THE UNIVERSITY
of EDINBURGH

BMP signalling via Id proteins in mesoderm progenitor cell differentiation

Amy Katrina Pegg

A thesis submitted in fulfilment of requirements for the degree of
Doctor of Philosophy

Institute for Stem Cell Research MRC Centre for Regenerative Medicine
School of Biological Sciences, University of Edinburgh

November 2018

Declaration

I declare that the work presented in this thesis is my own, unless otherwise stated. The work described in this thesis has not been submitted for any other degree or professional qualification.

Amy Katrina Pegg

Acknowledgements

Firstly, I would like to extend my deep thanks and gratitude to Professor Val Wilson and Doctor Sally Lowell for providing me with the opportunity to undertake this PhD. You let someone who had studied neither development nor stem cells before loose on a project examining cell fate during development.

I value having had the chance to work between both research groups and have greatly benefitted from diverse inputs from colleagues with varying research backgrounds. It was always entertaining to guess which bits of data each group would be excited about – definitely not always the same! Lab members both past and present have provided practical help and teaching at the bench, as well as providing valuable suggestions and feedback during lab meetings – thank you. A special thank you goes to Ron Wilkie who carried out sectioning for me, an endless supply of pens and was a lovely desk neighbour.

I would also like to thank the input from Dr Anestis Tsakiridis and Dr Tilo Kunath, both of whom were members of my PhD committee, for their encouragement and advice. Morning breakfasts over weekly meetings with the developmental biology group provided (slightly bleary eyed) stimulating discussion, and the odd meteorologically challenged day out. I am also grateful to the expertise and help offered by Claire and Fiona in the flow cytometry facility, and the Bertrand for imaging advice. Huge thanks go to Helen and Marilyn from tissue culture - two unsung heroes at SCRM. Buried away in a windowless room they not only kept the very busy tissue culture facility running throughout my time as a PhD student but also always had a smile, kind words, and a laugh to share.

This thesis would not have come to be without the kindness and support of friends both near and far, as well as old and new. Your help has been invaluable in so many ways, be it gibberish phone calls, cups of tea, coffee by post, burritos or hugs. All have helped through the tough moments.

Finally, I express an immense gratitude to my family. Although what I have spent the last few years working on seems a bit mysterious it would not have been achieved without you.

This project was supported by the BBSRC.

Abstract

Historically the three germ layer of the body: endoderm, ectoderm, and mesoderm, were considered to diverge early in development with the derivatives of each to progress along differentiation routes independent of one another. However, it is now known that neuromesodermal progenitors (NMPs) are present during axial elongation, after the basic formation of the three germ layers during gastrulation. These bipotent cells generate neurectodermal tissue in the form of the neural tube, giving rise to the central nervous system, and mesoderm in the formation of somites.

NMPs are located within the anterior of the primitive streak, in the node streak border and the adjacent caudal lateral epiblast in the E8.5 mouse embryo. As axial elongation continues they are found in the chordoneural hinge within the tailbud until E13.5. Another progenitor population, denoted lateral and paraxial mesoderm progenitors (LPMPs) are found within the posterior of the primitive streak and the adjacent caudal lateral epiblast at E8.5. This progenitor population contributes to lateral and ventral mesoderm during embryonic development. However, grafting into NMP containing regions of the embryo has shown that these progenitors retain the ability to contribute to the paraxial mesoderm when in the appropriate environment.

As the embryo begins elongation, *Id* transcripts can be detected within LPMP containing regions and are largely excluded from the regions that contain NMPs. The expression data generated here combined with previously published work identifies BMP signalling via Id factors as a candidate system for regulating mesoderm specification from progenitor populations within the primitive streak. As such, the work presented here utilises a combination of embryology and cell culture to examine the effects of BMP signalling via Id1 on the differentiation of progenitor populations within the primitive streak.

Grafting data generated here indicates that NMPs possess plasticity in mesodermal differentiation, as with LPMPs. NMP regions were grafted into LPMP containing regions of the embryo and contributed well. An *in vitro* system was created to model the differentiation of NMPs into paraxial mesoderm and neurectoderm. Inducing BMP activity within this system inhibited differentiation into neurectodermal and paraxial mesoderm lineages, and instead led to the upregulation of markers of lateral and ventral mesoderm. As expected, treatment with BMP in this context also induced Id1 expression suggesting that the effects of BMP were being mediated via Id1. Specific induction of Id1 during NMP differentiation *in vitro* mimicked the effects of BMP treatment.

The work described here extends expression data for the Id family in post implantation mouse development and presents a new cell based differentiation model. Utilising this system demonstrates that BMP signalling via Id1 can inhibit NMP differentiation into neurectoderm and paraxial mesoderm instead promoting differentiation into lateral and ventral mesoderm.

Contents

Declaration ii
Acknowledgements iii
Abstract iv
Contents vi
List of figures x
List of tables xii
List of abbreviations xiii
Chapter 1 – Introduction 1
1.1 Post-implantation mouse development 1
1.1.1 Gastrulation and the primitive streak 1
1.1.2 Neuromesodermal progenitors 3
1.1.3 Lateral and paraxial mesoderm progenitors 16
1.2 Epiblast stem cells 19
1.2.1 Origin and isolation 19
1.2.2 Signalling pathways involved in the maintenance of epiblast stem cell pluripotency 21
1.2.3 Epiblast stem cells as a model for post-implantation development 22
1.2.4 *In vitro* generation of NMPs 24
1.2.5 Relationship to other pluripotent cell types 27
1.3 The Id family 29
1.3.1 The helix-loop-helix family 29
1.3.2 Id family identification and structure 31
1.3.3 BMPs in early post-implantation mouse development 37
1.3.4 Id family member expression and function in post-implantation mouse development 42
1.3.5 Id family members in pluripotent stem cell culture 49
1.4 Scope of this thesis 50
Chapter 2 Materials and Methods 51

2.1 Cell culture 51
2.1.1 Cell lines 51
2.1.2 Culture conditions 52
2.1.3 Cell freezing and thawing 55
2.1.4 Differentiation protocols 56
2.1.5 Flow cytometry and fluorescent activated cell sorting 58
2.2 Embryology 58
2.2.1 Maintenance of mice 58
2.2.2 Collection of mouse embryos 59
2.2.3 In situ hybridisation 59
2.2.4 Embryo culture 62
2.3 Molecular biology 66
2.3.1 Plasmids used 66
2.3.2 Preparation of selective plates 66
2.3.3 Plasmid transformation into competent bacteria 67
2.3.4 Isolation of plasmid DNA 67
2.3.5 PCR methods 67
2.3.6 RNA methods 71
2.3.7 Antibody staining 75
Chapter 3 *Id* gene expression in the post implantation mouse embryo 77
Introduction 77
Id transcript expression in the pre-somitic mouse embryo 77
3.1.1 *Id* transcripts are expressed in proximal and extraembryonic tissue at E7.5 78
3.1.2 *Id* transcripts are expressed in lateral epiblast and the cardiac crescent 82
3.1.3 *Id1* transcript expression can be found surrounding the embryonic node 82
Id gene expression during early somitogenesis 85
3.1.4 *Id* genes have overlapping expression patterns in the E8.5 mouse embryo 85

Id gene expression during early organogenesis 88
3.1.5 Expression of the *Id* genes is similar but distinct at E9.5 89
Microarray analysis of post implantation *Id* transcript expression 93
Discussion 95
3.1.6 *Id* transcript expression 95
3.1.7 Id expression and mesoderm specification 97
Chapter 4 – An *in vitro* system for examining mesoderm differentiation of neuromesodermal progenitors 99
4.1 Introduction 99
4.2 Neuromesodermal progenitors can contribute to LPMP regions 100
4.3 Fgf activity induces differentiation of *in vitro* derived NMPs into prospective paraxial mesoderm and neurectoderm 105
4.3.1 Treatment of *in vitro* derived NMPs with Fgf induces rapid gene expression changes 105
4.3.2 *Tcf15* transcript expression can be detected prior to the onset of somitogenesis 113
4.3.3 Tcf15 induction during *in vitro* differentiation of NMPs 116
4.3.4 *In vitro* differentiation results in distinct populations of prospective paraxial mesoderm and neurectoderm 123
4.4 Discussion 127
Chapter 5 - The effect of BMP/Id on mesoderm specification 130
5.1 Introduction 130
5.2 BMP signalling perturbs NMP differentiation *in vitro* 130
5.2.1 BMP treatment during NMP differentiation induces Id1 expression 130
5.2.2 BMP treatment can redirect *in vitro* differentiation of NMPs 137
5.2.3 BMP stimulation can perturb the establishment of NMPs *in vitro* 149
5.2.4 Id1 has distinct expression patterns during differentiation into prospective paraxial and lateral mesoderm 153
5.3 Induction of Id1 in NMPs affects differentiation of NMPs 157
5.3.1 Induction of Id1 during NMP differentiation 158
5.3.2 Effect of Id1 induction during differentiation of NMPs 163
5.4 Discussion 175

Chapter 6 – Discussion 178
References 185
Appendix 1 202
Appendix 2 203

List of figures

Figure 1.1| Schematic displaying the location of NMPs and LPMPs. 7
Figure 1.2| Overview of culture methods used to generate NMPs *in vitro*. 25
Figure 1.3| Schematic of dominant negative inhibition by Id proteins. 35
Figure 3.1| *In vivo* expression of Id transcripts at E7.5. 79
Figure 3.2| Expression of Id transcripts at early head fold stage. 81
Figure 3.3| Expression of Id transcripts at E8.0. 83
Figure 3.4| *Id1* transcript expression surrounding the embryonic node. In situ hybridisation was performed using E8.0 embryos 84
Figure 3.5| Id transcript expression during early somitogenesis. 87
Figure 3.6| Expression of Id transcripts during early organogenesis. 90
Figure 3.7| Microarray analysis of embryonic subregions. 94
Figure 4.1| Schematic showing regions involved in grafting. 102
Figure 4.2| NMP containing regions contribute when grafted to the posterior CLE. 104
Figure 4.3| Differentiation of EpiSCs into NMPs. Culture of EpiSCs in Fgf and Chiron results in down regulation of Oct4, and co-expression of Sox2 and T...... 106
Figure 4.4| Differentiation of *in vitro* derived NMPs into prospective paraxial mesoderm. 109
Figure 4.5| Differentiated NMPs did not contribute when grafted into paraxial mesoderm and neurectoderm contributing regions.. 112
Figure 4.6| *Tcf15* transcript can be detected prior to the onset of somitogenesis. 115
Figure 4.7| Fgf stimulation of *in vitro* derived NMPs does not result in widespread upregulation of Tcf15-Venus. 117
Figure 4.8| Rspo3 treatment, and suppression of BMP activity does not increase the Tcf15-Venus positive population.. 122
Figure 4.10| Meox1 is upregulated during NMP differentiation in Fgf. 126
Figure 5.1| Id transcript expression during NMP differentiation.. 131
Figure 5.2| Id1-Venus is upregulated by BMP stimulation during NMP differentiation. 134
Figure 5.3| Id1-Venus is reproducibly upregulated by BMP4 treatment during NMP differentiation *in vitro*. 136
Figure 5.4| BMP treatment inhibits transcriptional upregulation of paraxial mesoderm and neural associated genes during *in vitro* differentiation of NMPs. 138
Figure 5.5| Sox2 and T are downregulated by BMP4 treatment. 141

Figure 5.6| BMP stimulation of differentiating NMPs downregulates Meox1 and upregulates Flk1-GFP. 143
Figure 5.7| Differentiation of NMPs in the presence of BMP4 results in strong increase in expression of Flk1-GFP. Flk1-GFP reporter cells were used to generate 147
Figure 5.8| Upregulation of Flk1-GFP following BMP4 treatment is reproducible. 148
Figure 5.9| BMP4 inhibits the establishment of NMPs *in vitro*.. 150
Figure 5.10| Manipulation of BMP signalling during NMP establishment *in vitro*. 151
Figure 5.11| Id1-Venus and Meox1 expression appear mutually exclusive during NMP differentiation. 155
Figure 5.12| A small subpopulation of NMPs co-express Id1-Venus and T. 156
Figure 5.13| Doxycycline treatment induces flag expression. 159
Figure 5.14| Doxycycline induced flag reports induced Id1 expression.. 160
Figure 5.15| Doxycycline treatment does not affect wild type cells. 162
Figure 5.16| Induced Id1-flag is mutually exclusive to Meox1. 164
Figure 5.17| Expression of Id1 and Meox1 during differentiation of NMPs *in vitro*. 165
Figure 5.18| Induction of Id1 redirects differentiation of NMPs *in vitro*. 169
Figure 5.19| NMP differentiation is not redirected when *Id1* is not induced. 172
Figure 5.20| Doxycycline mediated induction of Id1 varies in efficiency depending on context. 174
Figure 6.1| Model of the stages at which BMP/Id regulates mesoderm differentiation. 179

List of tables

Table 1.1| Additional conserved domains present within subset of the HLH superfamily and example bHLH proteins that contain them……..…30
Table 1.2| Summary of phenotypes observed in mutant mice for select BMP signalling components……...40
Table 1.3| Embryonic lethality of Id mutant genotypes……..48
Table 2.1| LIF and serum culture media composition…….....52
Table 2.2| EpiSC culture media composition……..……..54
Table 2.3| Embryo culture media composition……...……..64
Table 2.4| qPCR reaction composition……68
Table 2.5| qPCR cycling parameters……69
Table 2.6| qPCR primers and probes…….……70
Table 2.7| Plasmids and enzymes used to generate in situ hybridisation probes…….73
Table 2.8| Primary antibodies……..……76

List of abbreviations

A	
AP	Anterior posterior
AVE	Anterior visceral endoderm
B	
B-gal	B-galactosidase
BMP	Bone morphogenic protein
Bmpr	BMP receptor
bHLH	Basic helix-loop-helix
C	
CLE	Caudal lateral epiblast
CNH	Chordoneural hinge
D	
DEPC	Diethyl pryocarbonate
DIG	Digoxigenin
DMSO	Dimethyl sulfoxide
DVE	Distal visceral epiblast
E	
E	Embryonic day
EMT	Epithelial to mesenchymal transition
EpiSC	Epiblast stem cell
ExE	Extraembryonic endoderm
F	
FACS	Fluorescent activated cell sorting
FCS	Fetal calf serum
Fgf	Fibroblast growth factor
Fgfr	Fibroblast growth factor receptor
G	
GFP	Green fluorescent protein

GMEM	Glasgow minimal essential medium
	H
hES	Human embryonic stem
HLH	Helix-loop-helix
	I
ICM	Inner cell mass
Id	Inhibitor of differentiation
	K
KOSR	Knock out serum replacement
	L
L/St	Caudal lateral epiblast/primitive streak
LB	Lysogeny broth
LIF	Leukaemia inhibitor factor
LPMP	Lateral and paraxial mesoderm progenito
LVM	Lateral and ventral mesoderm
	M
mES	Mouse embryonic stem
mRNA	Messenger ribose nucleic acid
	N
NM	Neuromesodermal
NMP	Neuromesodermal progenitor
NSB	Node-streak border
	P
PCP	Planar cell polarity
PCR	Polymerase chain reaction
PD	Proximal-distal
PGC	Primordial germ cell
PS	Primitive streak
PSM	Pre-somitic mesoderm
pSmad	Phospho-Smad

Q	
qPCR	Quantitative real time PCR
T	
T	Brachyury
TBM	Tailbud mesoderm
V	
VE	Visceral endoderm

Chapter 1 – Introduction

1.1 Post-implantation mouse development

1.1.1 Gastrulation and the primitive streak

The development of the primitive streak (PS) begins shortly after implantation of the mouse embryo; at around E6.5. Prior to this however, the proximal-distal (PD) axis is formed in the developing embryo. This involves the establishment of gradients of Nodal, Wnt, and bone morphogenic protein (BMP) signalling components through the egg cylinder. In the proximal region of the epiblast at E5.5, Nodal signalling drives BMP4 expression in the extraembryonic ectoderm. This extraembryonic bone morphogenic protein (BMP) activity positively drives Wnt activity in the proximal epiblast of the embryo proper, which in turn is part of a positive feedback loop on Nodal expression. Local signalling from the epiblast and the extraembryonic tissue establishes regionalised patterns in the visceral endoderm (VE). A subset of VE cells become a signalling source known as the distal visceral endoderm (DVE) that is specified distally within the epiblast. The DVE is a strong source of Nodal and Wnt antagonists, and diminishes the expression of Nodal in the adjacent distal epiblast. As gestation progresses into E6.0, the DVE migrates to the presumptive anterior of the embryo, establishing the anterior VE (AVE) and thus the anterior-posterior axis (AP) of the embryo (Arkell & Tam 2012; Arnold & Robertson 2009).

The onset of gastrulation is marked by the establishment of the PS in the proximal posterior of the embryo. Historically, gastrulation is understood to mark the separation into and generation of the three distinct germ layers: ectoderm, endoderm and mesoderm. Extension of the PS into the distal region of the embryo occurs, with cells of the posterior epiblast migrating through the PS. These cells undergo epithelial to mesenchymal transition (EMT) as they ingress and become nascent mesoderm and definitive endoderm.

Distinct lineages of epiblast cells are acquired via exposure and response to specific signals, achieved in a spatial and temporal manner. A proximal source of Bmp4 from the extraembryonic endoderm (ExE) creates a gradient of Bmp activity along the developing PS in the posterior of the embryo (Di-Gregorio et al. 2007). This activity is contrasted with a strong distal source of Nodal signalling originating in the distal epiblast of the embryo.

Epiblast cells, which migrate early and within the posterior most region of the PS are exposed to high levels of Bmp4, and contribute to extraembryonic mesoderm; visceral yolk sac mesoderm, mesodermal component of the chorion and blood islands. Epiblast cell contribution to lateral mesoderm occurs following cell migration through the intermediate level of the PS and contribute to connective tissue and heart development (Kinder et al. 1999). As migration occurs at increasingly distal and anterior regions of the PS contribution to intermediate and paraxial mesoderm occurs, which generate kidney tissue and somites, respectively.

Axial mesoderm arises following epiblast migration through the anterior most portion of the PS and generates the node and notochord.

Definitive endoderm also arises from epiblast cells that have undergone migration through the PS at the anterior region (Kinder et al. 1999). Within the epiblast there are presumptive axial mesoderm and endoderm populations present prior to ingression through the PS (Burtscher & Lickert 2009). The predominant contribution to endoderm is from these cells, which are distinct to the mesoderm lineage. There does appear to be a more minor contribution to mesoderm and endoderm from a common bipotent progenitor population (Tzouanacou et al. 2009). Ectoderm is generated from epiblast cells that do not ingress through the PS, and generate the surface ectoderm and neural tissues.

1.1.2 Neuromesodermal progenitors

Traditionally, the three germ layers of the body: endoderm, ectoderm, and mesoderm, were considered to diverge early in development and the derivatives of each to progress along differentiation routes independent of one another. However, it is now known that neuromesodermal progenitors (NMPs) are present during axial elongation, after the basic formation of the three germ layers during gastrulation. These bipotent cells generate neurectodermal tissue in the form of the neural tube, giving rise to the central nervous system, and mesoderm in the

formation of somites (Tzouanacou et al. 2009). Somitic tissue gives rise to skeletal muscle, tendons, cartilage and bone.

1.1.2.1 Location and identification

Examination of potential stem cells or progenitor cells during axial elongation was facilitated via the use of a *laacZ* reporter. This reporter consisted of a construct containing an internal duplication of the *laacZ* gene, and thus no β-galactosidase (β-gal) activity (Bonnerot et al. 1987). This activity can however be restored following randomly occurring recombination restoring the *laacZ* open reading frame and leading to β-gal expression in the cell within which recombination occurred, and its descendants. The rarity and heritability of this event makes clonal analysis of populations of interest possible. Authors placed *laacZ* under the control of αAChR, which is a myotome-specific promoter. Analysis revealed multiple clones with contribution to seven or more somites with extension of labelled cells seen as far as the posterior most end of the myotome on the left and right sides of the embryo. These clones suggest a pool of self-renewing cells, which are present during the formation of the axis. The observation of bilaterally labelled clonal cells and observation of some labelled cells in particularly anterior somites indicates that this population of progenitor cells originated in the PS, in the progenitors of paraxial mesoderm (Smith et al. 1994). Further to the clonal analysis of the myotome, the lineage of the neural tube was also examined. This was achieved via placing *laacZ* under the control of the *neuron specific enolase* promoter. This resulted in a subset of

clonally labelled embryos where labelling extended from a variable anterior border to the posterior end of the neural tube, suggesting that stem cell-like progenitor cells also contribute to the spinal cord (Mathis & Nicolas 2000).

To examine these prospective progenitors in a non-lineage specific manner, *laacZ* was inserted into the Rosa26 locus. This is a ubiquitously expressed locus and allowed for retrospective clonal analysis (Tzouanacou et al. 2009). Clones were produced with contribution to both neurectodermal and mesodermal tissues, thus demonstrating the existence of bipotent NMPs. The presence of neuromesodermal clones in E8.5 and E10.5 embryos which extended from a variable anterior border to the PS, or tail bud in older embryos, is consistent with the presence of a progenitor population with stem cell-like properties in the posterior region of the developing mouse embryo.

In order to pinpoint the specific embryonic locations of these axial progenitors, transplantation studies using GFP positive donor embryos was used. The PS can be dissected into five arbitrary segments of equal length to provide anterior-to-posterior map references, beginning with streak 1 at the anterior most point, and streak 5 at the posterior most point (See Figure 1.1). When microdissected tissue from any position between streak 1 and 4 tissue was homotopically grafted, cells were observed within somites and the tailbud mesoderm (TBM) following 48 hours of culture, whereas the rostral node resulted in notochord contribution (Cambray & Wilson 2007). The grafts of the border between the node and the PS, the node-streak

border (NSB), contributed to the developing ventral neural tube and somites and some cells in the notochord. Descendants of these grafted cells also colonised the TBM and the chordoneural hinge (CNH); a structure appearing in the posterior-most region of the embryo at E10.5, formed by the posterior end of the ventral neural tube and the underlying notochordal plate. These grafting experiments in combination with previous work showing the ventral layer of the NSB forms notochord exclusively (Cambray & Wilson 2002) indicate that neuromesodermal bipotent cells reside within the dorsal region of the NSB.

Figure 1.1| Schematic displaying the location of NMPs and LPMPs. (A) Schematics of the E8.5 embryo highlighting the locations containing NMPs (NSB and L1-3) and LPMPs (L/St5). **(B)** Transverse section of a DAPI stained E8.5 embryo with reference points for the NSB and L/St5 regions. **(C)** Schematic of the 10.5 mouse embryo identifying the location of the CNH, within which NMPs are located. NSB, node streak border; L1-3, transverse lateral fifths of the CLE; L5, posterior most transverse segment of the CLE; St5, posterior most fifth of the primitive streak; RN, rostral node. Modified from (Wymeersch et al. 2016).

In addition to the above grafting experiments, heterochronic grafting of CNH tissue from E10.5-E12.5 embryos into the E8.5 NSB showed axial contribution to both neurectoderm and mesodermal tissues. Cells derived from these grafts also contributed to the TBM and the CNH like cells originating from the NSB. Grafts of the TBM did not repopulate the TBM or the CNH, and some failed to incorporate altogether. The potency of cells of the CNH did not appear to be lost, as serial grafting through three generations of host embryos continued to display axial and CNH contribution (Cambray & Wilson 2002).

The findings from these grafting experiments indicate that both the NSB of the E8.5 mouse embryo, and the later occurring CNH of the E10.5-E12.5 embryo are equivalent regions; both containing NMPs that are capable of self-renewal with involvement in axial elongation through contribution to the neural tube, somitic mesoderm and notochord.

Examination of additional posterior regions of the developing mouse embryo was performed to assess whether NMPs are present within a broader region. As discussed above, the PS can be annotated 1-5 in an anterior to posterior manner. This charting can also be applied to the regions flanking either side of the PS, the caudal lateral epiblast (CLE). When the anterior most region (L1) was homotopically grafted, the derived cells contributed to the neural tube, paraxial and TB mesoderm and the CNH; indicating the presence of prospective NMPs. More posterior regions of the CLE, L2-3 still contributed to paraxial mesoderm when grafted but did not

incorporate into the TBM, neural tube or CNH. However, when the L2-3 tissue was heterotopically grafted into the NSB, it retained mesoderm contribution, but also populated the neural tube. This indicates that L2-3 of the CLE contains cells that are NM potent, but in their natural environment generate mesoderm, implying that a cell autonomous bias is not present within NMPs, rather that extrinsic cues from the local environment directs their differentiation along neurectodermal or mesodermal lineages (Wymeersch et al. 2016).

A classic test for pluripotency is transplantation under the kidney capsule followed by observation of teratocarcinoma formation (teratocarcinomas contain derivatives of all three germ layers together with undifferentiated cells). When cells of the NSB, the L1-3 of the CLE and the CNH were subject to this, tissue masses were formed containing mesodermal and neurectodermal tissues, but lacking other cell types (Wymeersch et al. 2016). This corroborates the bipotential restriction of these cells to contribute to mesodermal and neurectodermal lineages, rather than being pluripotent stem cells.

Taken together, the data discussed within this subsection identifies NMPs as a population of bipotent progenitors, which contribute to axial elongation. NMPs are located within the NSB and L1-3 of the CLE within the E8.5 mouse embryo, and within the CNH of E10.5 to E12.5 mouse embryos (Figure 1.1).

1.1.2.2 Markers of NMPs

Expression of genes associated with axial elongation such as Wnt3a, Fgf8, T, Cdx2 and Evx1 can be detected within the NMP containing NSB, CLE (L1-3) and CNH regions. However, this expression is not specific to NMPs, as tissue of the PS, nascent mesoderm, posterior CLE regions, and TBM also express these genes (Cambray & Wilson 2007). Attempts to identify a unique marker of NMPs were made through microdissection of posterior progenitor zones taken from E8.5 to E13.5 mouse embryos, followed by microarray analysis. Unfortunately, no single unique marker could be identified (Wymeersch et al, submitted).

However, in mouse and other vertebrate species, the regions within which NMPs reside show co-expression of the PS and nascent mesoderm marker T and the neural marker Sox2 (Tsakiridis et al. 2014a; Martin & Kimelman 2012; Olivera-Martinez et al. 2012). Examination within the mouse embryo of these two transcription factors identified the first instance of double positive cells within the E7.5 epiblast, close to the NSB (Wymeersch et al. 2016). Extending this analysis throughout the period of axial elongation in the mouse embryo revealed the presence of T/Sox2 double positive cells in all NMP containing regions. The number of these cells was found to be highest at E9.5, followed by a decrease and eventual ablation upon the completion of somitogenesis at around E13.5.

Applying this data to mapping generated from grafting work (described above), it was observed that in the mouse embryo regions fated to differentiate into mesodermal or neural lineages showed high expression of T and Sox2, respectively.

The cells showing co-expression of these two factors typically displayed low or medium expression levels of both proteins. Within the CLE of the E8.5 mouse embryos the density of T/Sox2 double positive cells was highest in L1, declining posteriorly towards L3. This correlates with the observation of NM fated cells within L1 of the CLE, and NM potent cells within L2-3.

T(bra)

T is a T-box transcription factor, with expression observed and considered characteristic of the PS. Its expression is also detected within the tailbud and CNH as axial elongation continues until the end of somitogenesis, and within the node and the notochord (Wilkinson et al. 1990; Wilson & Beddington 1997; Kispert & Herrmann 1994; Wilson et al. 1995; Cambray & Wilson 2007). T is a direct target of Wnt3a signalling (Yamaguchi, Takada, et al. 1999). Gastrulation does occur in homozygous null T mouse embryos, but the axis shows truncations and loss of notochord, a kinked neural tube and thickened PS (Wilkinson et al. 1990; Rashbass et al. 1991). These embryos die at E10.5, most likely as a result of disruption of the allantois. Additionally, ectopic neural tissue develops at the expense of paraxial mesoderm in homozygous T mutants (Yamaguchi, Takada, et al. 1999). Heterozygous embryos also show an accumulation of cells at the PS and have short and typically kinked tails (Wilson & Beddington 1997).

Sox2

Sox2 is one of three members of the SoxB1 subfamily of transcription factors, sharing a homologous HMG-box DNA binding domain (Schepers et al. 2002). Sox2 and its subfamily members show expression within neural cells of adult and embryonic tissue in addition to pluripotency related expression in early development (Pevny et al. 1998; Sarkar & Hochedlinger 2013; Wood & Episkopou 1999). At the preimplantation stage, Sox2 is expressed within the inner cell mass (ICM) and throughout the epiblast initially after implantation. At around E7.0 as the PS is elongating, Sox2 becomes restricted to the anterior portion of the embryo. Once somitogenesis begins, there is strong Sox2 expression within neurectoderm, though it can also be detected within endoderm and the developing germ cells (Avilion et al. 2003). Homozygous mutation of Sox2 results in embryonic lethality around implantation. The expression of Sox2 in PS and CLE regions has been demonstrated to be regulated via a specific enhancer, designated N1 (Yoshida et al. 2014). Examination of the activation via this enhancer has revealed it to be dependent upon the combined actions of Wnt3 and Fgf8 signalling (Takemoto et al. 2004). NMPs can be identified via low co-expression of Sox2 and T (Wymeersch et al. 2016) and it has been shown that these two factors mutually repress one another's expression (Koch et al. 2017).

The co-expression of Sox2 and T shows extensive overlap with cells possessing NMP identity. However, it should be noted that double positive cells were also observed within the E8.5 midline PS, posterior to the CNH at E10.5 and within the

hindgut and notochord, hence not all T/Sox2 double positive cells are bona fide NMPs.

1.1.2.3 Pathways affecting NMPs and axis elongation

There are several signalling pathways that regulate the elongation of the axis (see (Wilson et al. 2009) for an overview). Fgf and Wnt signalling can be manipulated to generate NMPs from pluripotent cells *in vitro* (See 1.1.2.3 below) and to affect neurectoderm and mesoderm tissue formation.

Wnt signalling

Modulation of the transcriptional activity of β-catenin is the means through which canonical Wnt signalling is mediated (reviewed in (Komiya & Habas 2008)). Briefly, in the absence of Wnt β-catenin is subject to phosphorylation within the cytoplasm enabling it to be recognised by an E3 ubiquitin ligase. This results in ubiquitination and subsequent degradation of β-catenin by the proteasome. However, when Wnt is present, it binds to a heteromeric receptor formed by Frizzled and Lrp5/6, disrupting the phosphorylation complex and inhibiting the degradation of β-catenin which can then translocate to the nucleus. Once in the nucleus, β-catenin can drive transcription of target genes (Clevers 2006).

Wnt signalling can also be occur via non-canonical pathways that are not mediated via β-catenin signalling (Komiya & Habas 2008). A key non-canonical Wnt signalling pathway is planar cell polarity (PCP) signalling. This pathway was

originally identified via work in Drosophila where epithelial structure orientation was disrupted. Examination of the molecular cause of this phenotype identified mutation of Frizzled and Dishevelled, both of which are components of Wnt signalling (Seifert & Mlodzik 2007). The PCP pathway, play key roles in the differential cellular localisation of proteins, establishing and mediating polarisation of cells (reviewed in (Komiya & Habas 2008).

During early post implantation mouse development Wnt activity via β-catenin signalling can be detected within the PS and node, posterior epiblast, mesoderm and the developing notochord (Ferrer-vaquer et al. 2010). As axial elongation and somitogenesis continues, Wnt activity is also detectable within the tail bud.

Of the 19 proteins that comprise the Wnt family, three are found expressed within the posterior of the embryo; along the PS and in the tailbud, Wnt3a, Wnt5a and Wnt5b (Takada et al. 1994). Two of these proteins, Wnt3a and Wnt5a have robust developmental phenotypes when their activity is perturbed.

In Wnt3a null mouse embryos, somitogenesis does not occur posteriorly to the forelimb and the notochord does not develop correctly (Yoshikawa et al. 1997). Additionally, there is expansion of neurectoderm in the form of an ectopic neural tube, which forms at the expense of the paraxial mesoderm. Conversely, when Wnt3a is overexpressed within the epiblast, mesodermal differentiation occurs, and neural differentiation was prevented (Jurberg et al. 2014). In the instance of both loss of Wnt3a expression and its overexpression, embryos showed axial truncation. Further examination of Wnt3a activity during axial elongation has shown it to be

dose dependent, with higher levels of activity required for appropriate formation of increasingly posterior somites (Greco et al. 1996). These findings imply a regulatory role of Wnt3a signalling in NMP differentiation into neurectodermal or mesodermal tissue. Also, the expression of Wnt5a within NMP containing regions throughout axial elongation is appropriate for a potential role in NMP maintenance.

Unlike Wnt3a, signalling via Wnt5a stimulates β-catenin independent, or the non-canonical Wnt signalling pathway. Knock out of *Wnt5a* results in embryos with a shortened PS and small or absent posterior vertebrae (Yamaguchi, Bradley, et al. 1999). In *Wnt5a* mutant embryos a tail bud does form but the establishment of new paraxial mesoderm ceases prematurely. The interference with mesoderm differentiation and elongation of the axis when Wnt5a activity is manipulated and its absence from the developing somites suggest a role in NMP maintenance.

Fgf signalling

The fibroblast growth factor (Fgf) family of molecules are key signalling components utilised throughout embryonic development. The typical mode of action of Fgfs is via binding and activation of the cell surface Fgf receptors (Fgfr), (Goetz & Mohammadi 2013). Signalling then progresses via three intracellular cascades involving downstream mediators Ras/Mapk, PI3K/Aktl or Plcγ1.

During gastrulation and early somitogenesis Fgf4 and Fgf8 are expressed within the posterior of the embryo, in the PS, tail bud and CLE. A conditional deletion of either of these genes within the posterior regions of the developing embryo does not lead

to observable defects in axial elongation (Boulet & Capecchi 2012). However, double conditional mutant embryos showed truncation to the axis with reduced paraxial mesoderm and somite formation blocked after the generation of 15-20 somites. Additionally, these mutants appear to develop an ectopic neural tube, which suggests an altered fate resulting in the generation of additional neurectodermal tissue at the expense of mesoderm. Further examination of Fgf4 and Fgf8 activity was performed using cre-mediated excision driven via *T(bra)* to inactivate both Fgfs within the presomitic mesoderm (Naiche et al. 2011). In these embryos the presomitic mesoderm showed premature differentiation, suggesting involvement of Fgf signalling in the suppression of presomitic mesoderm differentiation.

Loss of function of Fgfr1 results in a phenotype reminiscent of that of Fgf8-/- embryos. These mutants undergo aberrant gastrulation as cells ingress at the PS but fail to migrate and undergo EMT correctly (Sun et al. 1999). Fgfr1 has also been shown to exert regulation over the specification of mesoderm cell fate through the expression of T and Tbx6 in the PS (Ciruna & Rossant 2001).

1.1.3 Lateral and paraxial mesoderm progenitors

The fate of and mesodermal plasticity of NMPs led to further examination of the PS and CLE (Wymeersch et al. 2016). The posterior most regions of the CLE and PS, designated L/St5 (See Figure 1.1) contains high and ubiquitous expression of the PS and pan-mesodermal marker T, but no expression of Sox2 is detectable within these

regions. The absence of Sox2, which is required for neural differentiation, suggests the cells in this area may not possess neurectodermal potency.

Kidney capsule grafts were utilised for an unbiased test of potency. When L/St5 grafts were performs, all derived growths contained mesodermal tissue but no neurectodermal tissue. When L/St5 with ubiquitous GFP expression was grafted homotopically in E8.5 mouse embryos, lateral and ventral mesoderm (LVM) contribution was routinely observed. Homotopic grafts of the slightly more anterior region of the CLE, (L2-3) did also show low contribution to LVM, in addition to paraxial mesoderm and TBM. Exclusive contribution to LVM was only seen with the posterior most region of the PS and CLE; L/St5 (Cambray & Wilson 2007; Wymeersch et al. 2016).

Examination of the plasticity of L/St5 was examined via heterotopic grafts and *ex vivo* embryo culture. The anterior of the PS (St1-3) has been previously shown to provide extensive contribution to paraxial mesoderm (Cambray & Wilson 2007). When L/St5 cells were grafted to this site, robust contribution to both the paraxial mesoderm and LVM was observed (Wymeersch et al. 2016). The grafts did not show contribution to the CNH following embryo culture, but there was some restricted contribution to TBM.

Cells of L/St5 were grafted into a region that generates neurectoderm as well as paraxial mesoderm to determine whether these cells could respond to such local signalling as NMPs can. When grafted into the NSB area, cells incorporated into the paraxial mesoderm with good extension along the AP axis. Only one graft resulting

in a small patch of cells in the neural tube. These experiments demonstrated that there are cells contained within the posterior of the CLE and PS (L/St5), which do have the ability to respond to paraxial mesoderm inducing signals; that they have plasticity in their mesodermal differentiation routes. This with the lack of neurectodermal contribution seen, led the authors to designate this population of cells lateral and paraxial mesoderm progenitors (LPMPs).

As the L/St5 region of the E8.5 mouse embryo is devoid of Sox2 expression (Wymeersch et al. 2016), and ectopic expression of this transcription factor can divert differentiation into neurectoderm (Takemoto et al. 2011), manipulation of this protein was used to further examine the differentiation potential of LPMPs. Regions of L/St5 were microdissected and electroporated with a CAG driven Sox2 expression plasmid with a tdTomato label. These cells were then grafted into the anterior region of the NSB of host embryos and cultured. There was incorporation into the paraxial mesoderm in grafted cells that had not taken up the expression vector well. However, those cells that did take up vector and thus express td-Tomato formed non-integrated clumps.

Taken together, the work discussed in this section describes a distinct population of mesodermal progenitors found in the posterior of the PS and CLE. These LPMPs normally contribute to lateral and ventral mesoderm, but display plasticity in mesodermal differentiation in their ability to generate paraxial mesoderm when presented with the appropriate environmental cues. Unlike, the more anteriorly

found NMPs, LPMPs do not generate neurectoderm in situ, and do not appear to be able to respond to neurectodermal inducing signals.

1.2 Epiblast stem cells

1.2.1 Origin and isolation

The isolation of pluripotent cell lines from mouse blastocysts, termed mouse embryonic stem (mES) cells (see section 1.2.5), led the way to the culture of ES cells from human blastocysts, hES cells. These resembled mES cells since they could differentiate into derivatives of all germ layers, but differed from mES cells in several important respects. They did not self-renew in response to LIF and serum, but instead required Fgf and Activin, suggesting they represented a later pluripotent cell state than that of the mouse blastocyst.

The derivation of pluripotent mouse cell lines bearing resemblance to human embryonic stem cell lines was achieved simultaneously by two independent research groups in 2007 (Brons et al. 2007; Tesar et al. 2007). These stem cells were denoted epiblast stem cells (EpiSCs) on account of their tissue of origin, the post-implantation mouse epiblast. EpiSCs are derived and maintained using hES culture conditions; activin/nodal and Fgf signalling, with mES cell culture conditions (LIF and 10% serum, see 2.1.2.1 for full media composition) being unable to sustain EpiSC self renewal and instead promoting their differentiation. Alternatively,

EpiSCs can also be derived *in vitro* from mES cells through sustained culture in Activin A and Fgf2 (Acampora et al. 2013).

The gene expression profile of EpiSCs is distinct from that of mES cells and the ICM, instead reflecting their source tissue; the E5.5 mouse epiblast (Brons et al. 2007; Tesar et al. 2007). EpiSCs maintain expression of the core pluripotency markers Oct4, Nanog and Sox2, but in contrast to mES cells do not express several of the naïve pluripotency markers including Stella, Klf4, and Essrb. In addition, EpiSCs express lineage-associated genes including T (Brachyury), Fgf5, Sox17, Nodal, Foxa2 and Eomes.

In line with an identity distinct from pre-implantation pluripotency, blastocyst injections and morula aggregations have failed to show incorporation of EpiSCs despite recurrent attempts (Brons et al. 2007; Tesar et al. 2007). Rather, grafting experiments have demonstrated that EpiSCs can incorporate into the post-implantation mouse epiblast; proliferating and dispersing from the original graft site (Huang et al. 2012). Historic fate mapping data revealed the routes and future contributions of cell populations across the developing epiblast of the post implantation epiblast (Beddington 1982). Comparison to this data shows that the tissue contribution of EpiSCs seen when grafted into host embryos was appropriate, with immunohistochemistry showing expression fitting to the tissue of integration.

Pluripotency of EpiSCs was confirmed using teratoma assays, in which derivatives of all three germ layers were produced. The differentiation potential of EpiSCs was additionally examined *in vitro* using EB-mediated and monolayer differentiation

protocols to confirm that these cells can generate endoderm, mesoderm and neurectoderm (Brons et al. 2007; Tesar et al. 2007).

Although originally isolated from E5.5 mouse epiblast, several studies have attempted to derive EpiSCs from embryos of varying ages (Osorno et al. 2012; Kojima et al. 2014). A study comparing the derivation of EpiSCs from E5.5 to E8.25 (late bud) stage embryos found that the established lines did not vary greatly in Oct4, Nanog and Sox2 expression or their transcriptome (Kojima et al. 2014). Lines derived from all stages were confirmed to be pluripotent based on the observation that all generated teratomas.

1.2.2 Signalling pathways involved in the maintenance of epiblast stem cell pluripotency

As mentioned above, EpiSC maintenance is achieved via culture with Fgf2 and Activin A. When Fgf2 and Activin A are simply excluded from culture medium, EpiSCs give rise to cells reminiscent of the anterior neural plate of the E7.5 mouse embryo (Iwafuchi-Doi et al. 2012).

Signalling via the Fgf pathway has been shown to exert inhibition over the exit of EpiSCs from pluripotency, specifically having a negative effect on neural differentiation (Sterneckert et al. 2010). EpiSCs can be readily derived from mES cells in culture, and can also be forced to revert to a mES cell-like state. The conditions required to achieve this include media supplementation with Fgf signalling inhibitors (Bao et al. 2009; Greber et al. 2010). This data is complementary

to data demonstrating that Fgf signalling is required for mES cells to exit the naïve pluripotent state and enter a state capable of lineage specification (Kunath et al. 2007). The active inhibition of activin/nodal signalling via the treatment of EpiSCs with inhibitors causes widespread differentiation of cells, highlighting the importance of this pathway for the maintenance of EpiSC pluripotency (Tesar et al. 2007).

Although the presence of Activin A and Fgf2 maintains EpiSCs, this state can be overridden by the addition of Bmp4 to standard EpiSC culture conditions; generating mesoderm and endoderm-like cells (Vallier et al. 2009). The EpiSC state can be further challenged by the manipulation of the Wnt/β-catenin pathway generating distinct subpopulations dependent upon activity level (Tsakiridis et al. 2014b). The presence of low Wnt activity produces cells reminiscent of the early PS, which maintain their pluripotency, whilst high levels of Wnt activity result in exit from pluripotency and generation of mesoderm and NMPs.

1.2.3 Epiblast stem cells as a model for post-implantation development

As mentioned briefly above, EpiSCs can contribute to the post-implantation epiblast when grafted into *ex vivo* cultured mouse embryos (Huang et al. 2012; Kojima et al. 2014). These studies examined the incorporation of EpiSCs when grafted into PS stage mouse embryos, showing efficient contribution to various PS and epiblast graft sites. In the vast majority of cases grafted cells proliferated and dispersed from the graft site over 24 and 48 hours of culture with nuclear and actin staining

showing that the grafted cells had morphologies similar to their native neighbours (Huang et al. 2012). Immunohistochemical analysis demonstrated protein expression appropriate to the tissue of incorporation of grafted cells; Sox2 expression in the neural tube, T expression in nascent mesoderm and PS, AP-2α in surface ectoderm, Cdx2 in cells in the allantois, and Foxa2 in the floorplate and endoderm. As Sox2 is widely expressed in EpiSCs under self-renewing culture conditions, it is of note that this pluripotency and neural progenitor marker is downregulated in graft derived cells in non-neural tissues. Incorporation into regions containing PGCs, the junction between the base of the allantois and the posterior PS, was also observed with donor cells showing upregulation of the PGC marker Stella. In addition to tissue appropriate expression, donor cells could be observed in the beating heart, having upregulated the cardiac marker Nkx2.5. Taken together, the contribution of EpiSCs to derivatives of all three germ layers and expression of markers appropriate to the host tissue validate these pluripotent cells as an appropriate *in vitro* system to attempt to model the post implantation epiblast.

As EpiSCs show functional equivalence to the post-implantation epiblast, they have been utilised as a resource to examine post-implantation lineage specification, such as the specification of and differentiation within the PS and neural development (Najm et al. 2011; Iwafuchi-Doi et al. 2012; Tsakiridis et al. 2014; Gouti et al. 2014).

1.2.4 *In vitro* generation of NMPs

In vivo examination has identified the WNT and FGF signalling pathways as involved in tissue formation during axial elongation and in the maintenance of NMP populations. As such, manipulation of these pathways has been utilised to establish NMPs *in vitro* ((Henrique et al. 2015) (Figure 1.2).

Figure 1.2| Overview of culture methods used to generate NMPs *in vitro*. Culture conditions and the starting cell populations that have been used to produce NMPs or prospective NMPs *in vitro*. Co-expression of the PS and pan-mesodermal marker T and the pluripotent and neural associated protein Sox2 are used as a read out of successful establishment of NMPs. Adapted from (Henrique et al. 2015) using information from: (Tsakiridis et al. 2014c; Gouti et al. 2014; Turner et al. 2014; Lippmann et al. 2015; Denham et al. 2015).

Culturing EpiSCs in the presence of CHIRON99021 (Chiron), which activates Wnt signalling via GSK3β inhibition, and elevated Fgf2 produces a high proportion of NMPs, with approximately 80% of the resulting population co-expressing Sox2 and T; an *in vivo* indicator of NMPs (Gouti et al. 2014). Under these culture conditions, minimal or undetectable expression of Nanog and Oct4 were observed, indicating an exit from the pluripotent state of EpiSCs. Additionally, elevation of trunk Hox gene and anterior PS associated gene expression was observed. The potency of *in vitro* derived NMPs was tested via grafting into mouse embryos: they gave rise to neural and mesodermal tissues, similarly to *in vivo* NMPs. Plating individual T-GFP positive cells derived from this *in vitro* protocol to generate NMPs results in clones containing both prospective neural and mesoderm (Tsakiridis & Wilson 2015). This indicates that *in vitro* derived NMPs have the bipotent differentiation potential appropriate to their *in vivo* counterparts.

Culture medium supplement with Fgf and Chiron can also induce an NM potent state from pluripotency in mES cells (Gouti et al. 2014; Turner et al. 2014). Grafting of the derived cells into chick embryos confirmed an appropriate differentiation potential *in vivo*, with derived cells incorporating into the somites and the neural tube (Gouti et al. 2014). Subsequent *in vitro* differentiation of these NMPs was also achieved. MyoD positive prospective paraxial mesoderm was established when NMPs were cultured in Chiron, and treatment with retinoic acid and a Shh antagonist produced cells with a prospective posterior neural identity. This prospective posterior neural identity was not established when the derivation of

NMPs was attempted without Wnt stimulation: instead prospective neural cells were obtained that showed anterior characteristics.

The above findings also extend to hES cells too, where stimulation of Wnt and Fgf activity can also induce an NMP state (Gouti et al. 2014; Lippmann et al. 2015). When the EpiSCs to NMP protocol discussed above is sufficient to generate a culture of 80% T/Sox2 double positive cells from hES cells. These cells likely resemble the T/Sox2 positive cells that are present in caudal epiblast of human embryos (Olivera-Martinez et al. 2012). These *in vitro* derived double positive cells subsequently became distinct populations expressing either the neural marker Sox2, or mesodermal markers T and Tbx6.

Protocol modification has enabled the generation of a more homogeneous population of NMP-like cells from human ES cells (Lippmann et al. 2015). These modifications resulted in 75-100% T/Sox2 double positive cells that could also be maintained for up to seven days, unlike the more transient state achieved with other reported protocols.

1.2.5 Relationship to other pluripotent cell types

As discussed in the above sections, EpiSCs provide an *in vitro* model system of the post implantation epiblast. This notion, their distinction from mES cells, and similarities to hES cells have been further analysed through gene expression.

The similarities between mouse EpiSCs and hES cells is striking in terms of the comparable culture conditions required for the maintenance of these two pluripotent populations. In addition to using the same signalling pathways to maintain pluripotency, differentiation protocols developed for hES cells have in several cases been used successfully for EpiSCs to achieve similar differentiation; indicating comparable responses to differentiation stimuli (Brons et al. 2007; Tesar et al. 2007; Gouti et al. 2014) ChIP-on-chip examination suggests that there are also epigenetic regulation mechanisms common to both populations (Tesar et al. 2007).

The ICM of the pre-implantation embryo is the source of the embryo proper, and can be used to derive mES cells *in vitro* (Evans & Kaufman 1981; Martin 1981). mES cells can be cultured in multiple conditions such as LIF/FCS or 2i/LIF. ES cells cultured in the presence of LIF and serum (FCS) are not considered homogeneous, and the serum component of the culture media can be variable. As a population ES cells are viewed as an *in vitro* counterpart to the preimplantation epiblast and display appropriate identity and potency when introduced in to host embryos (Nichols & Smith 2009). 2i/LIF refers to culture with the addition of a MEK/Erk inhibitor PD0325901 and the GSK3β inhibitor Chiron, along with LIF (Silva & Smith 2008). Under these conditions mES cells show higher homogeny, with reduced spontaneous differentiation and lineage marker expression as compared to culture in LIF/FSC. This state is considered more naïve and typically referred to as ground state pluripotency, and considered distinct from the primed pluripotency of the post implantation embryo and EpiSCs.

Although EpiSCs can be derived *in vitro* from ES cells, examination of the transcriptome of EpiSCs, mES cells and the ICM of the blastocyst show that independently-derived EpiSC lines cluster together. Their transcriptome is distinct from that of mES cells and the ICM, instead shows a closer association with post implantation epiblast (Kojima et al. 2014; Brons et al. 2007). Other studies confirm that EpiSC have a transcriptional profile distinct from that of mES cells, exemplified by a reduced expression of Pecam1, Tbx3 and Gbx2 in EpiSCs (Tesar et al. 2007). This is accompanied by higher expression of lineage associated genes such as T, Eomes, Foxa2, and Sox17.

1.3 The Id family

1.3.1 The helix-loop-helix family

The basic helix-loop-helix (bHLH) protein family of transcription regulators are found in a wide variety of organisms ranging from vertebrates to the yeast *Saccharomyces cerevisiae* (Massari & Murre 2000; Skinner et al. 2010). More than 100 bHLH proteins have been identified in mouse and human, where members of this large protein family are implicated in an array of biological processes and regulation. Since their discovery, various approaches have been taken in phylogenetic classification of bHLH proteins leading to the 5, 6 or 7 subfamilies being proposed (Atchley & Fitch 1997; Massari & Murre 2000; Ledent et al. 2002; Stevens et al. 2008; Skinner et al. 2010). These varying classifications have been

performed based on sequence analysis, DNA binding properties, function and *in vivo* expression specificity.

1.3.1.1 Basic helix-loop-helix protein structure

bHLH factors share a similarly structured protein domain first identified in 1989 (Murre et al. 1989); two α-helices separated by a flexible loop region, which is adjacent to a stretch of basic amino acids (Villares & Cabrera 1987; Ferré-D'Amaré et al. 1993; Ellenberger et al. 1994; Murre et al. 1989). In addition to the highly conserved HLH domain, there are other domains shared amongst some subfamily members including a PAS dimerisation motif, DNA binding leucine zipper domain, an Orange protein interaction domain and WRPW motif functioning in transcriptional repression (See Table 1.1 below for examples) (Blackwood & Eisenman 1991; Prendergast et al. 1991; Huang et al. 1993; Dawson et al. 1995; Kewley et al. 2004; Hooker & Hurlin 2006; Sun et al. 2007).

Domain	Examples
PAS	ARNT, AhR, SIM, HIF
Leucine zipper	Myc, Max, Mad, SREBP
Orange protein interaction domain	HEY1, HEY2, HEYL
WRPW	Hes family members

Table 1.1| Additional conserved domains present within subset of the HLH superfamily and example bHLH proteins that contain them. Data compiled using (Jones 2004; Kewley et al. 2004).

1.3.1.2 Regulation of transcription

bHLH proteins interact with DNA at E-boxes; specific recognition sequences of CANNTG. DNA-protein contact is mediated via the basic region, with the HLH domain of the transcription factors enabling protein dimerisation. bHLH factors must form homo- or heterodimers to interact with DNA. These dimers possess high specificity as recognition of specific E-box sequences is achieved only by certain bHLH subsets (Ellenberger et al. 1994; Ruzinova & Benezra 2003; Jones 2004). The standard model of bHLH regulation centres around ubiquitously expressed E proteins, which form heterodimers with those bHLH proteins expressed in a tissue specific manner to then interact with DNA (Murre et al. 1989; Norton 2000). Alternative splicing of the *E2a* genes (also known as *Tcf3*) generates the E12 and E47 proteins, the E2-2 protein is encoded by *Tcf4* and the HEB E protein is encoded by *Tcf12* (Massari & Murre 2000).

1.3.2 Id family identification and structure

1.3.2.1 Identification of Id family members

The identification of *Id1* occurred through examination of a mouse erythroid cell line attempting to identify further bHLH factors, which may be involved in the determination of this lineage (Benezra et al. 1990). This screen was performed using the sequence of the second α-helix of the bHLH factors *Myc, MyoD* and *Myog* as a probe for the cDNA library. A factor was identified that contained the highly

conserved HLH domain, but did not possess the adjacent basic (DNA-binding) domain. The authors demonstrated interaction between the protein product of this factor and E12, E47 and MyoD, where heterodimerisation inhibits the association of these bHLH proteins with DNA. As such, this protein was name Id; Inhibitor of DNA binding.

A second *Id* gene, *Id2*, was identified when an unintended λ phage clone weakly hybridised to a cDNA probe for *Id1* (Sun et al. 1991). Sequence analysis of this clone found the presence of the HLH motif showing high homology to the corresponding domain within Id1. This new HLH protein also lacks the basic domain common to most HLH proteins. Despite the high homology between Id1 and Id2 within the HLH motif, these two proteins vary considerably within other regions.

Id3 (termed *HLH462* at the time of discovery) was initially identified during experiments to detect early response genes following stimulation of cells by serum or PDGF (Christy et al. 1991). A cDNA clone previously isolated from the early mRNA of induced 3T3 cells was used to probe mRNA. From sequencing isolated fragments and using antisense oligonucleotide primers, the authors concluded that this gene generates mRNA of 955 nucleotides plus a polyA tail. The mRNA generates a protein with a HLH domain of striking similarity to that of Id1 and also lacks a basic domain. Using interspecific backcross analysis *Id3* was mapped to the distal region of mouse chromosome four.

The fourth *Id* gene was identified using a degenerate oligonucleotide with sequence homology to the helix two region of the HLH motif of Id1 and Id2 (Riechmann et al.

1994). This was used to probe a cDNA library generated from mouse bone marrow cells. A novel clone sequence was identified and the full length cDNA obtained one of the two identical novel clones was used to probe a cDNA library prepared from E12.5 mouse embryos. Three exons make up the *Id4* gene, with the coding region contained within the first and second exons (van Crüchten et al. 1998).

Homologs to the murine *Id* genes were subsequently identified in the human genome. *ID1* and *ID2* were discovered using a cDNA expression library prepared from fibroblasts (Hara et al. 1994) and later mapped to chromosomes 20 and 2, respectively (Mathew et al. 1995). Cloning of chromosome-specific CpG islands led to the annotation of *ID3* to human chromosome 1 (Ellmeier et al. 1992) and *ID4* was mapped to chromosome 6 following probing of a cDNA library with a DNA fragment corresponding to part of the HLH motif (Pagliuca et al. 1995).

1.3.2.2 Interaction with and regulation of bHLH transcription factors

Id1 can heterodimerise with lineage-associated bHLH factors such as MyoD, though co-immunoprecipitation shows that they have a much higher binding affinity to E12 and E47 (Benezra et al. 1990; Sun et al. 1991). The binding of Id1 to E12 or E47 prevents these bHLH factors from binding DNA. Thus it seems that the predominant mode of action of Id1 is sequestering E proteins, preventing them from forming homodimers or heterodimers with lineage associated bHLH factors (Figure 1.3). Further support for this model has been provided through a yeast-two-hybrid screen where E12 and E47 were identified as the only confirmed Id1 interactors in

mES cells (Davies et al. 2013). This dominant negative mode of regulation has also been identified for the other Id proteins showing interaction with E proteins to inhibit homodimerisation or heterodimerisation with lineage specific bHLH factors (Sun et al. 1991; Christy et al. 1991; Riechmann et al. 1994). There is variation between Id family members in their strength of interaction with specific E proteins. Id1 shows a reduced preference for interaction with HEB than the comparable propensity for interaction seen with E12, E47 and E2-2. Id2 preferentially interacts with E47, and Id3 shows more similar interaction propensity across the E proteins (Langlands et al. 1997).

Id proteins have also been shown to interact with non-bHLH proteins such as Pax and Ets proteins, although the functional significance of these interactions remains unclear (Yates et al. 1999; Ohtani et al. 2001).

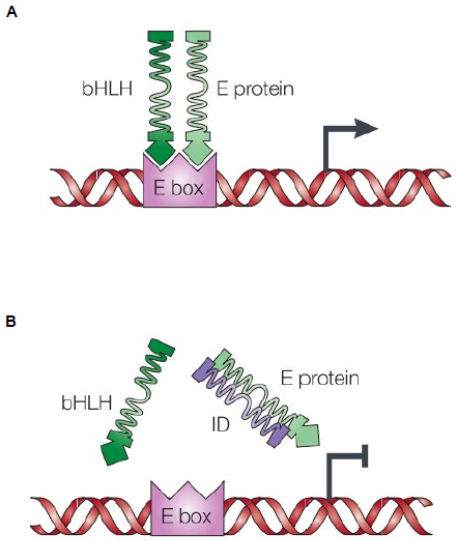

Figure 1.3| Schematic of dominant negative inhibition by Id proteins. (A) Lineage specific bHLH and E proteins require homo- or heterodimerisation to bind DNA via their basic region. **(B)** Id proteins display a high affinity for binding to E proteins. Forming such heterodimers sequesters the cofactor E proteins, preventing bHLH protein binding to the target gene E box. Adapted from (Perk et al. 2005).

1.3.2.3 BMP regulation of Id family members

The TGFβ superfamily of signalling molecules includes the subfamily of BMPs. These secreted extracellular proteins form dimers and bind to transmembrane serine/threonine protein kinase receptors. These heterotetrameric receptors are comprised of two Type I and two Type II receptors that interact with specific ligands within the TGFβ superfamily. BMP4 activity is achieved via interaction with BMP receptors (Bmpr) Bmpr1a, Bmpr1b (Type I), Bmpr2, Acvr2a, Acvr2b (Type II) (Allendorph et al. 2006; Koenig et al. 1994; Nagaso et al. 1999; Rosenzweig et al. 1995).

When a TFGβ ligand, such as BMP4, binds, phosphorylation of the Type I receptor is achieved via the kinase domain of the Type II receptor; this results in kinase activity activation (Chen & Weinberg 1995; Wrana et al. 1994). Once activated, the receptors can phosphorylate specific Smad proteins. In the case of BMP4 signalling, Smads 1, 5, and 8 are phosphorylated and can then complex with Smad4 to drive the transcription of target genes (Chen & Weinberg 1995; Kretzschmar et al. 1997; Nishimura et al. 1998). It is through this mechanism that BMP signalling drives expression of the directly targeted Id genes (Hollnagel et al. 1999; Katagiri et al. 2002).

1.3.3 BMPs in early post-implantation mouse development

During the early post implantation of the mousse embryo, expression of *Bmp2* and *Bmp4* can be found in the allantois and proximal epiblast of the embryo proper at E7.5 (Danesh et al. 2009; Aoyama et al. 2012; T Fujiwara et al. 2001). As development progresses to E8.0, expression of these two Bmps can still be found in the allantois, and also in the cardiac crescent and the lateral edges of the head fold (Danesh et al. 2009). At E8.5 and E9.0 *Bmp2* and *Bmp4* expression continues to be detected within the developing heart and laterally within the neural folds. Additionally, expression is observed within the tail bud, limb buds and otic vesicle. Bmp4 expression is seen in the ventral tail at E9.0. *Bmp7* is similarly seen in the cardiac crescent at E8.0, and in the developing heart, limb buds and otic vesicles at E9.0. *Bmp7*, is however also detectable in the distal epiblast, in cells surrounding the node at E7.5. This expression is not shared with other Bmps.

Bmpr1a expression can be detected within the neural folds and lateral plate mesoderm at E8.5 (Danesh et al. 2009). The expression within lateral plate mesoderm is maintained into E9.5, as is neurectodermal expression that can be found in the dorsal neural tube. At this stage of development *Bmpr1a* is also detectable within the limb buds and the developing head. *Bmpr1b* expression is detectable within lateral plate mesoderm, the neural folds, the otic vesicle and within a localised area in the developing hindbrain at E8.5. The expression in these tissues is maintained into E9.0 where *Bmpr1b* is also expressed within the limb buds, dorsal neural tube, optic vesicle, branchial arch and the somites. A similar pattern of

expression is observed for *Bmpr2* which is also expressed within the dorsal neural tube, limb buds, somites and developing brain at E8.5 to E9.0. Expression of this receptor was however, also detectable within the tail bud mesoderm.

As described in the section above (1.3.2.3 BMP regulation of Id family members), BMP signalling occurs via BMPRs and phosphorylation of Smad1, Smad 5 and Smad8. As such, Bmp expression alone is does not confirm BMP signalling activity. To capture spatial information about BMP activity within the mouse embryo, staining for phosphorylated-Smad (p-Smad) proteins and bmp-responsive element driven β-galactosidase reporter mice have been utilised to support the expression patterns of Bmps and Bmprs (Chuva de Sousa Lopes et al. 2003; Javier et al. 2012). These studies have captured indications of BMP activity within the allantois and proximal posterior epiblast at E7.5, and in the branchial arch and optic vesicle at E8.5. In E9.0 stage embryos, these studies found indicators of BMP activity within the dorsal neural tube and surrounding mesenchyme as well as the ventral tail bud.

To elucidate the requirements of BMP signalling during embryonic development, numerous mutant mouse stains have been created (reviewed in (Chen et al. 2004). These mutant strains have covered a range of mutation across the genes and proteins involved in the BMP signalling pathway. As BMP signalling is involved in multiple contexts and stages of development, straight knock out approaches capture defects in multiple tissues. Although there is variation in the phenotypes of varying mutants, there are common traits such as the disruption of primordial germ cell

(PGC) development, disruption of allantoic and cardiac development (See Table 1.2 below for a summary of certain genotypes).

Gene	Phenotype	References
Bmp2	• Defects in heart development • Reduced extraembryonic mesoderm, including poor development of the allantois • Reduction in PGCs • Null embryos die between E7.5 and E10.5	(Zhang & Bradley 1996; Ying & Zhao 2001)
Bmp4	• Defects in heart development • Reduced or absent allantois • Lack of PGCs • Little mesoderm development • Truncated or disorganised posterior development • Null embryos die between E6.5 and E9.5	(Winnier et al. 1995; Takeshi Fujiwara et al. 2001; Lawson et al. 1999)
Bmp7	• Null mice develop to term but die shortly after birth due improper kidney development	(Zhao 2003)
Smad1	• Reduced or absent PGCs • Disruption and expansion of visceral endoderm and extraembryonic mesoderm • Allantoic development is disrupted • Disruption of epiblast and nascent mesoderm • Null embryos die by E10.5	(Tremblay et al. 2001)
Smad5	• Defects in angiogenesis in the yolk sac • Disruption in left-right asymmetry • Reduced mesoderm formation • Neural tube and embryo turning abnormalities • Improper PGC formation • Null embryos die between E9.5 and E11.5	(Chang et al. 1999; Yang et al. 1999)
Bmpr1a	• Mutants are first distinguishable by morphology at E7.5 • Fail to gastrulate • Failure in mesoderm formation • Null embryos die at E9.5	(Mishina et al. 1995)
Bmpr2	• Defects in gastrulation and a lack of mesoderm observed.	(Beppu et al. 2000)
Bmp2+/-;Bmp4+/-	• Milder phenotype than individual null embryos • Fewer PGCs are observed than in individual heterozygotes	(Ying & Zhao 2001)
Bmp5/Bmp7	• Development of the allantois, heart, branchial arches, and forebrain are disrupted	(Solloway & Robertson 1999)

Table 1. 2| Summary of phenotypes observed in mutant mice for select BMP signalling components.

As complete ablation of a gene of interest does not provide spatial and temporal control, conditional knock out lines have also been utilised. This approach is particularly useful to supplement global findings, especially if embryonic death occurs prior to the developmental stage of interest. As BMP signalling is utilised in multiple tissues and contexts during embryonic development temporal control of interfering with signalling is of great benefit. An example of this approach can be found in the use of a conditional *Bmpr1a* knock out mouse strain to examine Bmpr1a functionality at gastrulation and during subsequent development (Miura et al. 2006). This system utilised cre-mediated recombination within the epiblast of the mouse embryo, driven by Mox2 expression and reduces but does not ablate the expression of Bmpr1a within the epiblast. Unlike Bmpr1a-null embryos, the conditional Bmpr1a knock out embryos did progress through gastrulation, though the PS remained shorter than in control embryos. However, morphological defects were apparent following gastrulation with a noticeable posterior curvature, the cardiac crescent not forming, and delayed development of the amnion and chorion. As embryos progress into E8.5 and the early stages of somitogenesis, the mutant embryos showed a lateral expansion of pre-somitic and somitic mesoderm with ectopic somites forming. These ectopic structures, although aberrant in their presence, were largely patterned appropriately when markers of somitic mesoderm were examined. Additional effects on mesoderm development were observed in the reduced and abnormal lateral plate mesoderm, which did not show typical morphology or gene expression patterns. The axial mesodermal structure of the notochord however, did develop and showed appropriate marker expression. The

investigations carried out with these mutant embryos highlighted the need for BMPR1A for cell recruitment to the PS, with delays in cell recruitment resulting in disrupted mesoderm specification. The effect of this delay is that prospective paraxial mesoderm cells are recruited to the PS during the head fold stage of development, rather than the mid-PS stage. This means that these cells will ingress through the streak at a differing proximal/distal location and thus presumably migrate further laterally.

1.3.4 Id family member expression and function in post-implantation mouse development

1.3.4.1 Expression of Id family members in the post-implantation mouse embryo

In situ hybridisation data have been generated examining the expression of the four *Id* genes in post-implantation mouse embryos (Wang et al. 1992; Jen et al. 1997). However, these studies were dependent on radioactively labelled riboprobes and the images generated are not always clear. As such it is difficult to unambiguously determine which regions contain true hybridisation and where signal is suitably above background levels. However, more recent work has provided further data regarding the expression of *Id1* and *Id2* in E6.5 to E7.5 mouse embryos (Li et al. 2013).

At E7.5 *Id1* transcript expression can be seen within all germ layers in proximal epiblast spanning from anterior to posterior regions, in addition to extraembryonic expression seen in the allantois and chorion (Wang et al. 1992; Jen et al. 1997). This

pattern is reproduced by Li *et al* (2003) in addition to showing expression at the base of the allantois (Li et al. 2013). As the head fold emerges, *Id1* transcript can be detected here, as well as in the cardiac crescent and in lateral mesoderm.

At E7.5, hybridisation signal can be detected indicating *Id2* expression in the chorion (Jen et al. 1997). This strong extraembryonic expression may be accompanied by expression in the proximal epiblast, though this cannot be clearly discerned from the figure. The more recent *in situ* hybridisation for *Id2* confirms the extraembryonic expression of the transcript, showing strong signal in the chorion of at bud stage (Li et al. 2013). This *in situ* hybridisation also shows weaker expression in the proximal region of the embryo proper. *Id2* expression is maintained in the chorion as the headfold emerges, when it can also be detected in the cardiac crescent and in the posterior of the embryo. However, due to the orientation of the embryo shown it is not clear exactly where this expression is.

The available data regarding the expression of *Id3* and *Id4* in presomitic mouse embryos are somewhat unclear. The authors suggest that at E7.5 *Id3* signal can be detected throughout the epiblast and that no *Id4* signal can be detected at this stage (Jen et al. 1997). However, this interpretation of the data should be treated with caution (See Appendix 1).

Following the onset of somitogenesis, *Id1* transcript can be detected in multiple tissues (Wang et al. 1992; Jen et al. 1996; Jen et al. 1997). One report suggests that at E8.5, *Id1* can be detected throughout the embryo with expression becoming more restricted during organogenesis (Wang et al. 1992). Other studies report a more

restricted pattern of expression, with transcript detected at the edges of the neural folds prior to neural tube closure in both the developing torso and head, along with adjacent cephalic mesenchyme (Jen et al. 1996; Jen et al. 1997). At E9.75 strong expression has been reported in the limb buds and branchial arch, along with the neural folds, though the neurectoderm was largely negative for *Id1* signal. Looking at older embryos, *Id1* transcript expression is reported in the mandibular arch and sclerotome derived mesoderm by E10.5 and later between E12.5 and E13.5 see strong expression detected in facial structures, condensing vertebrae and spinal cord. During early somitogenesis, no *Id1* signal was detected in the heart, though expression is reported by E11.5 at which stage expression in the sclerotome is also reported.

As with *Id1*, *Id2* mRNA is detected in multiple tissues during organogenesis (Jen et al. 1996; Jen et al. 1997). *Id2* signal can be detected in the neural folds at E8.5, and as neurogenesis progresses, can be seen in the roof plate and in presumptive neurons. *Id2* transcript expression is also reported in the branchial arches and optic vesicles at E9.5, and in the limb buds between E9.5 and E10.5, when signal is also detected in the gut endoderm. By E11.5 *Id2* transcript can be detected in the developing heart, mesenchyme dorsal to the developing stomach and sclerotome.

At E8.5 it is reported that *Id3* transcript can be detected in the neural folds and floor plate in both trunk and cephalic neurectoderm (Jen et al. 1996; Jen et al. 1997). This pattern persists through to E9.5 with expression detected in the ventral and dorsal parts of the neural tube (Ellmeier & Weith 1995). At this stage *Id3* signal can also be

detected in the branchial arches, optic vesicles, olfactory placode, and mesenchyme surrounding the dorsal aorta. *Id3* mRNA was not detected in newly formed somites, but was reported in the sclerotome at E11.5.

The examination of *Id4* during organogenesis shows a somewhat more restricted expression pattern than the other three *Id* genes (Jen et al. 1996; Jen et al. 1997). *Id4* expression has been detected mainly in neuronal tissues, and is suggested to be expressed in presumptive neurons as with *Id2*. *Id4* mRNA can also be detected in the epithelium of the developing stomach and otic vesicle. No expression of *Id4* was detected in the heart at the developmental stages examined in these studies.

Although there is overlap in the expression patterns of *Id1*, *Id2* and *Id3*, though more striking between *Id1* and *Id3*, these genes are not expressed in an identical manner. This suggests that while the genes may possess functional redundancy in some tissues, they are also likely to be differentially regulated and may exert different regulation over developmental processes. It is worth noting that the findings from Jen *et al* (1997) looking at *Id* gene expression in E8.5 embryos were described in the publication, but the data was not shown (Jen et al. 1997). As such, the reported expression patterns are those deduced by the authors and not subject to independent interpretation.

1.3.4.2 Phenotypes of Id deletion during development

When *Id1* knockout mice were generated no effects on embryo viability or post-natal growth were seen with *Id1*-/- pups born at Mendelian frequency (Yan et al. 1997). Histological analysis of various organs did not highlight abnormalities and mice did not show any obvious phenotypic defects even up to two years of age, and both male and female mice are fertile. *Id2* null mice develop to term and are at birth indistinguishable from wild type pups at birth (Yokota et al. 1999). Although mice heterozygous for *Id2* remain indistinguishable from wild type mice throughout life, a quarter of *Id2* null pups die neonatally. These mice show stunted growth and lack lymph nodes and Payer's patches along with a reduced population of natural killer (NK) cells. The reduction in NK cells appears to be due to a defect in NK-cell precursors. Defects are also seen in mammary gland epithelia during pregnancy when females are unable to lactate (Mori et al. 2000). Similarly, *Id3* knock out does not prevent development to term, with *Id3*-/- pups born at the expected Mendelian ration following crosses of heterozygous mice (Pan et al. 1999). A modest reduction in the number of CD4+ and CD8+ thymocytes is seen in Id3-/- mice, which also show decreased proliferation of B-cells in response to stimulation with an anti-mouse IgM antibody. However, this defect can be rescued by ectopic expression of *Id1* within B-cells of *Id3*-/- mice. No observable phenotype is seen in *Id4* heterozygote mice, but homozygous null mice have smaller overall brain sizes, which become apparent from E11.5 (Yun et al. 2004; Bedford et al. 2005). The reduced brain size in *Id4*-/- mice occurs due to premature differentiation of neural

progenitor cells in the developing forebrain. Approximately 50% of *Id4*-null embryos do not survive gestation, rapid weight loss occurs in a number of surviving pups with only 20% survive into adulthood.

The modest phenotypes seen in single knock out of *Id1*, *Id2* and *Id3* led to the generation of compound mutant mice to examine possible redundancy between the Id gene products. The extensively overlapping expression patterns between *Id1* and *Id3*, along with an ability of *Id1* to compensate for loss of *Id3* are highly suggestive of functional redundancy. As such, knock out of these two genes in combination was performed (Lyden et al. 1999). No mice were born lacking all four alleles, but mice lacking three out of the four alleles in any combination developed to term and appeared indistinguishable from wild type animals. The authors set about examining when during development a lack of both *Id1* and *Id3* becomes lethal. Until E10.5 development of *Id1*-/-*Id3*-/- mice is relatively normal, though embryos were found to be smaller than wild type by E11.5. Cranial haemorrhage was seen in double knock out embryos by E12.5 and none of these embryos survived beyond E13.5. Defective angiogenesis around the nervous system was accompanied by premature neuroblast withdrawal from the cell cycle in *Id1*-/-*Id3*-/- embryos.

Combinatorial knock out of four or five of the *Id1*, *Id2* and *Id3* alleles in most configurations results in embryonic lethality by mid-gestation (Table **1.3**) (Fraidenraich et al. 2004). However, the *Id1*-/-*Id2*+/-*Id3*+/- genotype can be tolerated, with embryos developing to term at an observed birth rate of 7.0% (expected 6.2%).

Genotype	Time of death	No. of alleles mutated
Id1-/-Id2+/-Id3+/-	Developed to term	4
Id1+/-Id2+/-Id3-/-	1% observed at birth	4
Id1+/-Id2-/-Id3+/-	E15.5	4
Id1-/-Id2-/-Id3+/+	E13.5	4
Id1+/+Id2-/-Id3-/-	E13.5	4
Id1-/-Id2+/+Id3-/-	E13.5	4
Id1-/-Id2-/-Id3+/-	E11.5	5
Id1-/-Id2+/-Id3-/-	E12.5	5
Id1+/-Id2-/-Id3-/-	Not determined	5
Id1-/-Id2-/-Id3-/-	E11.5	6

Table 1.3| Embryonic lethality of Id mutant genotypes. Adapted from (Fraidenraich et al. 2004).

Embryos lacking four or five of these alleles show a reduction in overall embryonic size. This is coupled with severe defects of the developing heart, which have been observed at E11.5 to E13.5. These defects include issues with the ventricular septum, reduced myocardium and disorganisation of myoctes and endocardial cells. BrdU labelling of *Id1-/-Id3-/-* embryos shows a defect in myocardial wall cell proliferation, and *Id1*/*Id2* double knock out embryos appear to have an enlarged ventricular septum. *Id1*/*Id2* heterozygotes on an *Id3* null background display a reduction in the aventricular and outflow track endocardial cells, resulting in underdevelopment of the endocardial cushion.

The knock out of all six alleles of *Id1*, *Id2* and *Id3* also results in a reduction in embryo size, though to a greater degree than with mutation of four or five of these alleles. Defects in the development of the heart are observed earlier, by E9.5 and are suggested to be the cause of embryonic lethality by E11.5. In these embryos, an

incomplete separation of the atrium and ventricle is observed. Although *Id1* and *Id3* double knock out embryos display haemorrhage within the developing brain, this was not observed in these triple knock out embryos.

The developmental problems observed within the emerging heart in Id mutants suggests the Ids could exert a function in the signalling between the differing tissues, or the loss of these proteins could affect early myocardial precursors.

1.3.5 Id family members in pluripotent stem cell culture

Within serum containing culture, BMPs are an essential component to maintain pluripotency of mES cells. The addition of serum to culture media has also been shown to stimulate Id family member expression, the expression of which can aid self renewal. This has been demonstrated via sustained self-renewal of mES cells when cultured with LIF, and forced Id1 expression alone (Ying et al. 2003). Additionally, transfection of *Id1*, *Id2* or *Id3* into mES cells inhibited neuronal differentiation even under neural differentiation conditions.

In line with the role of BMP and Id as maintaining a naïve pluripotent state, downregulation of Id transcripts is observed as embryoid body differentiation of ES cells begins (Romero-Lanman et al. 2012). Examination of *Id1* null mES cells show that lower expression of naïve pluripotency markers, and higher level of epiblast markers such as *T, Fgf5* and *Otx2* than in wild type cells. This is consistent with Id1

maintaining naïve pluripotency, with *Id1* null cells displaying gene expression patterns more typical of EpiSCs.

Ids are however not able to block differentiation completely; when LIF is simply withdrawn from *Id1* transfected mES cells, differentiation occurs towards non-neuronal fates. Additionally, Id1 expression within undifferentiated cells is able to impose an identity reminiscent of that of the proximal posterior epiblast in the developing embryo (Malaguti et al. 2013). This altered prospective positional identity is a prospective mechanism through which Id1 expression could prime cell differentiation.

1.4 Scope of this thesis

The work presented here aims to address whether BMP signalling mediated via Ids exerts regulation over the establishment of mesodermal subtypes from progenitor populations found in the PS. To examine potential effects of BMP and Id signalling on NMPs and LVMPs a combination of embryology work and cell culture is described. Although cell culture provides a more simple system, a differentiation model has been created and presented.

Chapter 2 Materials and Methods

2.1 Cell culture

All cell culture was performed on Corning cell culture plastics, and cells incubated in a 37°C/5%CO_2 humidified incubator (Sanyo CO_2 Incubator).

2.1.1 Cell lines

2.1.1.1 Wild type cell lines

E14 Ju09 cells were used here as wild type cells. This clonal cell line was generated by the Transgenics Service at the Institute from chimeric embryos generated with E14tg2a ES cells. This line was generated on a 129/Ola background.

2.1.1.2 Transgenic cell lines

A cell line to report the expression of Tcf15 was used. This was generated using a Tcf15_SKO plasmid targeted to the Tcf15 locus to introduce Venus into the first intron of one of the Tcf15 alleles. The clone used (SKO-E6-1) is designated Tcf15-Venus here.

An Id1-Venus reporter line was generated by Dr Mattias Malaguti within Sally Lowell's research group (Malaguti et al. 2013). This was generated on an E14 Ju09 mES cell background using an adapted version of a plasmid kindly gifted by Dr. Robert Benezra and Dr Hyang-song Nam (Nam & Benezra 2009).

A Flk1-GFP reporter line was kindly gifted by Dr Alexander Medvinksy, originally described in Jacobsen et al 1998.

An Id1 inducible cell line used here was previously generated by Dr Mattias Malaguti within Sally Lowell's research group. This line was generated using an overexpression plasmid (Ying et al. 2003) where flag (MDYKDDDD)-tagged cDNA of Id1 follows a CAG promoter. This is followed by and IRES and puromycin resistance gene. Two independent clones were used here, designated tId1 cl9 and tId1 cl43.

2.1.2 Culture conditions

2.1.2.1 ES cell culture in LIF and serum

mES cells were maintained in LIF and serum in media of the following composition:

Component	Volume	Final Concentration
Glasgow Minimum Essential Medium (GMEM, Sigma)	500ml	
Foetal Calf Serum (FCS, Gibco)	51ml	10%
L-Glutamine/Sodium pyruvate solution	11ml	L-Glutamine 2mM, Sodium pyruvate 1mM
Non-essential amino acids (Gibco)	5.5ml	1x
0.1M 2-mercaptoethanol	570µl	100nM
Leukemic inhibitory factor (LIF)	570µl	100U/ml

Table 2.1| LIF and serum culture media composition.

mES cells were maintained in flasks, which had been coated with 0.1% w/v gelatin for ≥ 10 minutes prior to use. Cells were passaged at 70-80% confluency. To passage mES cells, media was aspirated and the adherent culture washed with pre-warmed, sterile PBS (Sigma), before addition of trypsin EDTA (0.05% in PBS) (Gibco). Cells were incubated at 37°C until detached when ≥ 5 volumes of LIF and serum medium were added to quench the reaction. Cells were pelleted in a 30ml universal (Sterilin) by centrifugation for 3 minutes at 290xg. Medium was aspirated and the pelleted cells resuspended in LIF and serum medium before plating on prepared gelatin plates at an appropriate density.

A hematocytometer (Heubauer) was used where cell counting was required.

2.1.2.2 Epiblast stem cell culture

Plates were coated with Bovine fibronectin (Sigma) in PBS (7.5μg/ml) at 37°C for at least 10 minutes prior to use. EpiSCs were maintained in pre-prepared 6 well plates, in the following medium:

Component	Volume	Final Concentration
Dulbecco's modified eagle medium (DMEM):F12 (1:1 v/v) (Gibco)	100ml	
Neurobasal (Gibco)	100ml	
Non-essential amino acids (Invitrogen)	2ml	1x
L-glutamine (Invitrogen)	2ml	2mM
N2 supplement (Gibco)	1ml	0.5x
B27 supplement (Gibco)	4ml	1x
2-mecaptoethanol	200µl	100nM
Activin A (20µg/ml in 0.1%BSA) (PeproTech)	200µl	20ng/ml
Fgf2 (10µg/ml in 0.1%BSA) (R&D)	200µl	10ng/ml

Table 2.2| EpiSC culture media composition.

This medium composition is based on previously reported culture conditions (Brons et al. 2007), with minor adjustments. These modifications are based on work carried out within our Institute by Dr. Anestis Tsakiridis and Dr. Rodrigo Osorno to optimise cell survival and proliferation.

To passage EpiSCs, medium was aspirated off and the cells washed gently in pre-warmed PBS. 300µl 1x accutase (Sigma) was added to one well of a six well plate and the plate returned to 37°C for three minutes. Dissociation was checked under a microscope following gentle tapping of the side of the plate. The dissociated cells were transferred to a 30ml universal and 10 volumes of EpiSC medium were added to quench the reaction. Cells were pelleted by centrifugation at 1300rpm for three minutes. Excess medium was aspirated from the pellet, which was gently

resuspended in 1ml of EpiSC medium into fragmented clumps, using wide pore pipette tips. Cells were split 1:10 into a pre-warmed plate, every 48 hours. Where counting of EpiSCs was required, a small aliquot of the fragmented re-suspension was transferred into fresh EpiSC medium and dissociated to single cells. Cell counting was performed using a hematocytometer (Neubauer).

2.1.3 Cell freezing and thawing

To freeze EpiSCs, one confluent well of a six well plate was dissociated and pelleted as described above. This pellet was resuspended in 1ml of 10% dimethyl sulfoxide (DMSO) in knock out serum replacement (KOSR) and transferred to a 1ml cryotube (ThermoScientific) on dry ice. Cells were stored at -80°C for short term storage and moved to liquid nitrogen for long term storage.

To freeze ES cells, one T25 flask of approximately 80% confluency was trypsinised and the cells pelleted. This pellet was resuspended in 10% DMSO in ES media (LIF and serum), and transferred to a 1ml cyrotube. Cells were then stored as described above for cryopreservation of EpiSCs.

Cells were thawed by short incubation in a water bath at 37°C, followed by transfer to falcon tubes containing pre-warmed medium of the appropriate composition to the cell type. The cells were then pelleted by centrifugation in a bench top centrifuge (Eppendorf) and plated.

2.1.4 Differentiation protocols

2.1.4.1 In vitro derivation of epiblast stem cells

Unless otherwise stated, EpiSCs used here were derived *in vitro* from mES cells.

To generate EpiSCs *in vitro*, mES cells were dissociated, pelleted and resuspended as described above. Cell counting was performed using a hematocytometer (Neubauer) and cells plated at 8,000 cells cm^2 in 6 well plates. Plates were pre-treated with fibronectin (7.5μg/ml), as described above. Cells were cultured in LIF and serum for 24 hours, before medium change to EpiSC medium. Cells were passaged every 2-3 days, depending on density.

2.1.4.2 Neuromesodermal progenitor differentiation

Differentiation of EpiSCs into NMPs was carried out in accordance with a protocol developed by Dr. Anestis Tsakiridis (Gouti et al. 2014).

6- or 12-well plates were treated with fibronectin (7.5μg/ml in PBS), as with standard EpiSC culture, prior to cell plating. For differentiation into NMPs, N2B27 medium was supplemented with human Fgf2 (20ng/ml) (R&D Systems) and Chiron (CHIR99021) (Axon Medchem) (3μM), rather than Activin A and Fgf2 as with normal EpiSC culture. Cells were dissociated, pelleted and resuspended into fragmented clumps before plating at 1500 cells/cm^2. Cells were then cultured for 48 hours, at which point co-expression of Sox2 and T indicate successful differentiation into NMPs.

2.1.4.3 Mesoderm differentiation

After 48 hours of differentiation of EpiSCs into NMPs, as specified above, culture conditions were changed to induce differentiation into either prospective paraxial mesoderm, or prospective lateral and ventral mesoderm. Fgf2 and Chiron supplemented N2B27 medium was aspirated from the cells, which were briefly washed before addition of N2B27 medium supplemented with Fgf2 (20ng/ml) or Fgf2 (20ng/ml) and BMP4 (20ng/ml) to generate prospective paraxial, or lateral and ventral mesoderm, respectively. Following a further three days of culture cells were split 1:4 and re-plated in fresh medium.

Manipulation of WNT signalling was also examined within NMP differentiation into prospective paraxial mesoderm. NMPs were derived *in vitro*, then culture conditions changed to N2B27 media supplemented with the following: Fgf2 (20ng/ml) and LDN-193189 (0.1μM), Fgf2 (20ng/ml) and Chiron (3μM), Fgf2 (20ng/ml) and Rspondin-3 (30ng/ml), Fgf2 (20ng/ml) and Chiron (3μM) and Rspondin-3 (30ng/ml), Fgf2 (20ng/ml) and Chiron (3μM) and Rpondin-3 (30ng/ml) and LDN (0.1μM).

2.1.4.4 Id1 induction during mesoderm differentiation

A doxycycline inducible transgenic cell line was used to specifically induce expression of Id1 during *in vitro* differentiation. This mES cell line was made by M. Malaguti (detailed in section 2.1.1.2). These cells were differentiated into EpiSCs

before performing mesoderm differentiation as detailed above (2.1.4.3). Briefly, *in vitro* derived NMPs were cultured in Fgf2 (20ng/ml), with or without doxycycline (1μg/ml). Where LDN was included in the culture it was used at 0.1μM.

2.1.5 Flow cytometry and fluorescent activated cell sorting

2.1.5.1 Sample preparation

As with standard passaging, media was aspirated from adherent cell cultures and cells dissociated with accutase. Accutase was quenched using media and the cells pelleted by centrifugation. The pelleted cells were then resuspended in fluorescent activated cell sorting (FACS) buffer (4% FCS in PBS) and filtered prior to analysis or sorting. Cells were kept on ice until fluorescence analysis using a BD FACS Calibur, or until sorting using a BD FACS Aria II. FlowJo was used for analysis. For each sample tested, at least 10,000 events were analysed after gates were set to exclude cell debris.

2.2 Embryology

2.2.1 Maintenance of mice

Mice were house in the Animal Unit at the Centre for Regenerative Medicine on a 12 hour light/dark cycle, in accordance with the provisions of the Animals (Scientific Procedures) Act 1986 and the 2010/63/EU Directive.

2.2.2 Collection of mouse embryos

Mouse matings were set up overnight and females checked for vaginal plugs the following morning. Noon on the day of finding a vaginal plug was denoted embryonic day (E) 0.5. Cervical dislocation was used to cull pregnant females, the uterus was removed, and embryos were dissected from the uterus in M2 media (Sigma-Aldrich) at room temperature using a dissection microscope.

2.2.3 In situ hybridisation

Dissected embryos were fixed in 4% paraformaldehyde (PFA) overnight at 4^{o}C then dehydrated with increasing methanol (Fisher Scientific) concentrations (25%, 50%, 70%, and 100% in PBS). Dehydrated embryos were stored in 100% methanol at -20^{o}C.

Rehydration was performed using the same methanol series in reverse, and followed with three washes in RNase free PBS. Embryos were bleached in 6% H_2O_2 (Sigma) in PBS and Tween20 (PBT) for one hour at room temperature, and then washed three times in PBT. Following these washes embryos were permeabilised with proteinase K (10ug/ml in PBT) (Sigma) at room temperature, with incubation time dependent on embryo stage (7 minutes for E7.5, 10 minutes for E8.5, and 12 minutes for E9.5). Glycine (2mg/ml in PBT) (Sigma) treatment was used to stop the enzymatic reaction and embryos were washed twice in PBT. Re-fixing of the

embryos was performed with 4% PFA (Fisher Scientific), 0.2% glutaraldehyde (Sigma) in PBS. Embryos were transferred to a pre-hybridisation solution containing 50% formamide (Sigma-Aldrich), 25% 20x saline-sodium-citrate (SSC) in PBS (pH4.5), and 1% SDS. Following a short wash, the embryos were submerged in fresh pre-hybridisation solution and incubated in a humid box (containing tissue dampened with 50:50 H_2O and formamide), at 65°C with gentle rocking for at least two hours (Thermo Fisher Scientific oven was used for incubation). At the end of the incubation period, labelled riboprobes were denatured at 80°C for ten minutes then added to hybridisation solution containing 50% formamide (Sigma-Aldrich), 25% 20x SSC (pH4.5), 0.1% SDS, yeast tRNA (50ug/ml) (Promega/Ambion) and heparin (50ug/ml) (Sigma). Embryos were transferred to hybridisation solution containing denatured riboprobe (500ng/ml) and incubated in the same manner as for the pre-hybridisation incubation; 65°C overnight with gentle rocking.

Following hybridisation, embryos were washed twice for 30 minutes at 65˚C with Solution 1. This solution comprises 50% formamide (Sigma), 20% 20x SSC (pH4.5) and 1% SDS. Embryos were then transferred to a 1:1 mixture of Solution 1:Solution 2 and incubated for 10 minutes at 65˚C. Solution 2 consists of 10% 5M NaCL, 1% 1M Tris (pH7.5), 0.1% Tween20 in RNase free H_20 (Thermo Scientific). Three washes in Solution 2 were performed at room temperature, followed by 30 minute incubation in Solution 2 containing RNase A (100µg/ml) (Roche) at 37˚C. The RNase A containing solution was refreshed halfway through the incubation. Brief washes were performed with Solution 2, followed with Solution 3, which consists of 50%

formamide (Sigma), 10% 20x SSC (pH4.5) in diethyl pryocarbonate (DEPC) treated H_20. Embryos were washed for one hour at 37°C in Solution 3, with the solution replaced after 30 minutes. Embryos were washed three times in TBST (TBS and 0.1% Tween20) before blocking with 10% heat inactivated sheep serum (Sigma) in TBST at room temperature for at least 6 hours. Blocking solution was then replaced with 1% sheep serum in TBST with α-DigAP (1:2000) (Roche) and the samples incubated at 4°C overnight with gentle rocking. Following antibody incubation the embryos were washed three times in TBST followed by several extended washes at room temperature (at least five changes), and a final overnight wash at 4°C.

Prior to performing the colour reaction, the embryos were washed three times in NTMT (100mM NaCl, 100mM Tris-HCL pH9.5, 50mM $MgCl_2$, 0.1% Tween-20) at room temperature in embryo dishes. The staining solution consisted of 5-Bromo-4-chloro-3-indolyl phosphate/Nitro blue tetrazolium (BCIP/NBT) (Sigma-Aldrich), prepared in NTMT according to manufacturer instructions, and embryos incubated at room temperature in the dark. To stop the colour reaction, embryos were transferred to NTMT, before two final washes in PBT and re-fixing in 4% PFA at room temperature. Embryos were then transferred to 0.4% PFA in PBS and stored at 4°C. Whole mount embryos were imaged using a Nikon AZ100 dissecting microscope.

Preparation and sectioning of embryos previously used for whole mount in situ hybridisation was performed by Ron Wilkie. Fixed embryos were transferred to 15% sucrose in PBS, and incubated at 4°C for at least two hours. Embryos were then

transferred to 15% sucrose, 7% gelatin in PBS and incubated at 37°C until the embryo sank (time dependent on size of the embryo). The embedded embryo was then transferred in the sucrose and gelatin solution to an aluminium mould and orientated using a low powered dissecting microscope. Once set the block was partially submerged in liquid nitrogen then stored at -80°C until sectioning. Blocks were sectioned at -24°C by cryostat (Leica CM1900) and mounted on polylysine slides. Sections from in situ hybridisation samples were imaged using a Zeiss Axio Imager microscope.

2.2.4 Embryo culture

2.2.4.1 Preparation of host embryos

MF1 mouse embryos were used as host embryos.

To prepare embryos for culture, embryos were collected as described above, though with the following considerations. Care was taken when removing embryos from the decidua to avoid damage to the yolk sac, and Reichart's membrane removed to the base of the ectoplacental cone.

2.2.4.2 Grafting of cultured cells

rtO EpiSCs were used for all grafts of cultured cells described here. This cell line was derived directly from post-implantation mouse embryo epiblast. The line contains constitutively expressed GFP in addition to a doxycycline inducible Oct4 transgene, though the inducible transgene was not used here. Prior to *in vitro* differentiation into NMPs rtO EpiSCs were subject to fluorescent activated cell

sorting in case of silencing of the fluorescent label. GFP positive cells were plated into EpiSC culture conditions for 48 or 72 hours prior to differentiation into NMPs. NMP differentiation was performed as described above, and cells grafted following 48 hours of NMP differentiation.

Gentle scrapping using a 20-200μl pipette tip was used to detach clumps of cells from adherent culture. These clumps were sucked into hand drawn glass pipettes, which were used to graft the cells into host embryos. Host embryos were held in place gently with forceps and the graft-containing pipette inserted into the embryo at the desired graft site. The graft was expelled as the pipette was gently drawn out of the embryo. Embryos were then imaged as a record of the graft site and transferred into culture (see 2.2.4.4).

2.2.4.3 Grafting of embryo tissue

Microdissection and grafting of embryo tissue was performed by Val Wilson.

Dissection of donor embryos was performed in M2 medium using fine forceps to remove the embryos from the decidua and to remove Riechart's membrane. The posterior half of the embryo was separated from the anterior half by transverse cut posterior to the last fully formed somite. To isolate CLE the posterior portion of the embryo was segmented with transverse cuts made with fine glass needles. The resulting strips of tissue, containing PS flanked by CLE were then further dissected with lateral cuts to separate each CLE region. Finally, the mesoderm layer was

removed, again with a fine glass needle. The graft tissue was drawn into a hand-pulled glass pipette and deposited into the host embryo at the graft site as described above with grafting cultured cells.

2.2.4.4 Culture of host embryos

Embryos were cultured at 37°C in rolling culture (B.T.C Engineering precision incubator, 02767 DBS) at 5% CO_2 and 18-20% O_2 in the following medium:

Component	Volume	Concentration
Heat inactivated rat serum	1ml	
Glasgow Minimal Essential Medium (GMEM) (Invitrogen)	1ml	
L-glutamine/Pyruvate solution (Invitrogen)	20µl	2mM/1mM
Non-essential amino acids (Invitrogen)	10µl	1%

Table 2.3| Embryo culture media composition.

Rat serum was heat inactivated prior to use by incubation at 36°C for 15 minutes (performed by Ron Wilkie).

Culture medium was filtered through a 0.45µm filter, pre-warmed and pre-gassed prior to culture. Embryos were cultured in glass vials, with no more than two embryos per vial in 1ml medium per embryo. Following 24 hours of culture,

embryos were examined and culture was continued with those developing appropriately.

Embryos cultured for a further 24 hours were transferred to round-bottom universal tubes, transferred to 40% CO_2 and grown in rolling culture in a precision incubator (B.T.C Engineering, 029920 DBS). Again embryos were cultured in 1ml medium per embryo, with no more than two embryos per container. Tubes were sealed off with high vacuum silicone grease (VWR chemicals) and gassed by directing gas at embryo containing medium for one minute. This step of culture was performed in similar medium to the first 24 hours of culture, only composed of 75% heat inactivated rat serum with 25% Glasgow minimum essential medium (GMEM) (Invitrogen).

At the end of culture, embryos were transferred to M2 medium and dishes for dissection. The yolk sac was removed, and embryos imaged whole mount as a record of their development. Fine forceps were used to remove the anterior portion of the embryo including the heart.

To image incorporation of grafted tissue/cells, the posterior portion of embryo was imaged in bright field and green fluorescent channels on a Nikon stereoscope (Nikon AZ100). Embryo tissue was then washed in PBS to removed red blood cells and transferred to 4% PFA at 4°C overnight. The next morning the tissue was transferred to PBS at 4°C until further processing.

2.3 Molecular biology

2.3.1 Plasmids used

pGEM-T easy-Id1p was generated in house by linearization of pGEM-T easy and ligation of an Id1 insert to generate a plasmid to allow production of an Id1 in situ hybridisation plasmid. Restriction enzyme digestion and then sequencing was used to confirm orientation.

pBS/KS-Id2sp, pBS/KS-Id3sp and pBS/KS-Id4sp plasmids were obtained from Addgene. These plasmids were for the production of in situ hybridisation probes for Id2, Id3 and Id4 and were originally described and used in previous publication (Jen et al. 1997).

2.3.2 Preparation of selective plates

The Institute Wash Staff prepared lysogeny broth (LB)-agar by dissolving 1.5% Bacto™ Agar (BD) in LB. Stocks of ampicillin were prepared by dissolving 100mg ampicillin powder (Calbiochem) in 1ml nuclease free water (Gibco). The solution was then filtered through a 0.22μm filter (Millipore), and stored at -20°C. LB-agar was microwaved to melt the solution, and allowed to cool but not solidify. Antibiotic was added at a 1:1000 dilution and 15ml of this solution pipetted into 90mm standard petri dishes (Sterilin). The LB-agar plates were then left at room temperature to finish cooling and to solidify. Plates were stored at 4°C and used within four weeks.

2.3.3 Plasmid transformation into competent bacteria

Plasmids were transformed into chemically competent DH5α *Escherichia coli* (Invitrogen) according to the manufacturer's instructions. Briefly, less than 100ng of DNA was added to 50µl of bacteria on ice. This mixture was incubated on ice for 30 minutes, before heat shock at 42°C for 20 seconds, and a further 2 minutes on ice. 950µl LB was added to the tube and the mixture incubated at 37°C for 1 hour with shaking at 225rpm. 200µl of this solution were then plated onto a pre-warmed selective LB plates at 37°C overnight.

2.3.4 Isolation of plasmid DNA

To purify plasmid DNA, 5ml LB, supplemented with antibiotics was inoculated by picking one colony from transformation plates, and incubating overnight at 37°C, shaking at 225rpm. DNA was then purified using QIAprep Spin Miniprep Kit (Qiagen) in accordance with manufacturer's guidelines. DNA concentration was quantified by spectrometry (NanoDrop ND-1000 Spectrophotometer), followed by storage at -20°C.

2.3.5 PCR methods

2.3.5.1 Quantitative real-time PCR

The Roche LightCycler® 480 Real-Time PCR System was used to carry out quantitative real time PCR (qPCR). This system uses Taq DNA polymerase to amplify small DNA amplicons coupled with fluorescent molecules, which are used

to measure the number of DNA molecules present following each amplification cycle. I used the Roche Universal ProbeLibrary (UPL) system, which uses short probes coupled to a fluorophore at the 5′ end and a quencher at the 3′ end. During amplification, the fluorophore and quencher are separated, allowing detection of fluorescence by the instrument.

Primers for qPCR were designed using the online Roche UPL Assay Design Centre, which combines primer pairs with a suitable UPL probe for the gene of interest. The predicted specificity of the primers was then verified using Ensembl and Taq PCR with gel electrophoresis used to confirm that a single amplicons was produced. Amplicons were cloned into a pGem®T-Easy backbone (Promega) for use as serial dilutions.

10µl reaction volumes were used in 384 well plates

The reaction components used for qPCR were as follows:

Reagent	**Volume**	**Final Concentration**
LightCycler® 480 Probes Master	5µl	1X
Water	1.5µl	-
Forward primer (10µM)	0.45µl	450nM
Reverse primer (10µM)	0.45µl	450nM
Universal ProbeLibrary Probe	0.1µl	100nM
Template cDNA	2.5µl	-

Table 2.4| qPCR reaction composition.

Cycling conditions used for UPL qPCR were as follows:

Step	Temperature	Duration (min:sec)	No. of cycles
Denaturation	95°C	05:00	
Denaturation	95°C	00:05	45x
Annealing	60°C	00:10	
Extension	72°C	00:01	
Cooling	40°C	00:10	

Table 2.5| qPCR cycling parameters.

Lightcycler® 480 software was used to calculate the number of molecules of the amplicon of interest in each reaction. This was calculated using a serial dilution of pGem®-T Easy/amplicon plasmids as a reference within the same qPCR plate (6 10-fold dilutions at an initial copy number of 10^8/reaction). Each cDNA sample was loaded in triplicate. Normalised expression for a gene of interest in each biological sample was calculated by dividing the average expression value in the triplicate wells by the average expression value of the housekeeping gene *Tbp* (Turabelidze et al. 2010). To calculate biological average expression value for a gene of interest in biological replicate samples, the gene expression values in each sample were averaged across biological replicates. The table below details the primers and UPL probe combinations used for qPCR.

Primer	Sequence	UPL probe
Cdx2 F	caccatcaggaggaaaagtga	34
Cdx2 R	ctgcggttctgaaaccaaat	
Evx1 F	cagggagaactacgtttcaagac	66
Evx1 R	gccggttctgaaaccaca	
Flk1 F	ccccaaattccattatgacaa	18
Flk1 R	cggctctttcgcttactgtt	
Foxa2 F	aagtagccaccacacttcagg	32
Foxa2 R	tggcccatctatttagggac	
Hand1 F	caagcggaaaagggagttg	51
Hand1 R	gtgcgccctttaatcctctt	
Id1 F	tcctgcagcatgtaatcgac	78
Id1 R	ggtcccgacttcagactcc	
Id2 F	gacagaaccaggcgtcca	89
Id2 R	agctcagaagggaattcagatg	
Id3 F	catagactacatcctcgaccttca	53
Id3 R	cacaagttccggagtgagc	
Id4 F	agggtgacagcattctctgc	92
Id4 R	ccggtggcttgtttctctta	
Meox1 F	agacggagaagaaatcatccag	2
Meox1 R	ctgctgccttctggcttc	
Mesp1 F	acccatcgttcctgtacgc	89
Mesp1 R	gcatgtcgctgctgaagag	
Msgn1 F	aattacctgccgcctgtct	106
Msgn1 R	tgagtgtctggatcttggtga	
Oct4 F	gttggagaaggtggaaccaa	95
Oct4 R	ctccttctgcagggctttc	
Sox1 F	gtgacatctgcccccatc	60
Sox1 R	gaggccagtctggtgtcag	
Sox17 F	cacaacgcagagctaagcaa	97
Sox17 R	cgcttctctgccaaggtc	
Sox2 F	gtgtttgcaaaaagggaaaagt	43
Sox2 R	tctttctcccagccctagtct	
T(bra) F	actggtctagcctcggagtg	27
T(bra) R	ttgctcacagaccagagactg	
TBP F	ggggagctgtgatgtgaagt	97
TBP R	ccaggaaataattctggctca	
Tcf15 F	gtgtaaggaccggaggacaa	104
Tcf15 R	gatggctagatgggtccttg	
Wnt3a F	aatggtctctcgggagtttg	53
Wnt3a R	cttgaggtgcatgtgactgg	

Table 2.6| qPCR primers and probes.

2.3.6 RNA methods

2.3.6.1 RNA isolation

The isolation of whole RNA from cell samples was performed using the Agilent Absolutely RNA Miniprep Kit, according to the manufacture's protocol. Briefly, cells were either lysed directly on tissue culture plastics, or pelleted, resuspended and added to lysis buffer containing β-ME (7µl per 1ml of lysis buffer). Cell lysates were then stored at -20°C until RNA isolation. All steps were performed using filter tips and RNase free solutions. Pipettes, work surface and gloves were repeatedly cleaned with a cleaning agent for the removal of RNases (RNase Zap, Ambion), to minimise risk of contamination and degradation of samples with RNases. Samples were eluted in 50µl of elution buffer, into RNase free eppendorfs. The concentration and purity of the RNA samples was then determined through spectrometry (NanoDrop ND-1000 Spectrophotometer), and samples stored at -80°C.

2.3.6.2 cDNA synthesis

First strand cDNA was generated using M-MLV reverse transcriptase (Invitrogen) in accordance to manufacturers' guidelines. 500ng or 1µg RNA diluted in 10µl RNase free water was mixed with 50ng of random primers (Invitrogen) and 1µl 10mM dNTPs (Invitrogen). This mixture was heated to 65°C for 5 minutes, then cooled to 4°C before adding 4µl 5X First-strand buffer, 2µl 0.1M DTT and 1µl RNaseOUT™ Recombinant Ribonuclease Inhibitor (40U/µl) (Invitrogen). This

solution was mixed well and heated to 37°C for 2 minutes. 1µl M-MLV RT (200U) was then gently added to the solution, which was then subject to the following incubations: 25°C for 10 minutes, 37°C for 50 minutes, then heat inactivated at 70°C for 15 minutes. 1µl RNase H (5U) (New England Biolabs) was added to the solution to digest the RNA template and the samples incubated at 37°C for 20 minutes. The resulting cDNA was diluted 1 in 6 with RNase free water and stored at -20°C.

2.3.6.3 Generation of in situ hybridisation riboprobes

Dioxigenin labelled riboprobes were used for all in situ hybridisation experiments. Plasmids for Id2, Id3 and Id4 probes were obtained from Addgene, having been described and used in (Jen et al. 1997). The probe sequence for the Id1 probe was generated by PCR and ligation into pGEMT-easy, followed by sequencing (Gene Pool) to confirm that the sequence was correct and to determine sequence orientation in the plasmid. The primers used to amplify the probe sequence were described in (Gray et al. 2004).

Linearisation of plasmids was performed using the components detailed in Table 2.7, with restriction enzymes selected depending on the orientation of each probe sequence and appropriate to generate antisense riboprobes or control sense probes. Linearisation reactions were prepared in RNase free tubes and incubated overnight at 37°C.

Plasmid	Source	Riboprobe	Restriction enzyme	Restriction buffer	RNase pol
pGEM-T easy-Id1p	In house	Id1 antisense	NcoI	NEBuffer 3	Sp6
pGEM-T easy-Id1p	In house	Id1 sense control	PstI	NEBuffer 3 +BSA	T7
pBS/KS-Id2sp	Addgene	Id2 antisense	EcoRI	NEBuffer EcoRI	T7
pBS/KS-Id2sp	Addgene	Id2 sense control	BamHI	NEBuffer 3 +BSA	T3
pBS/KS-Id3sp	Addgene	Id3 antisense	SacI	NEBuffer 1 +BSA	T3
pBS/KS-Id3sp	Addgene	Id3 sense control	EcoRI	NEBuffer EcoRI	T7
pBS/KS-Id4sp	Addgene	Id4 antisense	XbaI	NEBuffer 4 +BSA	T3
pBS/KS-Id4sp	Addgene	Id4 sense control	EcoRI	NEBuffer EcoRI	T7

Table 2.7| Plasmids and enzymes used to generate in situ hybridisation probes.

The next day linearised plasmids were scaled to 500µl with RNase free water to perform purification. These 500µl solutions were mixed with 500µl Phenol:Chloroform:IAA (250:240:10µl) (Sigma Aldrich) and centrifuged for 10 minutes at room temperature (Heraeus Biofuge 13). The separated top layer was then removed and transferred to another RNase free tube and combined with 400µl phenol solution (ratio as above), and spun for another 10 minutes. This process was repeated once more, adding 300µl of phenol solution. After this final phenol step, the separated top layer was transferred to a new tube and precipitated with sodium acetate (Sigma) and ethanol with incubation at -20°C for at least 20 minutes. Plasmid DNA was then pelleted by centrifugation at 13,000 rpm for 15 minutes (Heraeus Biofuge 13) and the pellet washed with 70% ethanol in RNase free water. The pellet

was then air dried and resuspended in 10µl RNase free water (Thermo Scientific) and concentration determined by spectrometry.

To synthesise the digoxigenin labelled probe, 1µg of purified and linearised plasmid was combined with 1µl of appropriate RNA polymerase (see table X), 2µl transcription buffer (Roche), 2µl digoxigenin (DIG) labelled nucleotide mix (DIG-UTP) (Roche), 1.5µl RNase inhibitor (150U) (Roche) and scaled to 19µl. This reaction was incubated at 37°C for 1 hour, when another 1µl of RNA polymerase was added and the samples incubated for another hour.

DNase treatment was performed to digest the plasmid DNA template by adding 1µl DNase I (Promega) and 2µl 10x buffer (Promega) to the above solution, which was then incubated at 37°C for 30 minutes. The reaction was halted at the addition of 1µl STOP solution (Promega) and heat inactivation performed at 65°C for 10 minutes.

Ethanol precipitation was used to purify labelled riboprobes. Firstly, the probes were diluted to 50µl using RNase free water (Thermo Scientific), and mixed with 5µl RNase free sodium acetate (3M) (Sigma) and 2.5 volumes 100% ethanol. This solution was incubated at -20°C overnight. Next morning the riboprobes were pelleted by spinning at 13,000rpm for 10 minutes at 4°C, the resulting pellet washed twice in 70% ethanol (RNase free) and air dried. The pellet was then resuspended, RNA concentration determined by spectrometry, and aliquoted for storage at -80°C.

2.3.7 Antibody staining

2.3.7.1 Fixation of samples

Media was aspirated from adherent cell cultures and the cells washed gently in PBS. Cells were then fixed in 4% PFA (Fisher) in PBS (Sigma-Aldrich) for 20 minutes at room temperature. Fixed cells were washed twice in PBS then stored in PBS at 4°C until use for immunofluorescence.

2.3.7.2 Antibody staining of adherent cells

To prepare cells for antibody staining, culture media was removed by aspiration and the cells fixed in 4% PFA (Fisher) in PBS (Sigma) at room temperature for 20 minutes. Cells were then washed twice with PBS to remove the fixative. Cells were then either stained immediately or stored at 4°C for no more than 3 days before staining. Blocking and permeabilisation were performed by incubating samples in 3% donkey serum (Sigma) + 0.1% Triton™ X-100 in PBS for 30 minutes at room temperature. Incubation with primary antibodies was performed at room temperature over three hours in blocking solution, with optimised dilution for each antibody. At the end of the three hours, primary antibody containing solution was removed and cells were subject to three five minute washes in PBS at room temperature. Appropriate secondary antibodies were then added to the samples (1:1000) in blocking solution. Incubation with secondary antibodies was performed in the dark at room temperature for one hour. 100ng/ml Dapi (Biotium) was then

added to the samples for five minutes, followed by three five minute PBS washes at room temperature. Stained samples were stored in the dark at 4°C until imaged.

Primary antibodies used:

Target	Supplier	Species raised in	Catalogue number
Flag	Sigma	Mouse	F9291
Id1	Biocheck Inc	Rabbit	37-2
Meox1	Santa Cruz	Goat	sc10185
Oct4	Santa Cruz	Mouse	sc5279
Sox2	Abcam	Rabbit	ab97959
T(bra)	R&D systems	Goat	AF2085

Table 2.8| Primary antibodies.

Chapter 3 *Id* gene expression in the post implantation mouse embryo

Introduction

Aberrant BMP signalling has detrimental effects on embryonic development, with particularly striking effects on mesoderm specification. As BMP signalling is commonly mediated through Id signalling, and compound knock out of the *Id* genes results in cardiac defects it is of interest to examine the role of Id proteins in mesoderm specification. At the time of study, limited accurate spatial data were available on the expression of the *Id* genes during early post-implantation development (see 1.3.4.1). In situ hybridisation was utilised to examine in detail the expression of the four mammalian *Id* genes from E7.5, when the PS is formed through to early organogenesis. See Appendix 1 for schematic summary of developmental stages.

Id transcript expression in the pre-somitic mouse embryo

The formation of the PS begins around E6.5 within the proximal posterior region of the embryo leading to germ layer establishment. As development progresses through to E7.5 the neural plate begins to be defined in the anterior of the embryo; denoted head fold stage. As embryos progress into the late head fold stage and closer to the onset of somitogenesis, the earliest stages of heart development are seen, with the emergence of cardiac mesoderm. Around E7.0 is also the stage of development when the allantoic rudiment first appears, found in early bud stage embryos and this is accompanied by the formation of the amnion. To examine the

expression of the four *Id* genes prior to somitogenesis but after the onset of PS formation, embryos were selected at bud, and early and late head fold stages.

3.1.1 *Id* transcripts are expressed in proximal and extraembryonic tissue at E7.5

Examination of *Id* transcripts in bud stage mouse embryos shows expression of the transcripts in extraembryonic and proximal embryonic tissues, with the distal epiblast remaining negative for all four genes (Figure 3.1). *Id1* transcripts can be detected in extraembryonic ectoderm, the chorion and in the emerging allantoic rudiment (Figure 3.1 A, E, I, M). In the embryo proper, signal is detected in the anterior and lateral ectoderm of the proximal epiblast and the PS, in addition to weaker hybridisation seen in the anterior mesoderm (Figure 3.1 A, Q). At this developmental stage, strong extraembryonic hybridisation signal for *Id2* transcript is seen in the chorion though not detected in the allantoic bud (Figure 3.1 B, F, G, N). Compared to the strong *Id2* transcript expression seen in the chorion, weaker signal can be seen in the proximal region of the embryo, which sectioning reveals to be in the ectoderm and mesoderm (Figure 3.1 R). In bud stage embryos *Id3* transcript is detected in extraembryonic mesoderm where the allantoic bud begins to form (Figure 3.1 O), extraembryonic endoderm, amniotic fold and chorion (Figure 3.1. C, G, K). Some expression of *Id3* can also be detected in the ectoderm of the proximal most embryonic epiblast (Figure 3.1 S). Similarly to *Id2*, expression of *Id4* transcript

Figure 3.1| *In vivo* expression of Id transcripts at E7.5. In situ hybridisation was performed on whole mount E7.5 embryos at the bud stage using probes for *Id1* (**A**), *Id2* (**B**), *Id3* (**C**) and *Id4* (**D**) followed by transverse sectioning. Approximate locations of sections are indicated on each whole mount image. Images shown are of a representative embryo analysed for transcript expression of each gene of interest. *Id1* n = 5, *Id2* n = 4, *Id3* n = 4, *Id4* n = 5.

is clearly detected in the chorion (Figure 3.1 D, H, L, P), and there may also be some weak signal detected in the allantoic rudiment (Figure 3.1 P). The proximal anterior ectoderm also appears to show some hybridisation signal for *Id4*.

In E7.5 head fold stage embryos the distal regions of the embryos remain negative for expression of all four *Id* genes (Figure 3.2). *Id1* expression continues to be detected in the elongating allantois, and can also be seen in the chorion (Figure 3.2 A, E, I). In the proximal part of the embryo, *Id1* transcript is detected in mesoderm lateral to the PS in the posterior of the embryo, as well as in neurectoderm and the future cephalic mesenchyme of the developing head fold (Figure 3.2 A, M, Q). In the head fold stage embryo strong *Id2* signal continues to be detected in the chorion (Figure 3.2 B, F, J) and the allantois remains devoid of hybridisation signal (Figure 3.2 B and N). In the developing head fold, weak *Id2* signal can be detected, though it should be noted that this required prolonged exposure and is not clear in sections (Figure 3.2 B and R). As the head fold emerges, *Id3* transcript expression can be detected in the anterior of the embryo in neuroepithelium and cephalic mesenchyme (Figure 3.2 C, O, S). In the posterior of the embryo, *Id3* expression is seen in the ectoderm lateral to the PS region, and faint expression can be seen at the base of the allantois (Figure 3.2 C, G, K, O). At this stage of development *Id4* transcript expression is detected in the base of the allantois, the proximal posterior epiblast and mesoderm and emerging head fold (Figure 3.2 D, H, L, P, T). The expression described here for *Id1* and *Id2* is consistent with the whole mount images published whilst this project was ongoing (Li et al. 2013).

Figure 3.2| Expression of Id transcripts at early head fold stage. Whole mount in situ hybridisation was performed using E7.5 embryos at late bud and head fold stage embryos with probes to detect expression of *Id1* (**A**), *Id2* (**B**), *Id3* (**C**) and *Id4* (**D**) followed by transverse sectioning. Approximate locations of sections are indicated on each whole mount image. A representative embryo is shown displaying the transcript expression pattern detected for each gene of interest. *Id1* n = 5, *Id2* n = 5, *Id3* n =6, *Id4* n =3.

3.1.2 *Id* transcripts are expressed in lateral epiblast and the cardiac crescent

Examination of *Id* gene expression in late head fold stage embryos, when cardiac mesoderm begins to differentiate shows an overlapping expression pattern between the four genes (Figure 3.3). At the anterior of the embryo, *Id* transcripts can be detected in the cardiac crescent mesoderm, the underlying foregut primordium endoderm, and in lateral mesoderm found at the base of the crescent (Figure 3.3 A-D, I-P). In the posterior region of the embryo, signals are detected for Id1 and Id3 in the lateral ectoderm and mesoderm layers. This expression pattern does not appear to be shared by Id2 and Id4 transcripts (Figure 3.3 E-H, Q-T). Signals are detected for all for genes at the base of the allantois, with Id2 also detected within the chorion (Figure 3.3 E-H, M-P).

3.1.3 *Id1* transcript expression can be found surrounding the embryonic node

Extended exposure times to detect low level transcript localisation of *Id1* transcript expression in late head fold stage embryos reveals a broader expression of *Id1* (Figure 3.4). Figure 3.4 shows two such embryos. In addition to the tissues shown in Figure 3.3, additional hybridisation signal can be detected in a ring surrounding the embryonic node. This detection is reproducible when prolonged exposure is utilised, and is mirrored by findings seen in chimeric embryos containing high contribution of Id1-Venus reporter ES cells (Dr Mattias Malaguti). Based on the limited embryonic stage at which this distal expression has been detectable, it appears to be a somewhat transient expression.

Figure 3.3| Expression of Id transcripts at E8.0. Whole mount in situ hybridisation was performed on E8.0 embryos using probes for *Id1* (**A**), *Id2* (**B**), *Id3* (**C**) and *Id4* (**D**). Transverse sections were then obtained from the whole mount embryos shown. Approximate locations of sections are indicated on the whole mount images. Representative embryos are shown, displaying the transcript expression pattern detected for each gene of interest. *Id1* n = 6, *Id2* n = 4, *Id3* n = 6, *Id4* n = 4.

Figure 3.4| *Id1* transcript expression surrounding the embryonic node. In situ hybridisation was performed using E8.0 embryos with increased exposure time to alkaline phosphatase substrate during the process to enable the visualisation of low level *Id1* hybridisation signal. This reveals a ring of transcript expression detected around the node in addition to the more intense signal detected in the cardiac crescent, developing head, caudal lateral epiblast and base of the allantois. Two representative embryos at slightly different stages of development are shown, n = 4.

Id gene expression during early somitogenesis

Segmentation of presomitic mesoderm into somites begins in the mouse embryo around E8.0 to E8.5. Coinciding with somitogenesis, the head folds become increasingly prominent and neural folds begin to close in the cervical region. Patterning of the heart continues with atrial and ventricular regions that begin to beat and the foregut pocket is noticeable. During this stage of development further growth of the allantois is also seen.

3.1.4 *Id* genes have overlapping expression patterns in the E8.5 mouse embryo

To examine *Id* transcript expression during early somitogenesis, E8.5 mouse embryos of 2-5 somites were used. In embryos of this stage, *Id4* hybridisation signal was not observed above background levels despite prolonged exposure time. This may indicate a lack of *Id4* expression as suggested in previous work (Jen et al. 1997), or that in situ hybridisation is not a sensitive enough technique to detect potential low transcript expression.

Within the E8.5 embryo, *Id1* transcript expression can be detected in surface ectoderm (Figure 3.5 G) as well as clearly within the developing neural tube (Figure 3.5 D, J, M). *Id1* transcript can also be seen in the developing heart mesoderm (Figure 3.5 A, G) and in the lateral mesoderm and the endoderm (Figure 3.5 G). Anteriorly, *Id1* signal is detectable in lateral regions of the head fold (Figure 3.5 A, M). Within the posterior region of early somitogenesis stage embryos, *Id1* transcript

is detectable in the CLE, and is highest the posterior most region of the embryo; corresponding to lateral/streak 5 (Figure 3.5 D, G, J, M). Clear *Id1* transcript expression is also present from the allantoic base, extending through part of the allantois (Figure 3.5 A, M).

At this stage of development *Id2* hybridisation signal is detectable within neurectodermal tissue (Figure 3.5 E, H), though somewhat less widespread than that of *Id1* and *Id3*. In both the developing head and the trunk region of the embryo, strong lateral expression is detected (Figure 3.5 N). There may be weak signal detectable laterally in the embryo, especially the more posterior region of the embryo (Figure 3.5 N). In contrast to *Id1*, expression of *Id2* is not detected within the allantois (Figure 3.5 B, N).

Figure 3.5| Id transcript expression during early somitogenesis. Whole mount in situ hybridisation using probes for *Id1*, *Id2* and *Id3* was performed on E8.5, 2-5 somite embryos, followed by sectioning. Approximate locations of sections are indicated on whole mount images (**A-C**). Dorsal views of independent embryos are also displayed (**M-O**). cm; cephalic mesenchyme, g; gut, h; developing heart, lm; lateral mesoderm, nf; neural folds, nt; neural tube, se; surface ectoderm. *Id1* n = 7, *Id2* n = 6, *Id3* n = 7. Red dashed line indicated approximate length of the PS of 500μm.

The expression pattern detected for *Id3* at this stage of development closely resembles that of *Id1*, though with some subtle differences. *Id3* transcript is also detectable within surface ectoderm (Figure 3.5 I), and widely in developing neurectoderm (Figure 3.5 C, F, I, O). This expression is particularly clear along lateral edges of the neural folds (Figure 3.5 I), with this neurectodermal signal present in the head as well as along the trunk. *Id3* transcript is also detectable within cephalic mesenchyme along with the developing heart region and trunk mesenchyme (Figure 3.5 C, I, O). In line with the anterior lateral expression seen with *Id1* and *Id2*, *Id3* signal is clear along the headfolds and anterior of the embryo (Figure 3.5 C, O). No signal is detected within the somites (Figure 3.5 L). There appears to be some expression along the CLE and signal is present at the base of the allantois (Figure 3.5 C).

Id gene expression during early organogenesis

As the development continues into early organogenesis the mouse embryo turns, completing this process by E9.5. A single tube at this stage, the heart loops to bring the tissue for the chambers into the correct orientation and in late E9.5 embryos contractions can be seen. The fore- and hindgut become a continuous tube rather than being separated by pockets and otic and optic vesicles begin to form. The limb buds begin to form, followed by condensation with the anterior buds beginning to form prior to emergence of the posterior limb buds. AP axial elongation continues with somites continuing to be laid down. Analysis of NMPs has shown the absolute

number of these progenitors to peak at E9.5 before beginning to decline thereafter (Wymeersch et al. 2016).

3.1.5 Expression of the *Id* genes is similar but distinct at E9.5

Id1 transcript signal can still be detected within the developing head by E9.5 (Figure 3.6 A). Signal is detected weakly within the surface ectoderm and more clearly within the neural folds of the prospective hind brain. Expression of *Id1* is seen also within the neural folds and dorsal neural tube along the trunk of the embryo (Figure 3.6 E, I, M). Very strong signal is detected at the whole mount level within the first branchial pouch (Figure 3.6 A) with sectioning showing this expression to be present throughout the neural crest cells found within this structure (Figure 3.6 E). As indicated within the whole mount embryo, *Id1* transcript is excluded from the tissue of the otic pit though is expressed within the adjacent mesenchyme (Figure 3.6 A, I). *Id1* signal is expressed within the endodermal lining of the foregut, present along the AP axis (Figure 3.6 I, M). Expression of *Id1* was not detected within the somites, though can be seen within the lateral plate mesoderm (Figure 3.6 M) and in ventral TBM (Figure 3.6 Q). There is some expression of *Id1* observed within the atrial component of the developing heart, but this signal is very weak (Figure 3.6 E, M). Sections including more posterior regions of the embryo also reveal that the expression seen in the endodermal lining of the hindgut (Figure 3.6 Q).

Figure 3.6| Expression of Id transcripts during early organogenesis. Whole mount in situ hybridisation was performed on E9.5 embryos with between 15 and 20 somites using probes *for Id1, Id2, Id3* and *Id4*. Embryos were subsequently sectioned, though sections are not perfectly transverse due to curvature of the embryo. Approximate locations of sections are indicated on the whole mount images. bp. Branchial pouch, cm; cephalic mesenchyme, fg; foregut, h; heart, lm; lateral mesoderm, nt; neural tube, op; optic vesicle, ot; otic vesicle, s; somite. *Id1* n = 4, *Id2* n = 4, *Id3* n = 5, *Id4* n = 3.

Id2 transcript expression is observable within cephalic mesenchyme (Figure 3.6 B, F), neurectoderm and the emerging optic vesicle (Figure 3.6 B). It is possible that there is some signal detectable within the anterior most region of the notochord, but this is not clear (Figure 3.6 E). As seen with *Id1* (Figure 3.6 A), strong *Id2* signal is observed within the first branchial pouch (Figure 3.6 B), with sectioning revealing this expression to be widespread within the structure (Figure 3.6 E). In the developing neural tube, *Id2* signal is also detectable but within the more ventral region of the neurectoderm (Figure 3.6 E, J, N). Endodermal expression can be seen within the foregut and midgut (Figure 3.6 J, N, R) and there may also be weak expression within the thyroid primordium, found just ventral to the foregut (Figure 3.6 N). Although not clear from the sectioning of this sample, *Id2* transcript signal was found within the atrial chamber of the developing heart, though from the whole mount image it is clear to see that at this stage *Id2* is certainly not widespread throughout the heart (Figure 3.6 B). The whole mount sample suggests tailbud expression of *Id2* (Figure 3.6 B) similar to that of *Id1* (Figure 3.6 A). Sectioning however shows this to be less clear. Though there is gut endoderm expression within the tail, there does also appear to be some probe trapping within the posterior neural tube (Figure 3.6 R).

Broad similarities can be seen between in situ hybridisation performed probing for *Id3* expression (Figure 3.6 C) as with *Id1* (Figure 3.6 A) at the whole mount level. Within the head region, *Id3* transcript can be seen within the neurectoderm of the developing brain, laterally within cephalic mesenchyme, and within the developing

optic vesicle (Figure 3.6 G, K). As with the other Id factors, very clear *Id3* transcript signal is detected within the first branchial pouch (Figure 3.6 C) with sectioning confirming that this signal is present throughout the structure (Figure 3.6 K). Some *Id3* signal is observable within the surface ectoderm of the trunk region, adjacent to lateral mesenchymal expression, as well as expression found in the foregut endoderm (Figure 3.6 K). Although there appears to be some weak signal detectable in sub-regions of the developing heart (Figure 3.6 K), including the sinus venosus (Figure 3.6 O), this is difficult to discern and not widespread throughout the organ. The neurectodermal expression of *Id3* continues to be present through the trunk of the embryo, with localisation to the dorsal region of the neural tube (Figure 3.6 K, O, S). As with *Id1* and *Id2*, *Id3* transcript can be seen within the tailbud mesenchyme (Figure 3.6 C, O). Mesodermal expression can also be seen in lateral mesoderm parallel to the neural tube, and interestingly also laterally in some segmented somites (Figure 3.6 O).

Within the anterior region of the E9.5 mouse embryo, the expression pattern of *Id4* (Figure 3.6 D) resembles that of the other three *Id* genes (Figure 3.6 A-C). Expression is detected within the developing head in both neurectoderm and cephalic mesenchyme, and again strong signal is present within the first branchial pouch (Figure 3.6 D, H). The otic placodes appear to be negative for *Id4* signal once sectioned (Figure 3.6 H). Examination of the trunk reveals continued neurectodermal expression, though in contrast to *Id1* and *Id3* ISH reveals *Id4* expression to be restricted to the ventral neural tube (Figure 3.6 L, P). There is some

weak signal present in the foregut and midgut, and more clear expression of *Id4* detected within the sinus venosus of the developing heart (Figure 3.6 L, P, T). Unlike the other three Id factors, *Id4* signal is not observable within the tail at this stage of development (Figure 3.6 D).

Microarray analysis of post implantation *Id* transcript expression

Id transcript expression has also been examined via microarray analysis performed on microdissected embryonic regions. Pooling of embryonic tissue from multiple stage matched embryos was performed to obtain suitable sample volumes, and microarray performed on MouseWG-6 v2.0 Expression BeadChip arrays (Illumina) (Data generated by members of the Wilson and Tomlinson groups, not the author of this thesis). Comparisons were made between embryonic regions which are fated to become or that contain NMPs and LPMPs, and regions which appear to exclude such fates or populations (Figure 3.7 A, B).

At E7.5 Id transcripts are detected in tissue taken from the proximal regions (7A and 7PP) of the embryo with greater hybridisation signal detected from material sourced from the posterior region (7PP) (Figure 3.7 C). At E8.5 strong hybridisation signal is detected for transcripts of all four Id genes using tissue from the posterior most region of the PS (8ST5) (Figure 3.7 D). This is in contrast to the anterior of the PS (8ST1) and the embryonic node (8N) (Figure 3.7 D). The microarray analysis indicates higher expression of each transcript in the CLE (8L) than in the node or anterior PS (Figure 3.7 D).

Figure 3.7| Microarray analysis of embryonic subregions. Microdissection was performed on E7.5 and E8.5 embryos, with microdissected tissue from multiple embryos pooled to provide material for microarray analysis. Regions dissected from E7.5 and E8.5 embryos are indicated on the diagrams (**A** and **B**, respectively). Relative normalised expression displayed for probe data examining *Id1*, *Id2*, *Id3* and *Id4* expression within the E7.5 (**C**) and E8.5 (**D**) mouse embryo. 7A ; E7.5 anterior epiblast, 7P; E7.5 posterior epiblast, 7PP; E7.5 proximal posterior epiblast, 8N; E8.5 node, 8B; E8.5 border, 8L; E8.5 CLE, 8ST1; E8.5 anterior PS, 8ST5; E8.5 posterior PS.

Discussion

3.1.6 *Id* transcript expression

The study conducted here pairs whole mount in situ hybridisation with sectioning of the same samples to provide stage matched, detailed comparisons of transcript expression of the four *Id* genes. This clarifies existing spatial data and expands and adds detail to the expression of the Id factors during early post implantation mouse development. Select data generated in the course this study of Id expression has since been published (Malaguti et al. 2013; Row and Pegg et al. 2018).

The examination of presomitic stage embryos here largely supports that of data from other groups published prior to and during this study (Jen et al. 1997; Li et al. 2013). As discussed briefly in the Introduction (1.3.4.1), previously generated data using radioactive labelling can be difficult to interpret clearly. Authors of previous work concluded that at E7.5, *Id3* was expressed throughout the embryo and that no *Id4* signal was detectable (Jen et al. 1997) though I do not agree with this interpretation (for reference a copy of this data is included within Appendix 2). Instead the images presented appear to match with the data presented here where expression can be detected within the proximal region of the embryo proper and also in extraembryonic tissues.

Within E8.0 embryos expression of the four *Id* genes initially appear to have extensively overlapping expression patterns. The cardiac crescent and posterior lateral epiblast expression confirms previous reports for *Id1* and clarifies this

expression pattern for *Id2* (Li et al. 2013). This expression of *Id3* and *Id4* had not been previously reported. Additionally, the identification of *Id1* expression surrounding the node at this stage is a novel and somewhat unexpected expression pattern given that this is an area of high nodal activity (Zhou et al. 1993). Work within the Lowell laboratory supports this finding through the use of Id1-Venus transgenic mouse embryos, which also show expression of Id1 around the node (Dr M. Malaguti). The only BMP factor that has reported expression in this region at this stage of mouse development is Bmp7 (Arkell & Beddington 1997; Solloway et al. 1998). This raises the possibilities that this *Id1* expression could be BMP7 mediated or possibly BMP independent.

The expression detected here following the onset of somitogenesis highlights a highly concordant pattern of expression between *Id1* and *Id3*, with similar *Id2* expression and a slightly more disparate pattern seen with *Id4*. The data described here for E8.5 stage embryos supports findings reported in previously published papers (Wang et al. 1992; Jen et al. 1997). However, the data described here still provides novel observations as these studies provided short notes on some aspects of *Id* expression at this stage of development and the authors unfortunately did not display these data.

One particularly striking difference in the expression of the *Id* factors is the differential regional expression within the neural tube at E9.5 (Figure 3.6). Such dorsal-ventral distinction is not seen at E8.5 (Figure 3.5). Again, although this observation has been commented on (Jen et al. 1997), data was not presented within

that study. In E9.5 mouse embryos the expression of *Id1* and *Id3* are particularly similar to one another, whereas ventral tail bud expression highlights different patterns for *Id2* and *Id4*.

The pairing of whole mount and sectioned images provides clear spatial data of the transcript expression of the *Id* genes. Presentation of both types of data together allows accurate determination of embryonic stage and detailed investigation of tissue specific expression throughout the whole embryo, and comparison of the four genes in parallel.

3.1.7 Id expression and mesoderm specification

The in situ hybridisation data described here is also supported by microarray analysis performed on microdissected embryonic regions. The data obtained here, shows that in E7.5 mouse embryos *Id* transcripts are excluded from the distal region of the embryo instead being detected in the proximal embryo, with slightly more intense expression detected within the posterior region (Figure 3.1, Figure 3.2, Figure 3.7 C). As the PS develops further and the embryo begins elongation, *Id* transcripts can be detected in the posterior of the PS (annotated 8ST5 or St/L5) within the region that contains LPMPs with a lack of expression detected within the node and anterior PS (annotated 8ST1 or St1); the regions which contain NMPs (Figure 3.5, Figure 3.7 D). Although largely excluded from NMP containing regions, some *Id3* expression can be detected at the lateral edges of NMP containing tissue

regions (Figure 3.3 S). Additionally the microarray data and in situ hybridisation data also both show *Id* transcript expression within the CLE.

The expression patterns observed for *Id* transcripts coupled with the locations of, and behaviour of progenitor populations within the PS make the family attractive candidates for regulators of mesoderm patterns, and raise the hypothesis that Ids specify LPMPs and the lateral region of the CLE.

Chapter 4 – An *in vitro* system for examining mesoderm differentiation of neuromesodermal progenitors

4.1 Introduction

Previous fate map data generated from homotopic and heterotopic grafting provides a broad spatial framework for the investigation of sub-regions of continuous tissue. In the E8.5 embryo this can be achieved by artificial division of the PS and adjacent epiblast into transverse strips of tissue, annotated streak (St) and lateral (L)1-5, moving from the anterior to the posterior of the PS (Figure 1.1). As discussed in detail in the introduction (1.1.2.1), the PS contains distinct populations of progenitors. NMPs are found within the anterior of the PS, at the NSB and also in the adjacent CLE, which contribute to paraxial mesoderm and the neural tube throughout axis elongation (Tzouanacou et al. 2009). In the posterior most portion of the PS (St/L5) are found LPMPs, which contribute to lateral and ventral mesoderm (Wymeersch et al. 2016). Although these populations are spatially distinct, heterotopic grafting has shown that LPMPs can contribute appropriately to mesoderm but not neurectoderm when grafted into regions fated to generate paraxial mesoderm and neurectoderm (Wymeersch et al. 2016). This work demonstrates that LPMPs are restricted to mesoderm fates, and thus distinct from NMPs, which can form neurectoderm. Although not fated for paraxial mesoderm, the plasticity observed in heterotopic grafting demonstrates the LPMPs are potent to differentiate into paraxial mesoderm. These findings leads to the interesting

question of whether NMPs display similar plasticity and could contribute appropriately when grafted into LPMP containing regions.

To examine further what signalling pathways are important in establishing and regulating NMPs I chose to develop an *in vitro* system to model differentiation of these progenitors. There are many mesoderm differentiation protocols available using mES cells as starting material (Takenaga et al. 2007; Sakurai et al. 2008; Pucéat 2008; Torres et al. 2012; Nishikawa et al. 2012). However, to generate LPMPs *in vitro*, it would be an advantage to choose a starting cell population close to the developmental point of interest. As I am examining differentiation events that occur after implantation, and EpiSCs represent an *in vitro* equivalent of the post-implantation epiblast (Huang et al. 2012), they are a far more suitable starting population than mES cells. Dr Anestis Tsakiridis has established an *in vitro* differentiation protocol to generate NMPs from EpiSCs, with grafting showing that these cells behave appropriately when introduced into mouse embryos (Gouti et al. 2014). As such, I have used EpiSCs as a starting point to establish an *in vitro* system that examines the effect of BMP and Ids on the mesoderm differentiation of PS populations.

4.2 Neuromesodermal progenitors can contribute to LPMP regions

In the E8.5 mouse embryo NMPs are found within the NSB and the CLE in regions L1-2, and LPMPs at the posterior of the CLE (St/L5) ((Wymeersch et al. 2016), Figure

4.1 A). Microdissection of L1-2 epiblast from AGFP7 E8.5 (2-5 somites) mouse embryos was followed by grafting into St/L5 of MF1 host embryos (Figure 4.1 B) (grafting performed by Professor Val Wilson). Images were taken immediately following grafting to confirm and record graft site (

Figure **4.2**, Graft site), followed by 48 hour culture (details in Materials and Methods 2.2.4). These NMP grafts readily contributed to host embryos, showing lateral and ventral contribution with evident proliferation, and migration out of the graft site (

Figure **4.2**, 48 hour culture). Out of 7 successfully grafted embryos, 6 showed good contribution and development. One embryo did not develop well, and GFP positive cells could not be seen following 48 hours of culture. These manipulations indicate that given appropriate external stimulation, paraxial mesoderm-fated NMPs are capable of lateral mesoderm differentiation, incorporating and proliferating at a novel *in vivo* site.

Figure 4.1| Schematic showing regions involved in grafting. (**A**) Lateral and posterior view of an E8.5 mouse embryo showing the location of NMPs (blue) and the regions containing LPMPs (red). (**B**) L1-2 regions microdissected from ubiquitously expressing GFP epiblast is heterotopically grafted into wildtype host embryos, followed by 48 hour *ex vivo* culture. L1-2, caudal lateral epiblast 1 and 2; L/St5, caudal lateral epiblast and primitive streak 5.

Figure 4.2| NMP containing regions contribute when grafted to the posterior CLE. NMP containing anterior CLE from AGFP7 mouse embryos were grafted into MF1 host embryos. Images were taken immediately following grafting (Graft site), and following 48 hours of *ex vivo* culture (48 hour culture) to assess contribution and migration of cells away from the graft site. 1 grafting procedure failed, with no GFP positive cells observable immediately following grafting process. n = 8.

4.3 Fgf activity induces differentiation of *in vitro* derived NMPs into prospective paraxial mesoderm and neurectoderm

4.3.1 Treatment of *in vitro* derived NMPs with Fgf induces rapid gene expression changes

As mentioned above, an *in vitro* differentiation protocol has already been established to generate NMPs from mouse EpiSCs, and that these cells contribute appropriately when grafted into the NSB at E8.5 (Gouti et al. 2014).

I first confirmed that I could reproduce this protocol (Figure 4.3). EpiSCs were plated at low density and cultured in Fgf2 and Chiron supplemented media for 48 hours (full details are listed within Materials and Methods 2.1.4.2). Immunohistochemistry following the 48 hours of differentiation shows strong down regulation of Oct4 compared to EpiSCs grown in standard maintenance conditions, indicating loss of pluripotency over the two days (Figure 4.3 D and E). As with the published protocol (Gouti et al. 2014), *in vitro* derived NMPs have a high degree of co-expression of the nascent mesoderm and PS marker T, and the neural marker Sox2 (Figure 4.3 G, H, J, K, M, N). This is in line with the co-expression of T and Sox2 seen in embryonic regions that contain NMPs (Wymeersch et al. 2016). Since not all T positive cells express Sox2, this suggests that not all of the cells within the culture as NMPs (Figure 4.3 and (Gouti et al. 2014). The T positive, Sox2 negative cells may be recently formed mesoderm or PS-like cells.

Figure 4.3| Differentiation of EpiSCs into NMPs. Culture of EpiSCs in Fgf and Chiron results in down regulation of Oct4, and co-expression of Sox2 and T. EpiSCs were cultured in media supplemented with Fgf2 and Chiron for 48 hours to generate *in vitro* derived NMPs. Loss of pluripotency was assessed via Oct4 expression, and NMP status assessed via co-expression of Sox2 and T. No primary control represents EpiSCs that were incubated with secondary antibodies, with no preceding primary antibody exposure. n = 3 biological repeats, each of two technical repeats. 10 fields of view were imaged per replicate.

Having generated NMPs from EpiSCs I then set out to further differentiate these cells into the normal *in vivo* derivatives for these cells; paraxial mesoderm and neurectoderm. Several protocols to differentiate hES cells into mesoderm have relied on stimulation of Fgf signalling to induce markers of paraxial mesoderm (Lindsley et al. 2006; Cheung et al. 2012), and as such sustained culture in Fgf was used to differentiate NMPs further. As cells were not re-plated, culture was continued using fibronectin as a substrate. qPCR analysis was used to assess transcript changes occurring at the population level through several days of differentiation (Figure 4.4).

As expected *Oct4* transcripts were downregulated and remain low through the rest of the culture period (Figure 4.4 A). At the transcript level, little change is seen in *Sox2* expression between EpiSCs and NMPs (Figure 4.4 A). However, when NMPs are cultured in Fgf2 *Sox2* transcript is upregulated, which along with the downregulation of *Oct4*, suggests the presence of neurectodermal cells in the culture.

Examination of *T* and *Wnt3a*, both of which are expressed in the PS (Kispert & Herrmann 1994; Inman & Downs 2006; Nowotschin et al. 2012), show upregulation at day 2 of differentiation; when NMPs are present (Figure 4.4 B). The transcript level of both genes declines rapidly following change of culture conditions, with down-regulation seen within 24 hours. *Mesp1* is expressed in nascent mesoderm at the PS (Saga et al. 1996) and in presomitic mesoderm (PSM) just prior to segmentation into somites. As with *T* and *Wnt3a*, *Mesp1* transcript also increases

during differentiation of EpiSCs into NMPs (Figure 4.4 B). This upregulation is maintained during the first 24 hours of differentiation of NMPs into prospective NMP derivatives, beginning to decline by day 4 of the protocol. Once somitogenesis has begun, Msgn1 is expressed in the PSM, but unlike Mesp1 it has a broader expression domain. Slightly earlier in development, at E7.5, *Msgn1* transcript can be detected in tissue adjacent to the PS (Nowotschin et al. 2012). In this differentiation protocol, strong upregulation of *Msgn1* is seen at day 2 followed by a rapid downregulation within the next 24 hours of differentiation (Figure 4.4 C).

The expression of these transcripts suggests that during the differentiation from EpiSCs, the culture goes through a PS-like phase at day 2 when *in vitro* derived NMPs are found ((Gouti et al. 2014) and here). The rapid down-regulation of *T* and *Wnt3a*, which are associated with the PS, indicates that the NMP containing culture is rapidly changing during culture in Fgf2 without Chiron. The transient upregulation of *Mesp1* early in the protocol suggests that mesoderm is induced in the first 24 hours.

I next examined markers of more mature mesoderm, hoping to see upregulation of paraxial mesoderm markers during the mesoderm induction phase of the protocol. Both Meox1 and Tcf15 (also known as Paraxis) have very specific reported expression patterns during somitogenesis, where both are found in segmented somites (Burgess et al. 1995; Ang et al. 1996; Candia et al. 1992). From baseline expression of *Meox1* in EpiSCs and NMP cultures, a substantial upregulation is seen within 24 hours of culture in mesoderm inducing conditions (Fgf culture)

Figure 4.4| Differentiation of *in vitro* derived NMPs into prospective paraxial mesoderm. EpiSCs were differentiated into NMPs through 48 hour culture in Fgf2 and Chiron, followed by 5 days of culture in Fgf2 supplemented media. Cells were harvested every 24 hours for analysis of lineage associated gene expression. A subset of the starting population of EpiSCs was harvested as Day 0. Error bars represent standard deviation. n = three biological replicates. Only two independent samples used for Sox17 (**F**). Three technical replicates were loaded per biological sample, per gene of interest for qPCR analysis.

(Figure 4.4C). This upregulation continues with expression peaking at day 4, where after the transcript expression begins to decline. *Tcf15* shows downregulation at the NMP stage of this protocol, followed by upregulation during mesoderm induction (Figure 4.4 C).

Both published grafting work (Wymeersch et al. 2016) and the data previously discussed here (Section 4.2), indicate that NMPs and LPMPs have the potential to differentiate into both lateral and paraxial mesoderm if placed in the correct context. As such, the expression levels of genes marking mesoderm subtypes, such as lateral and ventral mesoderm were also assessed in this protocol. *Hand1* is a member of the bHLH family which can be found in the heart, lateral plate and extraembryonic mesoderm of the developing embryo (Cserjesi et al. 1995). *Flk1* (also known as *Kdr*) transcript is expressed in lateral mesoderm, the heart and allantois during development (Yamaguchi et al. 1993). During the *in vitro* differentiation of NMPs into prospective paraxial mesoderm, *Hand1* is not upregulated (Figure 4.4 D), and although there is some upregulation of *Flk1* this is still low (Figure 4.4 D).

Expression of the neural marker *Sox1* shows strong upregulation during this differentiation protocol (Figure 4.4 E). This suggests that as well as differentiation along PS- and paraxial mesoderm-like lineages, a population of neurectodermal cells is also generated in this culture. As contribution to both neural and paraxial mesoderm lineages are the differentiation fates of NMPs *in vivo* this is encouraging. Examination of the endodermally expressed *Sox17* did not show upregulation during differentiation (Figure 4.4 F).

The panel of markers examined here suggests that during this *in vitro* differentiation protocol, cells transition from a pluripotent epiblast starting point in the form of EpiSCs, into an NMP containing population (day 2) and then onto more differentiated states during subsequent days. Transcripts associated with the PS and nascent mesoderm, are upregulated early in the protocol, showing rapid downregulation as more mature markers such as *Meox1* and *Sox1* are upregulated. This temporal pattern is an encouraging observation when creating a model system.

In order to confirm the identity and potency of these *in vitro*-derived cells, limited attempts were made to graft differentiated NMPs into host mouse embryos with subsequent culture. A transgenic cell line containing ubiquitously expressed GFP was used to generate NMPs *in vitro*. These cells were then subject to 24 hours of Fgf stimulation to progress the population from an NMP state towards prospective paraxial mesoderm. While grafts were successful, with GFP positive clumps of cells visible at the paraxial mesoderm potent graft sites (L2-3 in 2-3 somite stage embryos), the host embryos did not develop well. The grafted cells remained in clumps rather than interspersing with wild type cells (**Figure 4.5**). These experiments however, do indicate that the cell population is no longer in the NMP state. The grafting in these experiments was carried out by Professor Val Wilson.

Figure 4.5| Differentiated NMPs did not contribute when grafted into paraxial mesoderm and neurectoderm contributing regions. Ubiquitously expressing GFP *in vitro* derived NMPs were differentiated for 24 hours in Fgf2 supplemented culture media then grafted into the anterior PS and CLE. Images were taken immediately after grafting (Graft site) and following 48 hours of ex vivo culture (48 hour culture) to assess contribution into host embryos. Cells did not proliferate and integrate into host tissue, instead remaining as a small clump.

4.3.2 *Tcf15* transcript expression can be detected prior to the onset of somitogenesis

During somitogenesis, Tcf15 is expressed in a very specific manner within segmented somites, and as such is considered a good indicator of somitic mesoderm during differentiation protocols. However, within the *in vitro* system described here, *Tcf15* transcript is only transiently induced (Figure 4.4 C), despite strong upregulation of the paraxial mesoderm marker *Meox1* (Figure 4.4 C), suggesting a partially differentiated population. Although the expression of Tcf15 is well documented during somitogenesis (Burgess et al. 1996), its expression earlier in post implantation development is not reported. It is possible that Tcf15 may be expressed at a later stage of developmental progress than the cells reach in this *in vitro* system. I therefore investigated *Tcf15* expression in earlier stage embryos.

As expected, and reproducing published work (Burgess et al. 1995), *Tcf15* transcript expression can be detected in segmented somites within embryos during stages of somitogenesis and axis elongation (Figure 4.6 A). Looking at younger embryos, some *Tcf15* signal is detectable as early as E7.5 in early bud stage embryos (Figure 4.6 B and C, arrowheads). As embryos progress through embryonic day seven into late bud and early headfold stage this distal band of *Tcf15* expression becomes clearer (Figure 4.6 D and E). By E8.0 around the onset of somitogenesis *Tcf15* can begin to be seen in separated blocks of expression (Figure 4.6 F) as expected from the well reported expression during somitogenesis. The expression pattern of Tcf15 during somitogenesis is well documented (Burgess et al. 1996) and additionally

confirmed here. However, the novel earlier expression detected here indicates that Tcf15 is one of the earliest paraxial mesoderm markers.

Figure 4.6| *Tcf15* transcript can be detected prior to the onset of somitogenesis. Whole mount in situ hybridisation was performed using a probe to detect *Tcf15* transcript expression. E9.5 mid-somitogenesis stage embryos were used as a positive control (**A**, n=3). Early post implantation expression of Tcf15 was examined in E7.5 bud stage embryos (**B, C, D**, n=15), E7.5 head fold stage embryos (**E**, n=8) and in E8.0 embryos at the onset of somitogenesis (**F**, n=6). Arrowheads indicate areas of low hybridisation signal.

4.3.3 Tcf15 induction during *in vitro* differentiation of NMPs

A Tcf15-Venus reporter cell line (generated within the Lowell laboratory) was utilised to examine the protein expression of Tcf15. This reporter cell line has been validated to Venus expression specifically throughout somites in high contribution chimeric embryos. Very few cells can be seen to express the Tcf15-Venus transgene (Figure 4.7 B and E). However, those which do are contained within the Meox1 positive population, indicating that Tcf15 is correctly expressed *in vitro* (Figure 4.7 C and F). Thus attempts were made to induce Tcf15 during the differentiation of NMPs.

To increase proportions of Tcf15 expressing cells, I added R-spondin and Chiron, which have previously been shown to enhance somitic mesoderm differentiation. R-spondins are secreted molecules that have been shown to activate β-catenin and canonical Wnt signalling (Carmon et al. 2011). R-spondins have been used to generate paraxial mesoderm and its derivatives from mES cells (Pourquié & Chal 2013; Chal et al. 2015). Using an Msgn1 reporter cell line, the researchers were able to show that the addition of Rspo3 in serum supplemented medium resulted in robust generation of Msgn1-positive cells. Based on the assessment criteria of proportion of Msgn1-positive cells, Rspo3 treatment had comparable efficiency as with Chiron treatment.

Using the Tcf15-Venus reporter line detailed above, I attempted to increase the Tcf15-Venus positive population within this protocol through manipulation of Wnt signalling. Flow cytometry was used to analyse the impact of adding Chiron and R-

Figure 4.7| Fgf stimulation of *in vitro* derived NMPs does not result in widespread upregulation of Tcf15-Venus. *In vitro* derived NMPs were differentiated into prospective paraxial mesoderm by culture in Fgf2 supplemented media for three days. Widespread expression of Meox1 is detected but Tcf15-Venus positive cells are rare within the culture. Tcf15-Venus positive cells appear to be contained within the Meox1-positive population. Two representative fields of view are shown; `1 = **A-C**, 2 = **D-F**. n=2 biological replicates with 10 fields of view imaged per experiment.

spo3 alone or in combination with Fgf2 supplemented media (

Figure **4.8**). EpiSCs were differentiated into NMPs as described previously. Continuation of culture in Fgf2 and Chiron resulted in an approximately three fold increase in the population of Tcf15-Venus positive cells (

Figure **4.8** D) compared to the original differentiation condition of media supplemented with Fgf2 alone (

Figure **4.8** B). Although continuous culture in Fgf2 and Chiron generated a substantial fold change in the proportion of Tcf15-Venus positive cells, the population still remains minor. The addition of R-spo3 to the original culture condition did not increase the positive population further (

Figure **4.8** E), and co-treatment of Chiron and R-spo3 (

Figure **4.8** F) did not increase the percentage of Tcf15-Venus positive cells detected above that seen with addition of Chiron (

Figure **4.8** D). LDN, a BMP inhibitor (Boergermann et al. 2010) was also tested to mitigate any endogenous BMP activity that may have arisen during the protocol, and thus potentially inhibit somitic mesoderm-associated gene expression. Neither the addition of LDN to the original differentiation condition (

Figure **4.8** C), nor to co-treatment with Chiron and R-spo3 (

Figure **4.8** G) improved the Tcf15-Venus positive population detected.

As Tcf15 is considered a robust marker of somitic mesoderm it is somewhat unexpected that it is not induced during this protocol. *Tcf15* knock out mice however, still form somites and make muscle (Burgess et al. 1996). Examination of these mutant mice indicates that *Tcf15* is required for the epithelialisation of somites and the appropriate patterning of somitic derivatives but not essential for maturation of the PSM into segmented somites. A failure in epithelialisation may offer an explanation for the lack of *Tcf15* induction during *in vitro* differentiation of NMPs. This two-dimensional culture system may not afford the cell-cell and cell-matrix interaction required for epithelialisation. As such, Tcf15 was not used to define the presence of paraxial mesoderm.

Figure 4.8| Rspo3 treatment, and suppression of BMP activity does not increase the Tcf15-Venus positive population. Wnt signalling (Chiron and Rspo3) and BMP signalling (LDN) were manipulated in attempt to increase the Tcf15 positive population during in vitro differentiation of NMPs. *In vitro* derived NMPs were established using Tcf15-Venus reporter cells and subject to a further three days of differentiation, in media supplemented with the following: Fgf2 supplemented media (**B**), Fgf2 and BMP inhibitor (LDN) (**C**), Fgf2 and Chiron (**D**), Fgf2 and Rspo3 (**E**), Fgf2 and Chiron and Rspo3 (**F**), Fgf2 and Chiron and Rspo3 and LDN (**G**). Negative control is wild type E14 cells (**A**). n = 1 biological replicate, 10,000 cells were analysed per sample.

4.3.4 *In vitro* differentiation results in distinct populations of prospective paraxial mesoderm and neurectoderm

As seen in the data discussed in section 4.3.1 Treatment of *in vitro* derived NMPs with Fgf induces rapid gene expression changesand shown in Figure 4.4, changing the conditions of *in vitro* derived NMPs to media supplemented with Fgf2 has quite dramatic effects on the transcript profiles of genes associated with the paraxial mesoderm lineage. The whole population data set shows a further increase in *Sox2* transcript as the *in vitro* derived NMPs are further differentiated (Figure 4.4 A). To confirm that this expression does not coincide with that of factors associated with the mesoderm lineage, immunohistochemistry was performed to examine Sox2, T and Meox1. Figure 4. shows co-staining of Sox2 with T in *in vitro* derived NMPs and further differentiated cells. As NMPs are differentiated into prospective paraxial mesoderm the prevalent co-expression of Sox2 and T seen in the *in vitro* derived NMPs is lost, and the two proteins become largely mutually exclusive (Figure 4.9). This indicates that the population of cells has differentiated into more restricted progenitor populations including prospective paraxial mesoderm and neural cells. Although there is maintained expression of Sox2, over three (Figure 4.9 F) and five days (Figure 4.9 K) of NMP differentiation, T expression begins to decline (Figure 4.9 J) and is only expressed in a small subset of cells at the later stage of differentiation (Figure 4.9 K).

Meox1, as mentioned above, is expressed strongly in somitic mesoderm. In this protocol, a rapid and sustained transcriptional upregulation is seen when *in vitro*

derived NMPs are cultured in Fgf2 supplemented media (Figure 4.4 C). This upregulation is mirrored at the protein level, with little to no detection of the protein by immunohistochemistry in NMPs, but robust expression once these progenitors are differentiated further (Figure 4.9 D and E). The upregulation seen in the Fgf2 treated cells is widespread amongst the population and appears mutually exclusive to the sustained expression of the Sox2 transcription factor (Figure 4.9 K).

Figure 4.9 | Sox2 and T co-expression is lost upon NMP differentiation. 48 hour culture of EpiSCs in Fgf and Chiron generates NMPs co-expressing Sox2 and T (NMPs, **A, E, I, M**). NMPs were differentiated further in Fgf2 supplemented media and fixed for antibody staining after 3 (**B, F, J, N**) and 5 days (**C, G, K, O**). Sox2 and T expression is still present following NMP differentiation in Fgf, though as increasingly distinct populations. Secondary only control (**D, H, L, P**) represents EpiSCs exposed to secondary antibodies without prior incubation with primary antibodies. n = 3 biological replicates, with 10 fields of view imaged per sample.

Figure 4.9| Meox1 is upregulated during NMP differentiation in Fgf. In vitro derived NMPs and NMPs differentiated in Fgf2 containing media were examined for expression of the paraxial mesoderm marker Meox1 and pluripotency and neural marker Sox2. In vitro derived NMPs show Sox2 expression but largely lack Meox1 expression (**A, D, G, J**). Fgf stimulation of NMPs over three days results in an upregulation of Meox1 in a largely mutually exclusive manner to Sox2 (**B, E, H, K**). No primary antibody control represents NMPs differentiated in Fgf2 for three days, exposed to secondary antibodies without prior incubation with primary antibodies (**C, F, I, L**). n = 3 biological replicates, 10 fields of view were imaged per sample.

4.4 Discussion

The combination of published and new grafting work discussed here identifies plasticity in the mesodermal differentiation potential between progenitor regions contributing to axial elongation. Although spatially distinct, it is clear that NMP and LPMP containing regions have the ability to behave appropriately when their locations are exchanged. As the fates of these progenitors are not determined by cell autonomous regulation, this raises the question of whether their fate is determined by signals from their respective local environments. The expression data discussed in Chapter 3 highlights disparate expression of the Id factors between the anterior and posterior PS and CLE in the developing mouse embryo. These expression patterns are consistent with the proposal that Id factors may regulate the fate of these progenitors.

The *in vitro* differentiation reported here provides further validation to the protocol developed previously to generate NMPs *in vitro* (Gouti et al. 2014); showing it to be reproducible by other researchers. I have extended this work, developing a protocol to generate prospective paraxial mesoderm and neurectoderm through the manipulation of FGF signalling. This model system has since been published (Row et al. 2018). The robust changes in RNA and protein expression observed during this protocol indicate the emergence of distinct and appropriate cell types from NMPs. The presence of both prospective paraxial mesoderm and neurectoderm also makes

this protocol suitable for further work addressing the balance between these two NMP derivatives. As well as the expression changes being robust, they are temporally appropriate (see transcript data) strongly suggesting that the population progresses sequentially through phases of pluripotency, PS/NMP stage, nascent and pre-somitic mesoderm and then into paraxial mesoderm.

The examination of *in vivo Tcf15* expression provides novel information regarding the post-implantation expression of this gene. The expression of *Tcf15* detected prior to the onset of somitogenesis was somewhat unexpected given previous reports of somite-specific expression of *Tcf15* during somitogenesis (Burgess et al. 1995). It is feasible that these early expressing cells remain Tcf15 positive until the onset of somitogenesis, and are fated to generate the first somite. This could be examined through lineage tracing of the Tcf15+ population. Four distinct blocks of Tcf15 hybridisation signal can be seen in the embryo in Figure 4.5 A. Posterior to the anterior most pair of these blocks, and anterior to the second pair is a visible 'groove' within the tissue of the embryo. This observation, paired with the *Tcf15* signal detected substantially prior to the onset of somitogenesis suggests that this morphological groove, whose identity as the anterior or posterior boundary of the first somite was unknown, is in fact the boundary between the first and second somite. Expression of *Tcf15* is not maintained uniformly during somitogenesis; as more somites are laid down, the expression of Tcf15 declines in the anterior most somites (Figure 4.5, A).

The newly developed protocol described in this chapter provides a useful, simple model system through which to examine the regulation of NMP differentiation. As there is prevalent BMP activity and Id expression in regions fated to contribute to lateral and ventral mesoderm, and broadly a lack of expression in regions containing NMPs, this signalling pathway is a suitable candidate for the local signals establishing and/or maintaining a distinction between these progenitors in the anterior and posterior PS.

Chapter 5 - The effect of BMP/Id on mesoderm specification

5.1 Introduction

As discussed in Chapter 4, I developed a method to differentiate *in vitro* derived NMPs further in culture, into prospective paraxial mesoderm and neurectoderm (Row et al. 2018). Efforts were made to minimise growth factor addition to the culture media used in this protocol. This facilitates the use of the system to examine multiple pathways which may mediate mesoderm differentiation of NMPs. This chapter details the examination of BMP treatment and Id induction to explore whether BMP or its direct target Id1 may function to ensure correct differentiation of mesoderm from either NMPs or LPMPs, induce differentiation into lateral mesoderm, and manipulate the plasticity for mesoderm potential in NMPs.

5.2 BMP signalling perturbs NMP differentiation *in vitro*

5.2.1 BMP treatment during NMP differentiation induces Id1 expression

To examine the effects of inducing BMP activity, EpiSCs were differentiated into NMPs over 48 hours. NMPs were then subject to differentiation in Fgf2 supplemented media (see Chapter 4) to produce prospective paraxial mesoderm and neurectoderm, or with the addition of BMP4 to challenge this differentiation. qPCR reveals a rapid induction of *Id1* transcript when NMPs were differentiated in the presence of BMP4 (Figure 5.1 A). *Id1* transcript peaks at the earliest time point

Figure 5.1| Id transcript expression during NMP differentiation. EpiSCs were differentiated into NMPs, which were then subject to differentiation into prospective paraxial mesoderm (FGF) and compared to the stimulation of BMP signalling via the addition of BMP4 to the culture media (FGF + BMP). At day 0 the starting material of EpiSCs was split in half, with one half used to for differentiation and the other half harvested as a biologically relevant day 0 sample. Error bars represent standard deviation of three biological replicates. qPCR samples were loaded in triplicate technical replicates per sample and per gene of interest. (**A**) * $p<0.05$. (**B**) * $p<0.01$.

examined in this experiment (24 hours of NMP differentiation), beginning to decline later in the protocol. Although there is a decline seen, the transcript levels remain substantially above that seen with Fgf2 treatment, confirming transcriptional upregulation of *Id1* when NMPs are treated with BMP4.

Examination of the other Id genes reveals that as NMPs are differentiated into prospective mesoderm the transcript levels for each gene increase compared to EpiSCs and *in vitro* derived NMPs (Figure 5.1). Robust transcriptional induction of *Id2* is detectable by qPCR, with higher levels observed in the culture of Fgf2 and BMP4 than with Fgf2 alone (Figure 5.1 B). In contrast, similar induction of *Id3* is seen with culture in Fgf2 alone, as with the addition of BMP4 at day 5 and day 7 of differentiation (Figure 5.1 C). Although increase in *Id4* transcript is seen during the differentiation of *in vitro* derived NMPs, the levels detected are very low when normalised to the housekeeping gene *Tbp* (Figure 5.1 D).

Prior to the availability of a suitable antibody, an Id1-Venus reporter cell line available in the laboratory (Malaguti et al. 2013) was utilised to examine Id1 protein expression through this differentiation. This cell line (detailed in 2.1.1.2) was generated by Dr Mattias Malaguti, a postdoctoral researcher in the Lowell research group using a targeting construct originally described by Nam & Benezra 2009.

Flow cytometry using the Id1-Venus reporter line reveals the presence of a positive subpopulation following the initial two days of differentiation (Figure 5.2), when an NMP containing population is produced. When further differentiation is carried out into prospective paraxial mesoderm, the percentage of Id1-Venus positive cells

Figure 5.2| Id1-Venus is upregulated by BMP stimulation during NMP differentiation. NMPs were differentiated *in vitro* into prospective paraxial mesoderm (Fgf2) and challenged with BMP stimulation (Fgf2&BMP4). Cells were analysed at 24 hour time points using E14 cells put through the same protocols. Plots are representative examples of one experiment. n=3 biological replicates, 10,000 cells were analysed per sample.

within the population remains similar over the next five days (Figure 5.2, Fgf). However, when cells are treated with Fgf2 and BMP4, a clear increase is seen in the percentage of Id1-Venus positive cells and their level of expression (Figure 5.2, Fgf&BMP). As with the Id1 transcript data (Figure 5.1 A), this increased expression declined over the course of the experiment. This decline resulted in a similar sized Id1-Venus positive population as is observed with Fgf treatment after five days of NMP differentiation. The induction of a larger Id1-Venus positive population following addition of BMP4 to the culture media is a reproducible pattern, though the absolute percentage of Venus positive cells does vary between replicate experiments (Figure 5.3).

Figure 5.3| Id1-Venus is reproducibly upregulated by BMP4 treatment during NMP differentiation *in vitro*. Id1-Venus cells were differentiated into NMPs, which were then subject to further differentiation in the presence of Fgf2 (**Fgf**), or Fgf2 and BMP4 (**Fgf & Bmp**). Samples were collected and analysed daily by flow cytometry utilising wild type E14 cells put through the same procedures as negative controls. Error bars represent standard deviation of three independent biological replicates. Each biological replicate experiment analysed 10,000 cells per sample. * $p = <0.01$.

5.2.2 BMP treatment can redirect *in vitro* differentiation of NMPs

Having confirmed that BMP4 addition to the differentiation protocol does induce Id expression, what effects this may have on the expression of mesodermal markers was then examined. I hypothesised that BMP activity would inhibit paraxial mesoderm differentiation and induce lateral/ventral mesoderm differentiation, and be inhibitory to neurectoderm. The data shown for the control condition of NMP differentiation in the presence of Fgf2 is replicated from that presented in Figure 4.3.

As seen previously, the early and pan mesoderm associated genes *T*, *Wnt3a* and *Mesp1* show a peak in transcript expression during the protocol when cells have been differentiated into NMPs. The addition of BMP4 when differentiating NMPs had limited effect on the transcript levels for these three genes, though it did result in a stronger downregulation of *T* and *Wnt3a* than with Fgf2 alone (Figure 5.4 B). Similarly a more pronounced downregulation in the PSM associated Msgn1 is observed when BMP4 is added to the culture to challenge differentiation into prospective paraxial mesoderm (Figure 5.4 C). A dramatic contrast is seen between these two culture conditions with regard to the somitic marker Meox1. As shown previously, this factor is strongly upregulated during the establishment of prospective paraxial mesoderm from NMPs (Figure 5.3 C). However, when BMP signalling is stimulated, a strong inhibition of this upregulation is observed (Figure 5.4 C). Stimulation of BMP signalling in this protocol also downregulated Tcf15 expression from NMPs, compared to Fgf2 treatment alone (Figure 5.4 C). This reinforces the conclusion that BMP suppresses paraxial mesoderm differentiation.

Figure 5.4| BMP treatment inhibits transcriptional upregulation of paraxial mesoderm and neural associated genes during *in vitro* differentiation of NMPs. EpiSCs were differentiated into NMPs (**Fgf+Chiron**), followed by culture in Fgf2 (**Fgf**), or Fgf2 and BMP4 (**Fgf+Bmp**). Samples were collected daily and analysed via qPCR for lineage associated gene expression. At day 0, the starting material of EpiSCs was halved, with one half used for differentiation and the other half harvested as a biologically relevant day 0 sample. Error bars represent standard deviation of three biological replicates. Only two independent samples used for *Sox17* (**F**). 3 technical replicates were loaded for qPCR analysis per sample and per gene of interest. Fgf values are replicated data from Figure 4.4. * $p < 0.01$.

Within 24 hours of differentiation of *in vitro* derived NMPs in the presence of BMP4 a sizeable and sustained upregulation of the bHLH factor *Hand1* occurs (Figure 5.4 D). In vivo, this factor is expressed within the lateral plate, heart and extraembryonic mesoderm (Cserjesi et al. 1995). A similar pattern of upregulation is seen with Flk1 (Figure 5.4 D), which during development can be detected in lateral mesoderm, the heart and the allantois (Yamaguchi et al. 1993). There is a rapid and continuing transcriptional upregulation of Flk1 when BMP signalling is stimulated to challenge the differentiation of NMPs into prospective paraxial mesoderm and neurectoderm. The upregulation of these two factors is in stark contrast to the down regulation and weak effects on transcript levels seen during differentiation into prospective paraxial mesoderm.

I have shown previously in Chapter 4 that the pluripotency factor Oct4 is down-regulated at the transcript and protein levels when NMPs are established from pluripotent EpiSCs (Figure 4.3 and Figure 4.4). Differentiating NMPs further *in vitro* shows continued down regulation of Oct4 transcript whether cells are exposed to BMP4 or not (Figure 5.4 A). The stimulation of BMP signalling in this differentiation protocol also has little effect on the transcriptional levels of Sox17 (Figure 5.4 F). This endoderm-associated factor does not show upregulation during differentiation of NMPs into prospective paraxial mesoderm and neurectoderm, nor when BMP4 is added to the culture conditions.

As discussed in the introduction, BMP signalling via Id factors has been shown to inhibit early neural specification from mES cells (Ying et al. 2003). As such, it is of

interest to examine whether stimulation of BMP signalling can affect genes associated with differentiation into the neural lineage within this protocol. *Sox2* is associated with both pluripotency and the neural lineage, and shows upregulation when NMPs are differentiated in the presence of Fgf2. This upregulation is lost upon the addition of BMP4, with transcriptional downregulation detected at the population level (Figure 5.4 A). This effect is also seen for expression of Sox1 (Figure 5.4 E). Fgf treatment of NMPs leads to a robust upregulation of *Sox1* transcript, peaking between 24 and 48 hours after changing culture conditions. However, when BMP4 is added to the culture, *Sox1* is rapidly downregulated as the population progresses away from an NMP state.

In overview of this data, it can be seen that stimulation of BMP signalling during this differentiation protocol can inhibit the differentiation of NMPs into prospective paraxial mesoderm and neurectoderm, instead resulting in the upregulation of genes associated with lateral and extraembryonic mesoderm.

I next asked whether the transcriptional changes of some key markers seen with the addition of BMP4 to the protocol are mirrored in protein expression. T and Sox2, which show a large degree of co-expression in NMPs both *in vitro* and *in vivo* ((Gouti et al. 2014; Wymeersch et al. 2016), Figure 4.3 and Figure 5.5 E, I, M), are robustly down regulated by treatment with Fgf2 and BMP4 (Figure 5.5 G, K, O). This is in contrast to the treatment of NMPs with Fgf2 alone, where the sustained expression of these two transcription factors shows a largely, but not entirely, mutually exclusive pattern of expression (Figure 5.5 F, J, N and Figure 4.3). This

Figure 5.5| Sox2 and T are downregulated by BMP4 treatment. *In vitro* derived NMPs (**A, E, I, M**) were differentiated for a further three days into prospective paraxial mesoderm via treatment with Fgf (**B, F, J, N**), or challenged with the addition of BMP4 to stimulate BMP signalling (**C, G, K, O**). Expression of the pluripotency and neural marker Sox2 and the PS and early mesoderm marker T were examined. No primary antibody control represents NMPs differentiated in Fgf containing media and exposed to secondary antibodies without prior incubation with primary antibodies. n = 3 biological replicates, with 10 fields of view imaged per experimental sample.

indicates that BMP4 treatment antagonises the production of maintenance of mesoderm progenitors and differentiation into the neural lineage.

In addition to the down regulation of the pluripotency and neural protein Sox2 and nascent-mesoderm-associated T, challenging NMPs with BMP signalling affects the protein expression of the somite marker Meox1. As expected from the down regulation in Meox1 transcript as compared to Fgf2 treatment (Figure 5.4 C), very few Meox1 positive cells are detected after three days of differentiation of NMPs (Figure 5.6 D and F). Where Meox1 positive cells can be detected, the signal intensity is far less than seen in Fgf2 treated cells (Figure 5.6 C, G). A Flk1-GFP reporter mES cell line was gifted from the Medvinsky laboratory and differentiated into EpiSCs to examine the expression of Flk1. The transcriptional upregulation of Flk1 when NMPs are subject to BMP signalling is replicated with detection of Flk1-GFP (Figure 5.6 F, H), which is not readily detectable when Fgf signalling is stimulated without BMP activity (Figure 5.6 E, G).

These data confirm that stimulating BMP signalling can affect the differentiation of NMPs *in vitro*. As previous studies have shown BMP signalling to inhibit neural specification from ES cell, the inhibition of Sox2 and Sox1 upregulation may be expected. The changes seen in mesoderm lineage related factors imply that BMP signalling may inhibit the typical paraxial mesoderm fate of NMPs, and instead may be redirecting differentiation towards other mesoderm subtypes. Although this data may be interpreted as such, it is also possible that a subpopulation of lateral mesoderm progenitors exists alongside NMPs following differentiation from

Figure 5.6| BMP stimulation of differentiating NMPs downregulates Meox1 and upregulates Flk1-GFP. *In vitro* derived NMPs were differentiated using Flk1-GFP reporter cells and subject to three days of further differentiation into paraxial mesoderm via culture with Fgf2 (**A, C, E, G**), or challenged with the addition of BMP4 to stimulate BMP signalling (**B, D, F, H**). In post implantation mouse development Flk1 is expressed in lateral and ventral mesoderm, and Meox1 is a marker of somitogenesis. n = 3 biological replicates, with 10 fields of view imaged per sample.

EpiSCs. If this is the case, the widespread expression of Flk1 seen with BMP4 treatment may be the result of an expansion of this subpopulation rather than redirecting the fate of NMPs. To address this question, further examination of the expression of Flk1 was carried out using a Flk1-GFP reporter ES cell line obtained from A. Medvinsky (Jakobsson et al. 2010).

Flow cytometry was used to examine the percentage of Flk1-GFP positive cells within the population at daily time points. Looking at *in vitro* derived NMPs, only a very minor population of Flk1-GFP positive cells can be found; between 1 and 3% of the whole population across replicate experiments (

Figure **5.7** and Figure 5.8). As NMPs are differentiated into prospective paraxial mesoderm and neurectoderm, the percentage of Flk1-GFP positive cells detected does not change dramatically, remaining a minor subpopulation (

Figure **5.7** and Figure 5.8, Fgf2). However, when the NMP to prospective mesoderm differentiation protocol is supplemented with BMP4 and rapid increase is seen with Flk1-GFP positive cells making up 60-70% of the population after 24 hours of differentiation (

Figure **5.7** and Figure 5.8, Fgf2&BMP4). This large percentage of positive cells is sustained over the next 24 hours of differentiation then begins to decline. Although there is a decline seen in the Flk1-GFP positive population, it remains a substantial subpopulation (~30%) and considerably higher than that seen with Fgf2 treatment. This pattern of Flk1-GFP expression is reproducible over independent experiments (Figure 5.8).

The rapid increase in the Flk1 positive cells from 2% to 62% of the population within 24 hours of BMP addition suggests that BMP signalling is redirecting cell fate rather than expanding a non-NMP subpopulation. It is highly unlikely that such a small subpopulation could be so readily expanded within a 24 hour time window.

Figure 5.7| Differentiation of NMPs in the presence of BMP4 results in strong increase in expression of Flk1-GFP. Flk1-GFP reporter cells were used to generate NMPs, which were then differentiated further in Fgf2, or in Fgf2 and BMP4 containing media. Cells were harvested at daily time points for flow cytometry with wild type E14 cells put through the same protocols were used as negative controls. Plots shown here are from one representative experiment. n = 3 biological replicates, with 10,000 cells analysed per sample.

Figure 5.8| Upregulation of Flk1-GFP following BMP4 treatment is reproducible. NMPs were derived *in vitro* from Flk1-GFP cells and differentiated further in the presence of Fgf2, or Fgf2 and BMP4, followed by flow cytometry and analysis. Scatter plots of one representative experiment are displayed in Figure 5.7. Error bars represent standard deviation of three independent biological replicates. 10,000 cells were analysed per sample, per experiment. * $p < 0.01$.

5.2.3 BMP stimulation can perturb the establishment of NMPs *in vitro*

The in situ hybridisation data presented in Chapter 3 shows that during early PS stages, *Id* transcripts are excluded from the distal region of the embryo; the region that will become NMP-potent and -fated. This, combined with the detection of *Id* expression in the posterior PS, where LPMPs are found, raises the possibility that exclusion of BMP activity is required to establish NMPs.

EpiSCs were differentiated into NMPs as previously described ((Gouti et al. 2014), Chapter 4), using co-expression of T and Sox2 as a readout of successful establishment of NMP state. Alongside, establishment of NMPs was attempted in either in the presence of BMP4 to stimulate BMP signalling, or in the presence of LDN, to inhibit BMP signalling (Boergermann et al. 2010). The addition of BMP4 to the culture for the 48 hours of differentiation resulted in a dramatic inhibition of both T and Sox2, indicating unsuccessful establishment of NMPs (Figure 5.9 G, K, O). The addition of LDN (Figure 5.9 F, L, N) led to a similar outcome as with the un-supplemented differentiation condition (Figure 5.9 E, I, M), with both producing populations with widespread co-expression of T and Sox2.

qPCR analysis confirms a BMP-mediated induction of both *Id1* (Figure 5.10 A) and *Id3* (Figure 5.10 B). It should be noted that the standard culture condition used to produce NMPs *in vitro* (Fgf2 and Chiron supplemented media) does result in a modest upregulation of both of these transcripts (Figure 5.10 A and B). Although addition of LDN attenuates this in the case of *Id3* transcript, this is not the case for *Id1*. It has been shown that Fgf signalling can induce Id1, and as the Fgf2

Figure 5.9| BMP4 inhibits the establishment of NMPs *in vitro*. EpiSCs were differentiated over 48 hours into NMPs by culture with Fgf2 and Chiron (**A, E, I, M**). BMP signalling was manipulated in this protocol by addition of LDN to inhibit BMP signalling (**B, F, J, N**), or the addition of BMP4 to drive BMP signalling (**C, G, K, O**). Establishment of NMP state was determined by co-expression of T and Sox2. No primary control represents EpiSCs differentiated in Fgf and Chiron for 48 hours then exposed to secondary antibodies without prior incubation with primary antibodies (**D, H, L, P**). n = 3 independent biological replicates, each of two technical replicates. 5 fields of view were imaged per sample.

Figure 5.10| Manipulation of BMP signalling during NMP establishment *in vitro*. Differentiation of EpiSCs into NMPs (Fgf+Chi) was compared with simultaneous stimulation of BMP signalling (Fgf+Chi+BMP) or suppression of BMP signalling (Fgf+Chi+LDN) following 48 hours of culture. qPCR analysis was performed to examine readouts of BMP signalling via *Id1* and *Id3* (**A, B**), the pluripotency marker *Oct4* (**C**), genes expressed within the PS; *Wnt3a, Cdx2* and *Evx1* (**D-F**), and the endodermally expressed *Foxa2* (**G**). At Day 0 the starting material of EpiSCs was halved; one subset used for the differentiation experiment, and the other half harvested as a biologically relevant EpiSC/Day 0 sample. Error bars represent standard deviation of three independent biological replicates.

concentration these cells are exposed to is increased to generate NMPs, this provides a possible explanation for this pattern.

It has been shown that BMP signalling via Id factors can inhibit the differentiation of mES cells, helping to promote pluripotency (Ying et al. 2003). Examination of the pluripotency factor Oct4 reveals that in the context of EpiSC differentiation into NMPs, modulating BMP activity has little effect on the transcriptional activity of this gene (Figure 5.10 C). As with the standard protocol condition, a robust downregulation is seen in the two test conditions as compared to the starting population of the experiment.

Wnt3a and *Cdx2* can both be detected in the PS and within nascent mesoderm, and transcriptional induction is seen for both of these genes during EpiSC differentiation into NMPs (Figure 5.10 D and E and (Gouti et al. 2014)). The inhibition of BMP signalling has little transcriptional effect on *Wnt3a* and *Cdx2* during this differentiation but the addition of BMP4 does show a trend for decreased or inhibited upregulation (Figure 5.10 D and E).

As *Id* gene expression can be detected in the posterior of the PS (Chapter 3), it is possible that BMP-mediated Id activity could impose a posterior identity on differentiating NMPs *in vitro*. *Evx1* is expressed in both nascent mesoderm of the PS and shows higher expression at the posterior end of the PS (Dush & Martin 1992; Faust et al. 1995). However, all three conditions tested provided similar results for the transcriptional level of this gene (Figure 5.10 F), suggesting this marker does not discriminate between anterior and posterior populations *in vitro*. Examination of the

endoderm and floor plate associated gene, *Foxa2* (Filosa et al. 1997) shows similar levels of transcript expression for in vitro derived NMPs, and differentiation in the presence of LDN as with EpiSCs (Figure 5.10 G). There is a small down-regulation seen when EpiSC to NMP differentiation is challenged with BMP4. This indicates that the manipulation of BMP signalling during in vitro NMP establishment is not affecting an endodermal population.

5.2.4 Id1 has distinct expression patterns during differentiation into prospective paraxial and lateral mesoderm

As can be seen from flow cytometry using an Id1-Venus reporter, Id1 positive populations can be detected both with and without the addition of BMP4 during the differentiation of NMPs into prospective mesoderm (Figure 5.2). Although widespread Meox1 protein expression can be seen during NMP differentiation into prospective paraxial mesoderm, this is not entirely homogenous throughout the population. As the addition of BMP4, resulting in Id1 upregulation has inhibited markers associated with paraxial mesoderm it raises questions over subpopulations during differentiation. Is there an overlap between cells expressing Meox1 and Id1 positive cells, or is the expression of these two proteins mutually exclusive, marking two distinct subpopulations?

The Id1-Venus reporter cell line detailed earlier was utilised to examine the pattern of Id1-Venus expression during the differentiation of NMPs. An Id1-Venus subpopulation during differentiation into prospective paraxial mesoderm has

already been identified via flow cytometry (Figure 5.2 Fgf), and this is reproduced by imaging (Figure 5.11 B). Where Id1-Venus expressing cells are observed, they are typically found in domed clumps of cells (as highlighted by the dense DAPI stain). The expression of Id1-Venus and Meox1 appear to be largely if not entirely mutually exclusive (Figure 5.11 D). This expression pattern contrasts strongly with that seen when the prospective paraxial mesoderm differentiation is challenged with the addition of BMP4. As shown previously the widespread Meox1 expression is not present during NMP differentiation in Fgf2 and BMP4 (Figure 5.11 G). As expected from flow cytometry data (Figure 5.2, BMP4), Id1-Venus expression is readily detectable (Figure 5.11 F) and unlike during Fgf treatment, expression is widespread across the population which is Meox1 negative. This data is compatible with a BMP mediated upregulation of Id1 preventing Meox1 expression, supporting the hypothesis that Id1 repression or absence is required for differentiation of NMPs into paraxial mesoderm.

There is *Id1* expression detected within posterior regions of the PS (Chapter 3) and flow cytometry identifies an Id1-Venus positive population within the culture following differentiation into NMPs (Figure 5.2). Immunohistochemistry was performed using Id1-Venus cells to identify any possible co-expression with T, which is expressed throughout the PS. Imaging of in vitro derived NMPs supports there being a small Id1-Venus positive population within the culture (Figure 5.12 D). Despite the widespread expression of T, there is only a very minor subpopulation that co-express T and Id1-Venus within the culture (Figure 5.12 J).

Figure 5.11| Id1-Venus and Meox1 expression appear mutually exclusive during NMP differentiation. Id1-Venus reporter cells were used for differentiation into NMPs followed by a further 3 days of differentiation in the presence of Fgf2 to generate prospective paraxial mesoderm (**A-D**), or challenged with the addition of BMP4 to the culture (**E-H**). The presence of prospective paraxial mesoderm was assessed by the presence of Meox1 positive cells. n = 2 biological replicates. 10 fields of view were imaged per sample.

Figure 5.12| A small subpopulation of NMPs co-express Id1-Venus and T. Id1-Venus reporter EpiSCs were differentiated into NMPs (**A, D, G, J**), which were subsequently differentiated into prospective paraxial mesoderm through culture with Fgf2 (**B, E, H, K**) or challenged with the addition of BMP4 to the culture (**C, F, I, L**). Id1-Venus expression was examined alongside the expression of the PS and early mesoderm marker T. n = 2 independent biological replicates. 10 fields of view were imaged per sample.

Following three days of differentiation of NMPs into prospective paraxial mesoderm, there are distinct populations of Id1-Venus positive and T positive cells, with little if any co-expression observed (Figure 5.12 E, H, K). This immunohistochemistry also reaffirms the downregulation of T and increased Id1-Venus positive proportion of cells (Figure 5.12 F, I, L). As Id gene expression is largely excluded from NMP containing regions with the embryo (Id transcript can be detected at the lateral edge of this region), it is encouraging that there is not widespread Id1-Venus expression within the T-positive NMP cells.

5.3 Induction of Id1 in NMPs affects differentiation of NMPs

The data discussed so far in this chapter has demonstrated that the differentiation of NMPs into prospective paraxial mesoderm and neurectoderm can be challenged by the addition of BMP4 to the culture. As expected, the addition of BMP4 stimulates the induction of Id factors, raising the possibility that that this is an effect of Id mediated BMP signalling. To address this possibility, an Id1 inducible cell line was utilised. This doxycycline inducible line was generated by Dr Mattias Malaguti, from the Lowell group (full cell line details in Materials and Methods 2.1.1.2). As at the time of creating this line there was not a reliable antibody available for Id1, it was designed with a 3xflag tag fused to the exogenous Id1 protein. More recently the availability of an Id1 antibody enables detection of both endogenous and exogenous Id1. The work discussed in the following sections was all performed using clonal lines which had been initially selected and validated for efficient and

non-leaky induction of Id1 within mES cells in previous work by Dr Mattias Malaguti. I then differentiated these lines into EpiSCs for use in this study.

5.3.1 Induction of Id1 during NMP differentiation

Two clones (tId1cl9 and tId1 cl43) of the Id1 inducible cell line were differentiated into EpiSCs and tested for Id1-flag induction following doxycycline treatment. Following 48 hours of culture in the presence of doxycycline, flag protein was detectable by immunohistochemistry in both lines (Figure 5.13). Expression was undetectable in the absence of doxycycline, and present after doxycycline induction although not in all cells in the culture.

To confirm that flag induction correctly reported on Id1 induction, EpiSCs were differentiated into NMPs then subjected to a further 24 hours of culture. As has been seen in wild-type and Id1-Venus reporter cells (Figure 5.1, Figure 5.2, Figure 5.3F) Id1 expression is induced during initial stages of differentiation into prospective paraxial mesoderm via Fgf2 treatment. This is reproduced with the Id1 doxycycline inducible line, with widespread, low level endogenous Id1 expressed in the absence of either doxycycline or BMP4 treatment (Figure 5.14 A-D). Following culture in Fgf2 and LDN, Id1 protein can be observed in a similar pattern to culture in Fgf2 alone (Figure 5.14 E-H). This shows that the Id1 expression that has been seen during the early stages of NMP differentiation into prospective paraxial mesoderm

Figure 5.13| Doxycycline treatment induces flag expression. Two clonal doxycycline inducible Id1 flag tagged EpiSCs (tId1) EpiSC lines were treated with doxycycline for 48 hours then immunostained to confirm flag-tag protein induction. No flag protein was detected when either clonal cell line was not exposed to doxycycline. No primary antibody represents clone 43 cells treated with doxycycline and treated with secondary antibodies without prior incubation with primary antibodies during immunostaining.

Figure 5.14| Doxycycline induced flag reports induced Id1 expression. Doxycycline inducible flag tagged Id1 EpiSCs (tId1 cl43) were differentiated and examined for flag and Id1 expression to assess the reliability of flag protein as a read out of induced Id1 expression. *In vitro* derived NMPs were differentiated for 24 hours in the presence of Fgf2 (**A-D**), Fgf2 and LDN (**E-H**), Fgf2 and BMP4 (**I-L**), Fgf2 and doxycycline (**M-P**), Fgf2, doxycycline and LDN (**Q-T**). Id1 expression shows a wider domain of expression than flag, but flag signal represents a subpopulation within the Id1 positive population, Arrowheads indicate examples of Id1-positive, flag-negative cells. No primary control represents cells that have been differentiated in Fgf and doxycycline then stained with secondary antibodies without prior incubation with primary antibodies. n = 2 independent biological replicates. 10 fields of view were imaged per sample.

is BMP-independent. Higher level of Id1 expression is observed following NMP differentiation in Fgf and BMP (Figure 5.14 I-L). When cells were cultured in the presence of doxycycline, widespread expression of both flag and Id1 protein can be observed, with flag positive cells defining a subpopulation within the larger Id1 positive population (Figure 5.14 M-P). The proportion of flag positive cells appears to become slightly higher when LDN is added to the culture, but there are still Id1 positive/flag negative cells within the culture (Figure 5.14 Q-T). The Id1 and flag protein expression seen following culture including doxycycline shows that induction is robust and entirely confined to Id1 expressing cells.

To ensure that any observable differences were due to exogenous Id1 and not exposure to doxycycline, parental wild-type cells were treated with doxycycline. When *in vitro* derived NMPs were differentiated into prospective paraxial mesoderm, no difference was seen in Id1 and Meox1 when doxycycline was added to the culture (Figure 5.15, A and B). Additionally, the presence of doxycycline did not prevent the establishment of NMPs in vitro, as assessed by T and Sox2 co-expression (Figure 5.15 C).

Figure 5.15| Doxycycline treatment does not affect wild type cells. NMPs were derived from wild type E14 EpiSCs, which were then differentiated into prospective paraxial mesoderm by culture with Fgf2, or with the addition of doxycycline. qPCR analysis of *Id1* (**A**) and *Meox1* (**B**) was performed to examine any effect of doxycycline on differentiation independent of induced Id1. T and Sox2 co-expression shows E14 EpiSCs can be differentiated into NMPs in the presence of doxycycline (**C**). Two independent biological replicates were performed.

5.3.2 Effect of Id1 induction during differentiation of NMPs

Differentiation of *in vitro* derived NMPs into prospective paraxial mesoderm was challenged with treatment of doxycycline to specifically induce Id1 (Figure 5.16). Following 48 hours of differentiation in the presence of Fgf2 and doxycycline (Figure 5.16 B, F, J, N) robust expression of flag protein can be detected, indicating cells which have upregulated exogenous Id1 (Figure 5.16 J). Flag protein and the paraxial mesoderm marker Meox1 are almost entirely mutually exclusive (Figure 5.16 N). This is in line with the hypothesis that Id1 expression is inhibitory to differentiation of NMPs into prospective paraxial mesoderm. Additionally, the cells within the culture that do express Meox1 appear to do so at lower levels than is seen in the differentiation into prospective paraxial mesoderm (Figure 5.16 A, E, I, M). Instead the protein intensity observed is reminiscent of that seen with addition of BMP4 to the culture (Figure 5.16 C, G, K, O).

However, as seen in Figure 5.14, flag positive cells consist of a subpopulation within an Id1 positive population of cells within the culture. Examination of Id1 expression across the whole population was examined at the same stage of differentiation; 48 hours of NMP differentiation into prospective paraxial mesoderm with the addition of doxycycline. In tId1 cl43 cells, areas of strong Id1 expression can be seen in addition to some low level expression (Figure 5.17 H) though still largely mutually exclusive to that of Meox1 (Figure 5.17 K). Similar to the data presented in Figure 5.16, the cells within the culture that do express Meox1, appear to do so at reduced intensity when compared to Id1 levels in the absence of doxycycline (Figure 5.17 D,

Figure 5.16| Induced Id1-flag is mutually exclusive to Meox1. Doxycycline inducible flag tagged Id1 (tId1 cl43) cells were differentiated into NMPs which were then differentiated into prospective paraxial mesoderm (Fgf), or challenged with the addition of doxycycline (Fgf and dox), or the additional of BMP (Fgf and BMP). Staining for flag (**I-L**) was used to assess doxycycline-mediated upregulation of Id1. Staining for Meox1 (**E-H**) was used to indicate differentiation into paraxial mesoderm. Arrowheads indicate Meox1-positive, Id1-flag negative cells. No primary antibody control represents cells treated with Fgf and doxycycline then stained using secondary antibodies without prior incubation with primary antibodies. n = 2 biological replicates. 10 fields of view imaged per sample per experiment.

Figure 5.17| Expression of Id1 and Meox1 during differentiation of NMPs *in vitro*. Doxycycline inducible flag tagged Id1 (tIdl cl43) NMPs were differentiated into prospective paraxial mesoderm (**A, D, G, J**) or challenged with Id1 induction (Fgf + dox) (**B, E, H, K**) for 48 hours. Weak Id1 expression is detectable during differentiation into paraxial mesoderm (**G**), but widespread Meox1 expression is lost upon strong doxycycline-mediated induction of Id1 (**H**). No primary antibody control is Fgf and doxycycline treated cells treated with secondary antibodies without prior incubation with primary antibodies. n = 3 biological replicates. 10 fields of view were imaged per sample.

E), therefore, high levels of Id1 appear incompatible with paraxial mesoderm differentiation.

To further examine the effects of Id1 induction on NMP differentiation, the expression of other mesoderm and neural lineage associated genes was examined. Examining both doxycycline-inducible clones (tId1 cl9 and tId1 cl43) shows that increased Id1 expression is maintained in the presence of doxycycline for at least five days (

Figure **5.18** A, B). Interestingly, following three days of differentiation, increased expression of the PS and pan-mesoderm marker T is seen with Id1 induction (

Figure **5.18** C, D). This increased transcriptional expression is not maintained throughout the course of the differentiation, with comparable levels seen with standard prospective paraxial mesoderm differentiation 48 hours later (day 7). This suggests that the increase in Id1 rather than BMP activity per se is delaying the exit of cells from a PS-like population. However, further replication and imaging is needed to determine whether this is specific to induced Id1-expressing cells or a paracrine effect on their neighbours.

Examination of more mature mesoderm and neural markers confirms that Id1 acts similarly to BMP to inhibit neural and paraxial mesoderm differentiation (Figure

5.4). As expected based on immunohistochemistry, Meox1 expression is reduced when differentiation is challenged with doxycycline mediated Id1 upregulation (

Figure **5.18** E, F). This inhibition is particularly evident following three days of differentiation of NMPs with detected transcript levels comparable to that seen in EpiSCs. This contrasts with the expression of the lateral and ventral mesoderm

Figure 5.18| Induction of Id1 redirects differentiation of NMPs *in vitro*. Two independent clones of a flag tagged Id1 doxycycline-inducible cells; tId1 cl9 (**A, C, E, G, I, K**) and tId1 cl43 (**B, D, F, H, J, L**) were differentiated into NMPs and then into paraxial mesoderm with and without doxycycline. qPCR analysis was performed to confirm induction of *Id1* (**A-B**), examine the expression of the PS and early mesoderm marker *T* (**C-D**), paraxial mesoderm marker *Meox1* (**E-F**), lateral and ventral mesoderm markers *Flk1* and *Hand1* (**G-J**) and the neural marker *Sox1* (**K-L**). n = one biological replicated per clonal cell line.

associated genes *Flk1* and *Hand1*. Both of these genes show transcriptional upregulation when differentiated in the presence of increased Id1 expression (

Figure **5.18** G-J). Expression of the neural lineage marker Sox1 is inhibited when Id1 expression is induced (

Figure **5.18** K, L).

The immunostaining and qPCR data discussed here is consistent with the hypothesis that specific induction of Id1 can mimic the effect of inducing BMP activity during the differentiation of NMPs. In both cases, the differentiation into prospective paraxial mesoderm and neurectoderm appears to be inhibited and redirected towards lateral and ventral mesoderm.

Although the transcript data covered in

Figure **5.18** shows reproducible findings with two independent clonal lines, the data represents a single biological replicate for each line. Unfortunately however, levels of Id1 induction began to decline in both of these lines at higher passage.

Only a minor upregulation of *Id1* became achievable, compared to the induction seen when differentiation of NMPs is challenged with BMP4 (Figure 5.19 A). The transcript levels detected for T, Flk1 and Sox1 are comparable between prospective

paraxial mesoderm differentiation and the addition of doxycycline to the culture (Figure 5.19 B, D, E). The dramatic difference in *Meox1* transcript levels seen when a robust doxycycline mediated *Id1* induction is achieved (

Figure **5.18**) is also lost here, with only a minor effect seen at one time point (Figure 5.19 C). However, the BMP4 mediated upregulation of Id1 does coincide with Flk1 upregulation (Figure 5.19 D) and strong inhibition of T, Meox1 and Sox1 (Figure 5.19 B, C, E), showing that these

Figure 5.19| NMP differentiation is not redirected when *Id1* is not induced. Id1 doxycycline inducible cells (tId1 cl43) were differentiated into NMPs and then into paraxial mesoderm (FGF), or challenged with addition of doxycycline or BMP to the culture. qPCR analysis was performed to examine *Id1* expression (**A**), the PS and early mesoderm marker *T* (**B**), the paraxial mesoderm marker *Meox1* (**C**), the lateral and ventral mesoderm marker *Flk1* (**D**), and the neural marker *Sox1* (**E**). *Id1* induction in response to doxycycline became weakened within this cell line, though BMP treatment still induced *Id1* expression. n = one biological replicate. Triplicate technical samples were loaded for qPCR analysis.

lines have not lost the ability to respond to BMP.

Immunohistochemistry reveals that the limited Id1 induction following doxycycline treatment is a result of very few cells responding with upregulation, rather than widespread but low level of induction (Figure 5.20 F). However, the cells within the culture that continue to respond and upregulate Id1-flag, do so with strong induction and are mutually exclusive to Meox1 expression (Figure 5.20 M). Despite the low level of induction, these results further reinforce the conclusion that Id1 expression cell-autonomously redirects prospective paraxial mesoderm to lateral mesoderm.

Figure 5.20| Doxycycline mediated induction of Id1 varies in efficiency depending on context. Flag tagged Id1 doxycycline inducible (tId1 cl43) NMPs were differentiated into paraxial mesoderm via culture with Fgf (**A, E, I, M**), challenged with addition of doxycycline to induce ectopic Id1 (**B, F, J, N**), or challenged with the addition of BMP4 (**C, G, K, O**). Following 48 hours of differentiation, cells were immunostained for the somitic marker Meox1 and for flag protein. Lack of flag positive cells indicates that only a small subset of the population is responding to doxycycline (**F, N**). The lack of Meox1 expression when cells are differentiated in the presence of BMP4 indicates that cells can still respond to BMP signalling (**K, O**). No primary antibody control represents cells treated with Fgf and doxycycline then fixed and stained with secondary antibodies without prior incubation with primary antibodies. n = two biological replicates. 10 fields of view were imaged per sample.

5.4 Discussion

The data presented within this chapter addresses the hypothesis that BMP activity, mediated via Id factors is inhibitory to the usual differentiation routes of NMPs; into neurectoderm and paraxial mesoderm. Although there does appear to be some BMP independent expression of Id during differentiation into prospective paraxial mesoderm and neurectoderm, BMP greatly further increases the expression of Id1.

The addition of BMP4 during NMP differentiation has a dramatic effect, robustly inhibiting paraxial mesoderm associated genes and instead upregulating lateral and ventral mesoderm associated genes. Additionally, the negligible population of Flk1-GFP cells detectable amongst NMPs strongly supports the idea that BMP/Id redirects cell fate rather than expanding a pre-existing subpopulation of lateral and ventral mesoderm or progenitors. The inhibitory effects of BMP and Id on neural differentiation have been described previously in cell culture experiments (Ying et al. 2003). The experiments conducted here, show that BMP and Id can inhibit neural differentiation in a different context; NMP differentiation into prospective paraxial mesoderm. These data have since been published (Row and Pegg et al. 2018) as part of a broader study that included similar observations made in zebrafish embryos.

Future work can be carried out to further validate that the effects of BMP and Id are exerted over NMPs. This will utilise a fluorescent Sox2 reporter line to obtain a purer population of NMPs. Cells will be differentiated into NMPs, then subjected to fluorescent activated cell sorting to obtain Sox2 positive and Sox2 negative populations for re-plating and further differentiation. The aim of this experiment

will be to confirm that BMP treatment and induced Id1 expression manipulates the differentiation of the Sox2 positive, and thus a purer NMP population.

The inhibition of NMP differentiation into prospective paraxial mesoderm and neurectoderm seen with addition of BMP4 is replicated when Id1 is induced independently of BMP activity. Id1 continues to show a mutually exclusive pattern of expression to the somitic marker Meox1, and mimics upregulation of lateral and ventral mesoderm associated genes. It supports the hypothesis that BMP activity via at least Id1 is inhibitory to differentiation into paraxial mesoderm and neurectoderm, and instead redirects NMPs into a lateral and/or ventral mesoderm fate.

There is also data presented here to support the hypothesis that the absence of BMP and Id activity is required to establish the state of NMPs. BMP treatment during *in vitro* differentiation into NMPs induces both *Id1* and *Id3* and inhibits the establishment of these progenitors. Although NMPs were not obtained during differentiation *in vitro* in the presence of BMP4, cells still exited pluripotency as indicated by the downregulation of Oct4. This suggests that BMP acts at multiple points in the differentiation of pluripotent epiblast cells.

Further support to the work presented here could be achieved via the generation of additional quantitative data. The immunohistochemistry data presented in Figure 5.5 displays co-expression of Sox2 and T in NMPs and in Figure 5.11 shows Id1-Venus- and Meox1-positive cells as predominantly mutually exclusive populations during NMP differentiation. These images were however captured with wide field

imaging, which in essence captures x and y dimensional information. Emitted light is captured from the entire z dimension of the sample, without capturing the thickness of cells in each field of view. Cells within a single field of view with varying local cell density, as indicated by DAPI staining, may appear to have different fluorophore intensity. We cannot determine from two dimensional imaging whether there is higher intensity detected in individual cells in high density areas, or if it is an artefact as a result of imaging multiple cells in the same x,y location.

In order to determine co-expression definitively in immunohistochemistry samples, three dimensional data is required. Through confocal microscopy, multiple two dimensional images are captured of the sample at progressive z planes. The collection of such data enables the three-dimensional reconstruction of the sample. Such data is required to perform digital quantification, whereby individual cells within a sample can be segmented using a nuclear- or cellular membrane stain and appropriate software. Individual cells can then be assessed for detection of fluorophore activity, intensity, and co-expression.

Chapter 6 – Discussion

The *in vitro* model for NMP differentiation developed here provides a simple, yet temporally appropriate system, which has been used to examine the effect of manipulating BMP/Id signalling (Row, Pegg et al. 2018). The data generated within this thesis show that BMP signalling mediated via Id1 can inhibit the differentiation of NMPs into paraxial mesoderm and neurectoderm, instead promoting lateral and ventral mesoderm. In situ hybridisation shows that *Id* transcripts are largely excluded from regions fated to become NMP containing regions, and NMP containing regions. This, combined with manipulation of BMP signalling during *in vitro* establishment of NMPs indicates that low or absent BMP/Id activity is required to establish NMPs. The mesodermal differentiation potential is shared between NMPs and LPMPs, with each able to respond to environmental signals. As Id transcript expression contrasts between these two locations, and can subvert NMP differentiation it is reasonable to hypothesise that BMP/Id activity is required for the establishment and differentiation of LPMPs. Taken together, this data suggests that BMP/Id acts at multiple points in the differentiation of pluripotent epiblast cells (Figure **6.1**).

Figure 6.1| Model of the stages at which BMP/Id regulates mesoderm differentiation. BMP/Id activity directs the differentiation of NMPs into lateral and/or ventral mesoderm, inhibiting Fgf mediated differentiation into neurectoderm or paraxial mesoderm. BMP may direct the establishment, or maintenance of LPMPs, which are restricted to mesodermal fates. BMP activity is then required to generate lateral and/or ventral mesoderm from these progenitors, with an absence of BMP/Id signalling facilitating differentiation into paraxial mesoderm. Necto; neurectoderm, Meso; mesoderm, PXM; paraxial mesoderm, LVM; lateral/ventral mesoderm, BMP; BMP signalling mediated via Id.

The work within this thesis covering the redirection of cell fate by BMP signalling via Id1 describes an unusual mode of action for members of the Id family. The typical action of Id proteins is to prevent early differentiation of progenitor cell populations, hence the namesake of inhibitor of differentiation. Examples of this mode of regulation in pluripotent cells can be found in the maintenance of mouse ES cells in an undifferentiated state via ID1 mediated interference with TCF15 upregulation (Davies et al. 2013). ID protein mediated inhibition of multipotent

progenitor differentiation is exampled in the inhibition of myogenesis (Benezra et al. 1990) and of neurogenesis (Bai et al. 2007; Jung et al. 2010; Liu & Harland 2003), instead promoting myoblast and neuroblast states, respectively. The data presented here shows a redirection of cell fate during NMP differentiation, into a lateral/ventral mesoderm identity. This finding parallels the observation of ID2 driven differentiation of white blood cells, where ID2 inhibits E2A driving differentiation into NK cells rather than differentiation into B-cells (Yokota et al. 1999).

The observation that NMPs exposed to Fgf signalling can generate neurectoderm and paraxial mesoderm and induction of BMP activity results in lateral and ventral mesoderm is mimicked in the zebrafish (Row, Pegg et al. 2018). During mediolateral patterning of the zebrafish embryo, bmp was observed to be a lateralising factor, with inhibition of bmp signalling resulting in the formation of ectopic somitic tissue. Induction of id1 or id3 replicated the phenotype seen when bmp signalling was induced. This indicates evolutionary conservation in mesoderm differentiation of NMPs, which have themselves been observed in numerous vertebrate species.

Msgn1 has been previously shown to activate a gene network that regulates presomitic mesoderm differentiation, with forced expression driving mES cell differentiation into presomitic mesoderm (Chalamalasetty et al. 2014). Additionally, ectopic expression of Msgn1 in the PS of mouse embryos led to an expansion of presomitic mesoderm at the expense of segmented somites. Taken together, this led to the conclusion of Msgn1 acting as a 'master regulator' of presomitic mesoderm differentiation and makes an appealing candidate for Id1 to act upon in the

disruption of NMP differentiation into paraxial mesoderm. In line with this, using morpholinos to disrupt *myf5, myod*, and *msgn1* in combination resulted in an a reduction of skeletal muscle, with expansion of differentiated endothelium instead (Row, Pegg et al. 2018). This phenotype was reminiscent, but less severe than ectopic *id3* activation during zebrafish gastrulation, which results in lateralisation. This indicates that these three bHLH factors are the primary determinants of somitic mesoderm differentiation in NMP specification in the zebrafish, and that the re-diverted differentiation into lateral mesoderm by BMP/Id is at least in part due to the inhibition of the function of these proteins. Generation of Id-resistant form of these proteins could be accomplished by tethering each bHLH factor to an E protein via a flexible linker. The *in vitro* NMP differentiation system developed here could then be used to assess whether BMP/Id can still subvert NMP differentiation into lateral and ventral mesoderm in a model mouse system.

Re-establishing EpiSC lines from the doxycycline inducible Id1 clonal lines will enable replication and thus further validation of the data presented in

Figure **5.18**. The data generated using specific Id1 induction in combination with BMP inhibition shows that Id1 expression alone rather than general activation of the BMP signalling pathway is sufficient to challenge NMP differentiation. An Id1 knock out cell line can be used to address whether Id1 is required to disrupt NMP differentiation into neurectoderm and paraxial mesoderm. To complement this *in vitro* experiment, labelled Id1 null cells either *in vitro* derived or homotopically

grafted from an Id1 null embryo could be grafted into L/St5. As this region contributes to lateral and ventral mesoderm is it an ideal context to test the requirement of Id1 for differentiation into these mesodermal subtypes. As Id1 knock out does not have a phenotypic effect on the organism as a whole (Yan et al. 1997), it is probable that this can be compensated for by another Id. *Id1* and *Id3* show strikingly similar expression patterns (Chapter 3), and induction of *id1* and *id3* show similar phenotypes (Row, Pegg et al. 2018). Thus, Id3 would be the stronger candidate for compensation and should be investigated in a similar manner to the Id1-related work here.

Further validation that the effects of BMP and Id are exerted over NMPs will utilise a fluorescent Sox2 reporter line to obtain a purer population of NMPs. Cells will be differentiated into NMPs, then subjected to fluorescent activated cell sorting to obtain Sox2 positive and Sox2 negative populations for re-plating and further differentiation. The aim of this experiment will be to confirm that BMP treatment and induced Id1 expression manipulates the differentiation of the Sox2-positive, and thus a purer NMP population.

Further extension of the work presented in this thesis can be achieved via manipulation of Id signalling within the embryo. As embryonic culture requires serum, which contains high levels of BMPs, broad treatment with BMP4 or BMP inhibitors is likely to prove problematic. However, specific plasmids can be electroporated into small numbers of cells in an embryo, followed by *ex vivo* culture (Huang et al. 2015). A labelled Id1 expression plasmid can be electroporated into the

L1-3 of the CLE, which includes NMPs and is fated to paraxial mesoderm. The hypothesised outcome of this experiment would be that paraxial mesoderm contribution would be disrupted in those cells that successfully take up the plasmid.

As discussed in chapter 4, the novel post implantation *Tcf15* expression suggests it could be an earlier marker of somitic mesoderm than currently thought. Lineage labelling should be used to ensure that those cells showing Tcf15 expression seen prior to the onset of somitogenesis (Figure 4.6 B-E) are fated to paraxial mesoderm. This could be achieved using a Tcf15-driven lineage label to label all descendants of cells that have switched on Tcf15. As *Tcf15* is expressed in the ICM (Davies et al. 2013), this system would require temporal control to avoid labelling all cells of the embryo proper. An alternative approach could be to electroporate a fluorescent protein plasmid into the embryo then culture *ex vivo* and image. This has the drawbacks of only labelling a small number of cells, not the entire Tcf15 expressing population. Additionally, it would not guarantee only labelling Tcf15 positive cells. As electroporation is dependent on manually orientating an embryo with regards to electroporation probes, and this early *Tcf15* expression is not in a morphologically distinct region, it is highly likely that non target cells would be labelled.

The work contained within this thesis provides a detailed and well stage matched comparison of early post implantation expression of the Id family combining both whole mount and section data. A model system has been developed to examine NMP differentiation *in vitro*, and used to show that BMP signalling via Id1 can

promote lateral and ventral mesoderm differentiation from NMPs at the expense of paraxial mesoderm and neurectoderm.

References

Acampora, D., Di Giovannantonio, L.G. & Simeone, A., 2013. Otx2 is an intrinsic determinant of the embryonic stem cell state and is required for transition to a stable epiblast stem cell condition. *Development (Cambridge, England)*, 140(1), pp.43–55. Available at: http://www.ncbi.nlm.nih.gov/pubmed/23154415 [Accessed May 23, 2014].

Allendorph, G.P., Vale, W.W. & Choe, S., 2006. Structure of the ternary signaling complex of a TGF- ℓ superfamily member. *PNAS*, 103(20), pp.7643–7648.

Ang, S. et al., 1996. A targeted mouse Otx2 mutation leads to severe defects in gastrulation and formation of axial mesoderm and to deletion of rostral brain. *Development*, 122, pp.243–252.

Aoyama, M. et al., 2012. Spatial restriction of bone morphogenetic protein signaling in mouse gastrula through the mVam2-dependent endocytic pathway. *Developmental cell*, 22(6), pp.1163–75. Available at: http://www.ncbi.nlm.nih.gov/pubmed/22698281 [Accessed June 5, 2014].

Arkell, R. & Beddington, R.S.P., 1997. BMP-7 influences pattern and growth of the developing hindbrain of mouse embryos. , 12, pp.1–12.

Arkell, R.M. & Tam, P.P.L., 2012. Initiating head development in mouse embryos : integrating signalling and transcriptional activity. *Open Biology*, 2.

Arnold, S.J. & Robertson, E.J., 2009. Making a commitment: cell lineage allocation and axis patterning in the early mouse embryo. *Nature reviews. Molecular cell biology*, 10(2), pp.91–103. Available at: http://www.ncbi.nlm.nih.gov/pubmed/19129791 [Accessed May 25, 2014].

Atchley, W.R. & Fitch, W.M., 1997. A natural classification of the basic helix-loop-helix class of transcription factors. *Proceedings of the National Academy of Sciences of the United States of America*, 94(10), pp.5172–5176.

Avilion, A.A. et al., 2003. Multipotent cell lineages in early mouse development depend on SOX2 function. *Genes & development*, 17, pp.126–140.

Bai, G. et al., 2007. Id sustains Hes1 expression to inhibit precocious neurogenesis by releasing negative autoregulation of Hes1. *Developmental cell*, 13(2), pp.283–97. Available at: http://www.ncbi.nlm.nih.gov/pubmed/17681138 [Accessed May 29, 2014].

Bao, S. et al., 2009. Epigenetic reversion of postimplantation epiblast cells to pluripotent embryonic stem cells. *Nature*, 461.

Beddington, R.S., 1982. An autoradiographic analysis of tissue potency in different

regions of the embryonic ectoderm during gastrulation in the mouse. *Journal of embryology and experimental morphology*, 69, pp.265–85. Available at: http://www.ncbi.nlm.nih.gov/pubmed/7119671.

Bedford, L. et al., 2005. Id4 is required for the correct timing of neural differentiation. *Developmental biology*, 280, pp.386–395.

Benezra, R. et al., 1990. The protein Id: a negative regulator of helix-loop-helix DNA binding proteins. *Cell*, 61(1), pp.49–59. Available at: http://www.pubmedcentral.nih.gov/articlerender.fcgi?artid=3318758&tool=pmcentrez&rendertype=abstract.

Beppu, H. et al., 2000. BMP type II receptor is required for gastrulation and early development of mouse embryos. *Developmental Biology*, 221(1), pp.249–258.

Blackwood, E.M. & Eisenman, R.N., 1991. Max: a helix-loop-helix zipper protein that forms a sequence-specific DNA-binding complex with Myc. *Science (New York, N.Y.)*, 251(4998), pp.1211–1217.

Boergermann, J.H. et al., 2010. Dorsomorphin and LDN-193189 inhibit BMP-mediated Smad, p38 and Akt signalling in C2C12 cells. *The international journal of biochemistry & cell biology*, 42(11), pp.1802–7. Available at: http://www.ncbi.nlm.nih.gov/pubmed/20691279 [Accessed May 23, 2014].

Bonnerot, C. et al., 1987. A / 3-galactosidase hybrid protein targeted to nuclei as a marker for developmental studies. *Proceedings of the National Academy of Sciences of the United States of America*, 84, pp.6795–6799.

Boulet, A.M. & Capecchi, M.R., 2012. Signaling by FGF4 and FGF8 is required for axial elongation of the mouse embryo. *Developmental biology*, 371(2), pp.235–45. Available at: http://www.pubmedcentral.nih.gov/articlerender.fcgi?artid=3481862&tool=pmcentrez&rendertype=abstract [Accessed June 13, 2014].

Brons, I.G.M. et al., 2007. Derivation of pluripotent epiblast stem cells from mammalian embryos. *Nature*, 448(7150), pp.191–195. Available at: http://www.ncbi.nlm.nih.gov/pubmed/17597762 [Accessed May 24, 2014].

Burgess, R. et al., 1995. Paraxis: A Basic Helix-Loop-Helix Protein Expressed in Paraxial Mesoderm and Developing Somites. *Developmental biology*, 168, pp.296–306.

Burgess, R. et al., 1996. Requirement of the paraxis gene for somite formation and musculoskeletal patterning. *Nature*, 384, pp.356–358.

Burtscher, I. & Lickert, H., 2009. Foxa2 regulates polarity and epithelialization in the endoderm germ layer of the mouse embryo. *Development (Cambridge, England)*, 136(6), pp.1029–38. Available at:

http://www.ncbi.nlm.nih.gov/pubmed/19234065 [Accessed June 10, 2014].

Cambray, N. & Wilson, V., 2002. Axial progenitors with extensive potency are localised to the mouse chordoneural hinge. *Development (Cambridge, England)*, 129(20), pp.4855–66. Available at: http://www.ncbi.nlm.nih.gov/pubmed/12361976.

Cambray, N. & Wilson, V., 2007. Two distinct sources for a population of maturing axial progenitors. *Development (Cambridge, England)*, 134(15), pp.2829–40. Available at: http://www.ncbi.nlm.nih.gov/pubmed/17611225 [Accessed June 3, 2014].

Candia, A.F. et al., 1992. Mox-1 and Mox-2 define a novel homeobox gene subfamily and are differentially expressed during early mesodermal patterning in mouse embryos. *Development*, 116, pp.1123–1136.

Carmon, K.S. et al., 2011. R-spondins function as ligands of the orphan receptors LGR4 and LGR5 to regulate Wnt / β -catenin signaling. *PNAS*, 108(28).

Chal, J. et al., 2015. Differentiation of pluripotent stem cells to muscle fiber to model Duchenne muscular dystrophy. *Nature Biotechnology*, 33(9), pp.962–969.

Chalamalasetty, R.B. et al., 2014. Mesogenin 1 is a master regulator of paraxial presomitic mesoderm differentiation. , pp.4285–4297.

Chang, H. et al., 1999. Smad5 knockout mice die at mid-gestation due to multiple embryonic and extraembryonic defects. *Development (Cambridge, England)*, 126(8), pp.1631–42. Available at: http://www.ncbi.nlm.nih.gov/pubmed/10079226.

Chen, D., Zhao, M. & Mundy, G.R., 2004. Bone morphogenetic proteins. *Growth factors (Chur, Switzerland)*, 22(4), pp.233–41. Available at: http://www.ncbi.nlm.nih.gov/pubmed/15621726 [Accessed May 24, 2014].

Chen, F. & Weinberg, R.A., 1995. Biochemical evidence for the autophosphorylation and transphosphorylation of transforming growth factor (3 receptor kinases. *Proceedings of the National Academy of Sciences of the United States of America*, 92, pp.1565–1569.

Cheung, C. et al., 2012. Articles Generation of human vascular smooth muscle subtypes provides insight into embryological origin – dependent disease susceptibility. *Nature Biotechnology*, 30(2), pp.165–175. Available at: http://dx.doi.org/10.1038/nbt.2107.

Christy, B.A. et al., 1991. An Id-related helix-loop-helix protein encoded by a growth factor-inducible gene. *Proceedings of the National Academy of Sciences of the United States of America*, 88(5), pp.1815–9. Available at: http://www.pubmedcentral.nih.gov/articlerender.fcgi?artid=51116&tool=pmce

ntrez&rendertype=abstract.

Chuva de Sousa Lopes, S.M. et al., 2003. Distribution of phosphorylated Smad2 identifies target tissues of TGFβ ligands in mouse development. *Gene Expression Patterns*, 3, pp.355–360.

Ciruna, B. & Rossant, J., 2001. Mesoderm Cell Fate Specification and Morphogenetic Movement at the Primitive Streak. *Developmental cell*, 1, pp.37–49.

Clevers, H., 2006. Wnt/β-Catenin Signaling in Development and Disease. *Cell*, 127(3), pp.469–480.

van Crüchten, I. et al., 1998. Structure, chromosomal localisation and expression of the murine dominant negative helix-loop-helix Id4 gene. *Biochimica et biophysica acta*, 1443(1–2), pp.55–64. Available at: http://www.ncbi.nlm.nih.gov/pubmed/9838043.

Cserjesi, P. et al., 1995. Expression of the Novel Basic Helix-Loop-Helix Gene eHAND in Neural Crest Derivatives and Extraembryonic Membranes during Mouse Development. *Developmental biology*, 170, pp.664–678.

Danesh, S.M. et al., 2009. BMP and BMP receptor expression during murine organogenesis. *Gene Expression Patterns*, 9, pp.255–265. Available at: http://dx.doi.org/10.1016/j.gep.2009.04.002.

Davies, O.R. et al., 2013. Tcf15 primes pluripotent cells for differentiation. *Cell reports*, 3(2), pp.472–84. Available at: http://www.pubmedcentral.nih.gov/articlerender.fcgi?artid=3607254&tool=pmcentrez&rendertype=abstract [Accessed May 23, 2014].

Dawson, S.R. et al., 1995. Specificity for the hairy/enhancer of split basic helix-loop-helix (bHLH) proteins maps outside the bHLH domain and suggests two separable modes of transcriptional repression. *Molecular and cellular biology*, 15(12), pp.6923–6931.

Denham, M. et al., 2015. Multipotent Caudal Neural Progenitors Derived from Human Pluripotent Stem Cells That Give Rise to Lineages of the Central and Peripheral Nervous System. *Stem Cells*, 33, pp.1759–1770.

Di-Gregorio, A. et al., 2007. BMP signalling inhibits premature neural differentiation in the mouse embryo. *Development (Cambridge, England)*, 134(18), pp.3359–69. Available at: http://www.ncbi.nlm.nih.gov/pubmed/17699604 [Accessed June 9, 2014].

Dush, M.K. & Martin, G.R., 1992. Analysis of mouse Evx genes: Evx-1 displays graded expression in the primitive streak. *Developmental Biology*, 151(1), pp.273–287. Available at: http://www.sciencedirect.com/science/article/pii/0012160692902326.

Ellenberger, T. et al., 1994. Crystal structure of transcription factor E47: E-box recognition by a basic region helix-loop-helix dimer. *Genes and Development*, 8(8), pp.970–980.

Ellmeier, W. et al., 1992. Mutually exclusive expression of a helix-loop-helix gene and N-myc in human neuroblastomas and in normal development. *The EMBO journal*, 11(7), pp.2563–2571.

Ellmeier, W. & Weith, a, 1995. Expression of the helix-loop-helix gene Id3 during murine embryonic development. *Developmental dynamics : an official publication of the American Association of Anatomists*, 203(2), pp.163–73. Available at: http://www.ncbi.nlm.nih.gov/pubmed/7655079.

Evans, M.J. & Kaufman, M.H., 1981. Establishment in culture of pluripotential cells from mouse embryos. *Nature*, 292, pp.154–156.

Faust, C. et al., 1995. The eed mutation disrupts anterior mesoderm production in mice. *Development (Cambridge, England)*, 121(2), pp.273–85. Available at: http://www.ncbi.nlm.nih.gov/pubmed/7768172.

Ferré-D'Amaré, a R. et al., 1993. Recognition by Max of its cognate DNA through a dimeric b/HLH/Z domain. *Nature*, 363(6424), pp.38–45.

Ferrer-vaquer, A. et al., 2010. A sensitive and bright single-cell resolution live imaging reporter of Wnt / ß-catenin signaling in the mouse. *BMC developmental biology*, 10.

Filosa, S. et al., 1997. goosecoid and HNF-3 β genetically interact to regulate neural tube patterning during mouse embryogenesis. , 2854, pp.2843–2854.

Fraidenraich, D. et al., 2004. Rescue of cardiac defects in id knockout embryos by injection of embryonic stem cells. *Science (New York, N.Y.)*, 306(5694), pp.247–52. Available at: http://www.pubmedcentral.nih.gov/articlerender.fcgi?artid=1351017&tool=pmcentrez&rendertype=abstract [Accessed June 16, 2014].

Fujiwara, T., Dunn, N.R. & Hogan, B.L., 2001. Bone morphogenetic protein 4 in the extraembryonic mesoderm is required for allantois development and the localization and survival of primordial germ cells in the mouse. *Proceedings of the National Academy of Sciences of the United States of America*, 98(24), pp.13739–44. Available at: http://www.pubmedcentral.nih.gov/articlerender.fcgi?artid=61111&tool=pmcentrez&rendertype=abstract.

Fujiwara, T., Dunn, N.R. & Hogan, B.L.M., 2001. Bone morphogenetic protein 4 in the extraembryonic mesoderm is required for allantois development and the localization and survival of primordial germ cells in the mouse. *Proceedings of the National Academy of Sciences of the United States of America*, 98(24), pp.13739–

13744.

Goetz, R. & Mohammadi, M., 2013. Exploring mechanisms of FGF signalling through the lens of structural biology. *Nature Reviews Molecular Cell Biology*, 14(3), pp.166–180. Available at: http://dx.doi.org/10.1038/nrm3528.

Gouti, M. et al., 2014. In Vitro Generation of Neuromesodermal Progenitors Reveals Distinct Roles for Wnt Signalling in the Specification of Spinal Cord and Paraxial Mesoderm Identity. *PLoS biology*, 12(8), p.e1001937. Available at: http://www.ncbi.nlm.nih.gov/pubmed/25157815 [Accessed August 27, 2014].

Gray, P. a et al., 2004. Mouse brain organization revealed through direct genome-scale TF expression analysis. *Science (New York, N.Y.)*, 306(5705), pp.2255–7. Available at: http://www.ncbi.nlm.nih.gov/pubmed/15618518 [Accessed June 13, 2014].

Greber, B. et al., 2010. Conserved and divergent roles of FGF signaling in mouse epiblast stem cells and human embryonic stem cells. *Cell stem cell*, 6(3), pp.215–26. Available at: http://www.ncbi.nlm.nih.gov/pubmed/20207225 [Accessed May 24, 2014].

Greco, T.L. et al., 1996. Analysis of the vestigial tail mutation demonstrates that Wnt-3a gene dosage regulates mouse axial development. *Genes & development*, 10, pp.313–324.

Hara, E. et al., 1994. Id-related genes encoding helix-loop-helix proteins are required for G1 progression and are repressed in senescent human fibroblasts. *Journal of Biological Chemistry*, 269(3), pp.2139–2145.

Henrique, D. et al., 2015. Neuromesodermal progenitors and the making of the spinal cord. *Development*, 142, pp.2864–2875.

Hollnagel, a et al., 1999. Id genes are direct targets of bone morphogenetic protein induction in embryonic stem cells. *The Journal of biological chemistry*, 274(28), pp.19838–45. Available at: http://www.ncbi.nlm.nih.gov/pubmed/10391928.

Hooker, C.W. & Hurlin, P.J., 2006. Of Myc and Mnt. *Journal of cell science*, 119(Pt 2), pp.208–216.

Huang, Y. et al., 2012. In Vivo differentiation potential of epiblast stem cells revealed by chimeric embryo formation. *Cell reports*, 2(6), pp.1571–8. Available at: http://www.ncbi.nlm.nih.gov/pubmed/23200857 [Accessed June 4, 2014].

Huang, Y., Wilkie, R. & Wilson, V., 2015. Methods for Precisely Localized Transfer of Cells or DNA into Early Postimplantation Mouse Embryos. *Journal of Visualized Experiments*, (106), pp.1–8. Available at: http://www.jove.com/video/53295/methods-for-precisely-localized-transfer-cells-or-dna-into-early.

Huang, Z.J., Edery, I. & Rosbash, M., 1993. PAS is a dimerization domain common to Drosophila period and several transcription factors. *Nature*, 364(6434), pp.259–262.

Inman, K.E. & Downs, K.M., 2006. Localization of Brachyury (T) in embryonic and extraembryonic tissues during mouse gastrulation. *Gene expression patterns : GEP*, 6(8), pp.783–93. Available at: http://www.ncbi.nlm.nih.gov/pubmed/16545989 [Accessed June 13, 2014].

Iwafuchi-Doi, M. et al., 2012. Transcriptional regulatory networks in epiblast cells and during anterior neural plate development as modeled in epiblast stem cells. *Development*, 139(21), pp.3926–3937. Available at: http://www.ncbi.nlm.nih.gov/pubmed/22992956 [Accessed June 13, 2014].

Jakobsson, L. et al., 2010. Endothelial cells dynamically compete for the tip cell position during angiogenic sprouting. *Nature Cell Biology*, 12(10), pp.943–953. Available at: http://dx.doi.org/10.1038/ncb2103.

Javier, A.L. et al., 2012. Bmp Indicator Mice Reveal Dynamic Regulation of Transcriptional Response. *PloS one*, 7(9), p.e42566.

Jen, Y., Manova, K. & Benezra, R., 1997. Each member of the Id gene family exhibits a unique expression pattern in mouse gastrulation and neurogenesis. *Developmental dynamics*, 208(1), pp.92–106. Available at: http://www.ncbi.nlm.nih.gov/pubmed/8989524.

Jen, Y., Manova, K. & Benezra, R., 1996. Expression Patterns of Id1, Id2 , and Id3 Are Highly Related But Distinct From That of Id4 During Mouse Embryogenesis. *Developmental dynamics*, 207, pp.235–252.

Jones, S., 2004. An overview of the basic helix-loop-helix proteins. *Genome Biology*, 5(6), p.226. Available at: http://genomebiology.com/2004/5/6/226%5Cnhttp://www.ncbi.nlm.nih.gov/pubmed/15186484%5Cnhttp://www.pubmedcentral.nih.gov/articlerender.fcgi?artid=PMC463060.

Jung, S. et al., 2010. Id proteins facilitate self-renewal and proliferation of neural stem cells. *Stem cells and development*, 19(6), pp.831–41. Available at: http://www.ncbi.nlm.nih.gov/pubmed/19757990 [Accessed June 13, 2014].

Jurberg, A.D. et al., 2014. Compartment-dependent activities of Wnt3a/B-catenin signaling during vertebrate axial extension. *Developmental Biology*, 394(2), pp.253–263. Available at: http://dx.doi.org/10.1016/j.ydbio.2014.08.012.

Katagiri, T. et al., 2002. Identification of a BMP-responsive element in Id1, the gene for inhibition of myogenesis. *Genes to cells : devoted to molecular & cellular mechanisms*, 7(9), pp.949–60. Available at: http://www.ncbi.nlm.nih.gov/pubmed/12296825.

Kewley, R.J., Whitelaw, M.L. & Chapman-Smith, A., 2004. The mammalian basic helix-loop-helix/PAS family of transcriptional regulators. *International Journal of Biochemistry and Cell Biology*, 36(2), pp.189–204.

Kinder, S.J. et al., 1999. The orderly allocation of mesodermal cells to the extraembryonic structures and the anteroposterior axis during gastrulation of the mouse embryo. *Development*, (126), pp.4691–4701.

Kispert, A. & Herrmann, B.G., 1994. Immunohistochemical analysis of the Brachyury protein in wild-type and mutant mouse embryos. *Developmental biology*, 161(1), pp.179–193.

Koch, F. et al., 2017. Antagonistic Activities of Sox2 and Brachyury Control the Fate Choice of Neuro-Mesodermal Article Antagonistic Activities of Sox2 and Brachyury Control the Fate Choice of Neuro-Mesodermal Progenitors. *Developmental Cell*, 42(5), p.514–526.e7. Available at: http://dx.doi.org/10.1016/j.devcel.2017.07.021.

Koenig, B.B. et al., 1994. Characterization and Cloning of a Receptor for BMP-2 and BMP-4 from NIH 3T3 Cells. *Mole*, 14(9), pp.5961–5974.

Kojima, Y. et al., 2014. Resource The Transcriptional and Functional Properties of Mouse Epiblast Stem Cells Resemble the Anterior Primitive Streak. *Cell stem cellStem Cell*, 13, pp.1–14. Available at: http://dx.doi.org/10.1016/j.stem.2013.09.014.

Komiya, Y. & Habas, R., 2008. Wnt signal transduction pathways. *Organogenesis*, 4(2), pp.68–75.

Kretzschmar, M. et al., 1997. The TGF- [family mediator Smadl is phosphorylated directly and activated functionally by the BMP receptor kinase. *Genes and Development*, 11, pp.984–995.

Kunath, T. et al., 2007. FGF stimulation of the Erk1 / 2 signalling cascade triggers transition of pluripotent embryonic stem cells from self-renewal to lineage commitment. *Development*, 134, pp.2895–2902.

Langlands, K. et al., 1997. Differential Interactions of Id Proteins with Basic-Helix-Loop-Helix Transcription Factors. *Journal of Biological Chemistry*, 272(32), pp.19785–19793. Available at: http://www.jbc.org/cgi/doi/10.1074/jbc.272.32.19785 [Accessed June 16, 2014].

Lawson, K.A. et al., 1999. Bmp4 is required for the generation of primordial germ cells in the mouse embryo. *Genes and Development*, 13(4), pp.424–436.

Ledent, V., Paquet, O. & Vervoort, M., 2002. Phylogenetic analysis of the human basic helix-loop-helix proteins. *Genome biology*, 3(6), pp.1–18.

Li, L. et al., 2013. Location of transient ectodermal progenitor potential in mouse

development. *Development (Cambridge, England)*, 140(22), pp.4533–43. Available at: http://www.ncbi.nlm.nih.gov/pubmed/24131634 [Accessed October 13, 2014].

Lindsley, R.C. et al., 2006. Canonical Wnt signaling is required for development of embryonic stem cell-derived mesoderm. *Development (Cambridge, England)*, 133(19), pp.3787–96. Available at: http://www.ncbi.nlm.nih.gov/pubmed/16943279 [Accessed May 24, 2014].

Lippmann, E.S. et al., 2015. Deterministic HOX Pattterning in Human Pluripotent Stem Cell-Derived Neurectoderm. *Stem Cell Reports*, 4, pp.632–644. Available at: http://dx.doi.org/10.1016/j.stemcr.2015.02.018.

Liu, K.J. & Harland, R.M., 2003. Cloning and characterization of Xenopus Id4 reveals differing roles for Id genes. *Developmental Biology*, 264(2), pp.339–351. Available at: http://linkinghub.elsevier.com/retrieve/pii/S0012160603005141 [Accessed June 16, 2014].

Lyden, D. et al., 1999. Id1 and Id3 are required for neurogenesis, angiogenesis and vascularization of tumour xenografts. *Nature*, 401(6754), pp.670–7. Available at: http://www.ncbi.nlm.nih.gov/pubmed/10537105.

Malaguti, M. et al., 2013. Bone morphogenic protein signalling suppresses differentiation of pluripotent cells by maintaining expression of E-Cadherin. *eLife*, 2, p.e01197. Available at: http://www.pubmedcentral.nih.gov/articlerender.fcgi?artid=3865744&tool=pmcentrez&rendertype=abstract [Accessed October 6, 2014].

Martin, B.L. & Kimelman, D., 2012. Canonical Wnt signaling dynamically controls multiple stem cell fate decisions during vertebrate body formation. *Developmental cell*, 22(1), pp.223–32. Available at: http://www.pubmedcentral.nih.gov/articlerender.fcgi?artid=3465166&tool=pmcentrez&rendertype=abstract [Accessed June 5, 2014].

Martin, G.R., 1981. Isolation of a pluripotent cell line from early mouse embryos cultured in medium conditioned by teratocarcinoma stem cells Developmental Biology : *PNAS*, 78(12), pp.7634–7638.

Massari, M.E. & Murre, C., 2000. Helix-Loop-Helix Proteins : Regulators of Transcription in Eucaryotic Organisms MINIREVIEW Helix-Loop-Helix Proteins : Regulators of Transcription in Eucaryotic Organisms. *Molecular and cellular biology*, 20(2).

Mathew, S. et al., 1995. Chromosomal Assignment of Human ID1 and ID2 Genes. , 387, pp.385–387.

Mathis, L. & Nicolas, J.F., 2000. Different clonal dispersion in the rostral and caudal mouse central nervous system. *Development*, 127, pp.1277–1290.

Mishina, Y. et al., 1995. Bmpr encodes a type I bone morphogenetic protein receptor that is essential for gastrulation during mouse embryogenesis. *Genes and Development*, 9(24), pp.3027–3037.

Miura, S. et al., 2006. BMP signaling in the epiblast is required for proper recruitment of the prospective paraxial mesoderm and development of the somites. *Development (Cambridge, England)*, 133(19), pp.3767–75. Available at: http://www.ncbi.nlm.nih.gov/pubmed/16943278 [Accessed June 16, 2014].

Mori, S., Nishikawa, S. & Yokota, Y., 2000. Lactation defect in mice lacking the helix ± loop ± helix inhibitor Id2. *The EMBO journal*, 19(21).

Murre, C.., McCaw, P.S.. & Baltimore, D., 1989. A New DNA-Binding and Dimerization Motif in Immunoglobulin Enhancer Binding, Daughterless, Myod, and Myc Proteins. *Cell*, 56(5), pp.777–783.

Nagaso, H. et al., 1999. Dual specificity of activin type II receptor ActRIIb in dorso-ventral patterning during zebrafish embryogenesis. *Development Growth and Differentiation*, 1, pp.119–133.

Naiche, L.A., Holder, N. & Lewandoski, M., 2011. FGF4 and FGF8 comprise the wavefront activity that controls somitogenesis. *Proceedings of the National Academy of Sciences of the United States of America*, 108(10).

Najm, F.J. et al., 2011. Rapid and robust gen of functional OPCs from EpiSCs SUPPL. *Nature Methods*, 8(11), pp.957–962. Available at: http://www.pubmedcentral.nih.gov/articlerender.fcgi?artid=3400969&tool=pmcentrez&rendertype=abstract [Accessed May 30, 2014].

Nam, H. & Benezra, R., 2009. High levels of Id1 expression define B1 type adult neural stem cells. *Cell stem cell*, 5(5), pp.515–26. Available at: http://www.pubmedcentral.nih.gov/articlerender.fcgi?artid=2775820&tool=pmcentrez&rendertype=abstract [Accessed November 18, 2014].

Nichols, J. & Smith, A., 2009. Perspective Naive and Primed Pluripotent States. *Stem Cell*, 4(6), pp.487–492. Available at: http://dx.doi.org/10.1016/j.stem.2009.05.015.

Nishikawa, M. et al., 2012. Stepwise renal lineage differentiation of mouse embryonic stem cells tracing in vivo development. *Biochemical and biophysical research communications*, 417(2), pp.897–902. Available at: http://www.ncbi.nlm.nih.gov/pubmed/22209845 [Accessed May 29, 2014].

Nishimura, R. et al., 1998. Smad5 and DPC4 Are Key Molecules in Mediating BMP-2-induced Osteoblastic Differentiation of the Pluripotent Mesenchymal Precursor Cell Line C2C12 *. *The Journal of biological chemistry*, 273(4), pp.1872–1879.

Norton, J.D., 2000. COMMENTARY ID helix-loop-helix proteins in cell growth ,

differentiation and tumorigenesis. , 3905, pp.3897–3905.

Nowotschin, S. et al., 2012. Interaction of Wnt3a , Msgn1 and Tbx6 in neural versus paraxial mesoderm lineage commitment and paraxial mesoderm differentiation in the mouse embryo. *Developmental Biology*, 367(1), pp.1–14. Available at: http://dx.doi.org/10.1016/j.ydbio.2012.04.012.

Ohtani, N. et al., 2001. Opposing effects of Ets and Id proteins on p16 INK4a expression during cellular senescence. *Nature*, 409, pp.1067–1070.

Olivera-Martinez, I. et al., 2012. Loss of FGF-dependent mesoderm identity and rise of endogenous retinoid signalling determine cessation of body axis elongation. *PLoS biology*, 10(10), p.e1001415. Available at: http://www.pubmedcentral.nih.gov/articlerender.fcgi?artid=3484059&tool=pmcentrez&rendertype=abstract [Accessed June 5, 2014].

Osorno, R. et al., 2012. The developmental dismantling of pluripotency is reversed by ectopic Oct4 expression. *Development (Cambridge, England)*, 139(13), pp.2288–98. Available at: http://www.pubmedcentral.nih.gov/articlerender.fcgi?artid=3367440&tool=pmcentrez&rendertype=abstract [Accessed May 24, 2014].

Pagliuca, A. et al., 1995. Molecular cloning of ID4, a novel dominant negative helix-loop-helix human gene on chromosome 6p21.3-p22. *Genomics*, 27(1), pp.200–3. Available at: http://www.ncbi.nlm.nih.gov/pubmed/7665172.

Pan, L. et al., 1999. Impaired Immune Responses and B-Cell Proliferation in Mice Lacking the Id3 Gene. *Molecular and cellular biology*, 19(9), pp.5969–5980.

Perk, J., Iavarone, A. & Benezra, R., 2005. ID FAMILY OF HELIX ◎ LOOP ◎ HELIX PROTEINS IN CANCER. *Nature Reviews Cancer*, 5, pp.603–614.

Pevny, L.H. et al., 1998. A role for SOX1 in neural determination. *Development*, 125, pp.1967–1978.

Pourquié, O. & Chal, J., 2013. Tepzz 565 64a_t (11). , 1(19), pp.1–48.

Prendergast, G.C., Lawe, D. & Ziff, E.B., 1991. Association of Myn, the murine homolog of Max, with c-Myc stimulates methylation-sensitive DNA binding and ras cotransformation. *Cell*, 65(3), pp.395–407.

Pucéat, M., 2008. Protocols for cardiac differentiation of embryonic stem cells. *Methods (San Diego, Calif.)*, 45(2), pp.168–71. Available at: http://www.ncbi.nlm.nih.gov/pubmed/18593613 [Accessed June 10, 2014].

Rashbass, P. et al., 1991. A cell autonomous function of Brachyury in T/T embryonic stem cell chimaeras. *Nature*, 353.

Riechmann, V., van Crüchten, I. & Sablitzky, F., 1994. The expression pattern of Id4,

a novel dominant negative helix-loop-helix protein, is distinct from Id1, Id2 and Id3. *Nucleic acids research*, 22(5), pp.749–55. Available at: http://www.pubmedcentral.nih.gov/articlerender.fcgi?artid=307878&tool=pmcentrez&rendertype=abstract.

Romero-Lanman, E.E. et al., 2012. Id1 maintains embryonic stem cell self-renewal by up-regulation of Nanog and repression of Brachyury expression. *Stem cells and development*, 21(3), pp.384–93. Available at: http://www.ncbi.nlm.nih.gov/pubmed/22013995 [Accessed June 13, 2014].

Rosenzweig, B.L. et al., 1995. Cloning and characterization of a human type II receptor for bone morphogenetic proteins. *Proceedings of the National Academy of Sciences of the United States of America*, 92(August), pp.7632–7636.

Row, R.H. et al., 2018. BMP and FGF signaling interact to pattern mesoderm by controlling basic helix-loop-helix transcription factor activity. *Elife*, Jun 7(7), p.e31018.

Ruzinova, M.B. & Benezra, R., 2003. Id proteins in development, cell cycle and cancer. *Trends in Cell Biology*, 13(8), pp.410–418. Available at: http://linkinghub.elsevier.com/retrieve/pii/S0962892403001478 [Accessed June 16, 2014].

Saga, Y. et al., 1996. MesP1: a novel basic helix-loop-helix protein expressed in the nascent mesodermal cells during mouse gastrulation. *Development (Cambridge, England)*, 122(9), pp.2769–78. Available at: http://www.ncbi.nlm.nih.gov/pubmed/8787751.

Sakurai, H. et al., 2008. Paraxial Mesodermal Progenitors Derived from Mouse Embryonic Stem Cells Contribute to Muscle Regeneration via Differentiation into Muscle Satellite Cells AND. , pp.1865–1873.

Sarkar, A. & Hochedlinger, K., 2013. Review The Sox Family of Transcription Factors : Versatile Regulators of Stem and Progenitor Cell Fate. *Stem Cell*, 12(1), pp.15–30. Available at: http://dx.doi.org/10.1016/j.stem.2012.12.007.

Schepers, G.E., Teasdale, R.D. & Koopman, P., 2002. Twenty Pairs of Sox : Extent , Homology , and Nomenclature. *Developmental cell*, 3, pp.167–170.

Seifert, J.R.K. & Mlodzik, M., 2007. Frizzled/PCP signalling: A conserved mechanism regulating cell polarity and directed motility. *Nature Reviews Genetics*, 8(2), pp.126–138.

Silva, J. & Smith, A., 2008. Capturing pluripotency. *Cell*, 132(4), pp.532–6. Available at: http://www.pubmedcentral.nih.gov/articlerender.fcgi?artid=2427053&tool=pmcentrez&rendertype=abstract [Accessed May 24, 2014].

Skinner, M.K. et al., 2010. NIH Public Access. *Differentiation*, 80(1), pp.1–8.

Smith, J.L., Gesteland, K.M. & Schoenwolf, G.C., 1994. Prospective fate map of the mouse primitive streak at 7.5 days of gestation. *Developmental dynamics : an official publication of the American Association of Anatomists*, 201(3), pp.279–89. Available at: http://www.ncbi.nlm.nih.gov/pubmed/7881130.

Solloway, M.J. et al., 1998. Mice lacking Bmp6 function. *Developmental Genetics*, 22(4), pp.321–339. Available at: http://dx.doi.org/10.1002/(SICI)1520-6408(1998)22:4%3C321::AID-DVG3%3E3.0.CO.

Solloway, M.J. & Robertson, E.J., 1999. Early embryonic lethality in Bmp5;Bmp7 double mutant mice suggests functional redundancy within the 60A subgroup. *Development (Cambridge, England)*, 126(8), pp.1753–68. Available at: http://www.ncbi.nlm.nih.gov/pubmed/10079236.

Sterneckert, J. et al., 2010. Neural induction intermediates exhibit distinct roles of Fgf signaling. *Stem cells (Dayton, Ohio)*, 28(10), pp.1772–81. Available at: http://www.ncbi.nlm.nih.gov/pubmed/20715182 [Accessed June 13, 2014].

Stevens, J.D., Roalson, E.H. & Skinner, M.K., 2008. Phylogenetic and expression analysis of the basic helix-loop-helix transcription factor gene family: Genomic approach to cellular differentiation. *Differentiation*, 76(9), pp.1006–1022. Available at: http://dx.doi.org/10.1111/j.1432-0436.2008.00285.x.

Sun, H., Ghaffari, S. & Taneja, R., 2007. bHLH-Orange Transcription Factors in Development and Cancer. *Translational oncogenomics*, 2, pp.107–20. Available at: http://www.pubmedcentral.nih.gov/articlerender.fcgi?artid=3634620&tool=pmcentrez&rendertype=abstract.

Sun, X. et al., 1999. Targeted disruption of Fgf8 causes failure of cell migration in the gastrulating mouse embryo. *Genes & development*, 13, pp.1834–1846.

Sun, X.H. et al., 1991. Id proteins Id1 and Id2 selectively inhibit DNA binding by one class of helix-loop-helix proteins. *Molecular and cellular biology*, 11(11), pp.5603–11. Available at: http://www.pubmedcentral.nih.gov/articlerender.fcgi?artid=361931&tool=pmcentrez&rendertype=abstract.

Takada, S. et al., 1994. Wnt-3a regulates somite and tailbud formation in the mouse embryo. *Genes & Development*, 8(2), pp.174–189. Available at: http://www.genesdev.org/cgi/doi/10.1101/gad.8.2.174 [Accessed June 3, 2014].

Takemoto, T. et al., 2004. Convergence of Wnt and FGF signals in the genesis of posterior neural plate through activation of the Sox2 enhancer N-1. *Development*, 133, pp.297–306.

Takemoto, T. et al., 2011. Tbx6-dependent Sox2 regulation determines neural or

mesodermal fate in axial stem cells. *Nature*, 470(7334), pp.394–8. Available at: http://www.pubmedcentral.nih.gov/articlerender.fcgi?artid=3042233&tool=pmcentrez&rendertype=abstract [Accessed June 5, 2014].

Takenaga, M., Fukumoto, M. & Hori, Y., 2007. Regulated Nodal signaling promotes differentiation of the definitive endoderm and mesoderm from ES cells. *Journal of cell science*, 120(Pt 12), pp.2078–90. Available at: http://www.ncbi.nlm.nih.gov/pubmed/17535850 [Accessed June 13, 2014].

Tesar, P. et al., 2007. New cell lines from mouse epiblast share defining features with human embryonic stem cells. *Nature*, 448(7150), pp.196–199. Available at: http://www.ncbi.nlm.nih.gov/entrez/query.fcgi?cmd=Retrieve&db=PubMed&dopt=Citation&list_uids=17597760 [Accessed May 24, 2014].

Torres, J. et al., 2012. Efficient Differentiation of Embryonic Stem Cells into Mesodermal Precursors by BMP , Retinoic Acid and Notch Signalling. *PloS one*, 7(4).

Tremblay, K.D., Dunn, N.R. & Robertson, E.J., 2001. Mouse embryos lacking Smad1 signals display defects in extra-embryonic tissues and germ cell formation. *Development (Cambridge, England)*, 128(18), pp.3609–21. Available at: http://www.ncbi.nlm.nih.gov/pubmed/11566864.

Tsakiridis, A. et al., 2014a. Distinct Wnt-driven primitive streak-like populations reflect in vivo lineage precursors. *Development (Cambridge, England)*, 141(6), pp.1209–21. Available at: http://www.pubmedcentral.nih.gov/articlerender.fcgi?artid=3943179&tool=pmcentrez&rendertype=abstract [Accessed August 13, 2014].

Tsakiridis, A. et al., 2014b. Distinct Wnt-driven primitive streak-like populations reflect in vivo lineage precursors. , pp.1209–1221.

Tsakiridis, A. et al., 2014c. Distinct Wnt-driven primitive streak-like populations reflect in vivo lineage precursors. , pp.1209–1221.

Tsakiridis, A. & Wilson, V., 2015. Assessing the bipotency of in vitro-derived neuromesodermal progenitors [version 2 ; referees : 2 approved , 1 approved with reservations] Referee Status : , (0), pp.1–17.

Turabelidze, A., Guo, S. & Dipietro, L.A., 2010. Importance of Housekeeping gene selection for accurate RT-qPCR in a wound healing model. *Wound Repair Regen*, 18(5), pp.460–466. Available at: http://medgen.ugent.be/~jvdesomp/genorm/.

Turner, D.A. et al., 2014. Wnt / β -catenin and FGF signalling direct the specification and maintenance of a neuromesodermal axial progenitor in ensembles of mouse embryonic stem cells. *Developmentevelopment*, 141, pp.4243–4253.

Tzouanacou, E. et al., 2009. Redefining the progression of lineage segregations

during mammalian embryogenesis by clonal analysis. *Developmental cell*, 17(3), pp.365–76. Available at: http://www.ncbi.nlm.nih.gov/pubmed/19758561 [Accessed May 24, 2014].

Vallier, L. et al., 2009. Early cell fate decisions of human embryonic stem cells and mouse epiblast stem cells are controlled by the same signalling pathways. *PloS one*, 4(6), p.e6082. Available at: http://www.pubmedcentral.nih.gov/articlerender.fcgi?artid=2700259&tool=pmcentrez&rendertype=abstract [Accessed May 26, 2014].

Villares, R. & Cabrera, C. V., 1987. The achaete-scute gene complex of D. melanogaster: Conserved Domains in a subset of genes required for neurogenesis and their homology to myc. *Cell*, 50(3), pp.415–424.

Wang, Y., Benezra, R. & Sassoon, D. a, 1992. Id expression during mouse development: a role in morphogenesis. *Developmental dynamics : an official publication of the American Association of Anatomists*, 194(3), pp.222–30. Available at: http://www.ncbi.nlm.nih.gov/pubmed/1361374.

Wilkinson, D.G., Bhatt, S. & Herrmann, B.G., 1990. Expression pattern of the mouse T gene and its role in mesoderm formation. *Letters to Nature*, 343.

Wilson, V. et al., 1995. The T gene is necessary for normal mesodermal morphogenetic cell movements during gastrulation. *Development (Cambridge, England)*, 121(3), pp.877–86. Available at: http://www.ncbi.nlm.nih.gov/pubmed/7720590.

Wilson, V. & Beddington, R., 1997. Expression of T protein in the primitive streak is necessary and sufficient for posterior mesoderm movement and somite differentiation. *Developmental biology*, 192(1), pp.45–58. Available at: http://www.ncbi.nlm.nih.gov/pubmed/9405096.

Wilson, V., Olivera-Martinez, I. & Storey, K.G., 2009. Stem cells, signals and vertebrate body axis extension. *Development*, 136(12), pp.2133–2133. Available at: http://dev.biologists.org/cgi/doi/10.1242/dev.039172 [Accessed June 5, 2014].

Winnier, G., Blessing, M. & Labosky, P.A., 1995. Bone morphogenetic protein-4 Is required for mesoderm formation and patterning in the mouse. *Genes & Development*, 9, pp.2105–2116.

Wood, H.B. & Episkopou, V., 1999. Comparative expression of the mouse Sox1 , Sox2 and Sox3 genes from pre-gastrulation to early somite stages. *Mechanisms of Development*, 86, pp.197–201.

Wrana, J.L. et al., 1994. Mechanism of activation of the TFG-b receptor. *Nature*, 370, pp.341–347.

Wymeersch, F.J. et al., 2016. Position-dependent plasticity of distinct progenitor

types in the primitive streak. *eLife*, pp.1–28.

Yamaguchi, T.P., Bradley, A., et al., 1999. A Wnt5a pathway underlies outgrowth of multiple structures in the vertebrate embryo. *Development*, 126, pp.1211–1223.

Yamaguchi, T.P. et al., 1993. flk-1 , an flt -related receptor tyrosine kinase is an early marker for endothelial cell precursors. *Development*, 118, pp.489–498.

Yamaguchi, T.P., Takada, S., et al., 1999. T (Brachyury) is a direct target of Wnt3a during paraxial mesoderm specification service T (Brachyury) is a direct target of Wnt3a during paraxial mesoderm specification. , pp.3185–3190.

Yan, W. et al., 1997. High incidence of T-cell tumors in E2A-null mice and E2A/Id1 double-knockout mice. *Molecular and cellular biology*, 17(12), pp.7317–27. Available at: http://www.pubmedcentral.nih.gov/articlerender.fcgi?artid=232588&tool=pmcentrez&rendertype=abstract.

Yang, X. et al., 1999. Angiogenesis defects and mesenchymal apoptosis in mice lacking SMAD5. *Development*, 126(8), pp.1571–80. Available at: http://www.ncbi.nlm.nih.gov/pubmed/10079220.

Yates, P.R. et al., 1999. Id helix – loop – helix proteins inhibit nucleoprotein complex formation by the TCF ETS-domain transcription factors. *The EMBO journal*, 18(4), pp.968–976.

Ying, Q.L. et al., 2003. BMP induction of Id proteins suppresses differentiation and sustains embryonic stem cell self-renewal in collaboration with STAT3. *Cell*, 115(3), pp.281–92. Available at: http://www.ncbi.nlm.nih.gov/pubmed/14636556.

Ying, Y. & Zhao, G.Q., 2001. Cooperation of endoderm-derived BMP2 and extraembryonic ectoderm-derived BMP4 in primordial germ cell generation in the mouse. *Developmental Biology*, 232(2), pp.484–492.

Yokota, Y., Mansouri, A. & Mori, S., 1999. Development of peripheral lymphoid organs and natural killer cells depends on the helix-loop-helix inhibitor Id2. *Nature*, 397, pp.702–706.

Yoshida, M. et al., 2014. Regulation of mesodermal precursor production by low-level expression of B1 Sox genes in the caudal lateral epiblast. *Mechanisms of Development*, 132, pp.59–68. Available at: http://dx.doi.org/10.1016/j.mod.2014.01.003.

Yoshikawa, Y. et al., 1997. Evidence That Absence of Wnt-3a Signaling Promotes Neuralization Instead of Paraxial Mesoderm Development in the Mouse. *Developmental biology*, 183, pp.234–242.

Yun, K. et al., 2004. Id4 regulates neural progenitor proliferation and differentiation

in vivo. *Development*, 131, pp.5441–5448.

Zhang, H. & Bradley, A., 1996. Mice deficient for BMP2 are nonviable and have defects in amnion/chorion and cardiac development. *Development (Cambridge, England)*, 122(10), pp.2977–86. Available at: http://www.ncbi.nlm.nih.gov/pubmed/8898212.

Zhao, G.-Q., 2003. Consequences of knocking out BMP signaling in the mouse. *Genesis (New York, N.Y. : 2000)*, 35(1), pp.43–56. Available at: http://www.ncbi.nlm.nih.gov/pubmed/12481298 [Accessed June 13, 2014].

Zhou, X. et al., 1993. Nodal is a novel TGF-b-like gene expressed in the mouse node during gastrulation. *Letters to Nature*, 361.

Appendix 1

Appendix 1| Schematic of stages of mouse embryonic development. Lateral views of representative diagrams showing the stages of development examined within this thesis. Diagrams are not to scale.

Appendix 2

Appendix 2| Data taken from (Jen et al. 1997), Figure 2. In situ hybridisation using probes for Id1, Id2, Id3 and Id4 in E7.5 mouse embryos. The authors stated "Id3 is expressed in the entire embryos proper as well as in the visceral yolk sac. Again, the Id4 signals were not detectable at this stage (Fig. 2G,H)."